

THE UNIVERSITY OF CALGARY

A Physical Simulation of Ball Lightning for Computer Graphics

by

Petri Matthew Varsa

A THESIS

SUBMITTED TO THE FACULTY OF GRADUATE STUDIES
IN PARTIAL FULFILLMENT OF THE REQUIREMENTS FOR THE
DEGREE OF MASTER OF SCIENCE

DEPARTMENT OF COMPUTER SCIENCE

CALGARY, ALBERTA

March, 2004

© Petri Matthew Varsa 2004

THE UNIVERSITY OF CALGARY
FACULTY OF GRADUATE STUDIES

The undersigned certify that they have read, and recommend to the Faculty of Graduate Studies for acceptance, a thesis entitled “**A Physical Simulation of Ball Lightning for Computer Graphics**” submitted by Petri Matthew Varsa in partial fulfillment of the requirements for the degree of Master of Science.

Supervisor, Dr. Jon Rokne,
Department of Computer Science.

Dr. Jörg Denzinger,
Department of Computer Science.

Dr. Gordon Sick,
Haskayne School of Business.

March 5th, 2004

Date

Abstract

Rendering images of outdoor scenes capturing the magnificence of the natural world is a challenging task for computer graphics. Some excellent images containing specific natural phenomena have been created, but much more work needs to be done so that realistic scenes can be rendered in all cases. Part of the difficulty is that many of the captivating natural phenomena are not fully appreciated and sometimes not even properly explained by scientists. The interface between physics and computer graphics may be a fertile ground for exploring such phenomena. The computer scientist can provide exploratory images which could support the physicist in developing theories to explain the phenomena. One natural phenomenon that has received no attention in the field of computer graphics and scarce attention in physics is ball lightning. It is likely the most infrequent and poorly understood aspect of physics today. Although its existence is disputed, the evidence quoted in the thesis is in favor of the existence of a type of manifestation that is commonly referred to as ball lightning. A computer graphics simulation of this rare feature would greatly improve animated sequences of thunderstorms. A physical model of ball lightning may also aid physicists in discovering its *true* nature. This thesis presents the first attempt at a computer graphics simulation of ball lightning. It is based on observations and physical theories which have attempted to describe its properties. None of the theories presented so far can explain all the manifestations of ball lightning reported in the literature. Consequently, it was not possible to develop a purely physical simulation.

In particular, little is known about the internal structure of ball lightning. Common computer graphics techniques that are efficient and easy to implement are therefore used to approximate the deformations of a ball lightning as it passes through small openings. An emphasis is placed on clearly defining a set of parameters that affect the visual qualities of the animation. In this way, the final output can be adjusted to suit the variety of observations that have been documented. Since ball lightning research is new to the field of computer graphics it necessitated an extensive introduction and survey of the current state of knowledge of the phenomenon for the thesis.

Acknowledgements

This work would not have been possible without the support and guidance of my supervisor, Dr. Jon Rokne. He was instrumental in its completion and I would like to acknowledge him for his continual help and encouragement.

I would like to thank Dr. Gladimir Baranoski for helping me find a few references and also for his support.

While writing this thesis I had several chats and conversations with my peers that have motivated me and given me valuable ideas. Although one might not think much of these little chats, I believe that these discussions were important ideation sessions. It is not easy to list all the individuals that have given me such inspiration, but they know who they are.

This work made use of the infrastructure and resources of MACI (Multimedia Advanced Computational Infrastructure), funded in part by the CFI (Canada Foundation for Innovation), ISRIP (Alberta Innovation and Science Research Investment Program), and the Universities of Alberta and Calgary.

I would like to acknowledge Alias for making the Maya product suite available to the University of Calgary. Maya was used indirectly for this thesis, and the presented material does not depend upon it in any way.

Finally, I would like to thank my family and friends for their loving support.

Contents

Approval Sheet	i
Abstract	ii
Acknowledgements	iv
Contents	v
List of Figures	viii
List of Tables	ix
List of Abbreviations	x
1 Introduction	1
1.1 What Is Ball Lightning?	2
1.1.1 Characteristics	6
1.1.2 Ball Lightning Reports	9
1.1.3 Similar Phenomena	12
1.1.4 Ball Lightning as a Category of Phenomena	14
1.2 Rendering Physical Phenomena	15
2 Ball Lightning Research	20
2.1 Overview of Ball Lightning Research	21
2.2 Typical Pitfalls in Ball Lightning Theory	24
2.3 Plasma	27
2.4 Lightning	30
2.5 Ball Lightning Models	35
2.5.1 External Energy Source Models	35
2.5.2 Erosion Discharge and Particulate Models	40
2.5.3 Lightning Impact Models and Vortex Containment	44
2.5.4 Other Models	46

3	Simulating Phenomena	49
3.1	Basic Ray Tracing	50
3.2	Splatting	56
3.3	Modelling of Phenomena	60
3.3.1	Modelling Rainbows	60
3.3.2	Modelling Aurora	65
3.3.3	Modelling Lightning	67
4	Simulating Ball Lightning	74
4.1	Non-deformable Motion	75
4.1.1	Numerical Solution	77
4.1.2	Initial Conditions	79
4.1.3	Examples	81
4.2	Deformation Through an Opening	83
4.2.1	Graphical Approximation	85
4.2.2	Voxel Volume Initialization	87
4.3	Rendering	96
4.3.1	Basic Ball Lightning	97
4.3.2	Compositing	99
5	Conclusion	101
5.1	Results	101
5.2	Efficiency Considerations	109
5.3	Future Considerations	114
5.4	Conclusion	117
	Bibliography	119

List of Figures

1.1	1868 W. von Haidinger sketch of ball lightning	4
1.2	1957 B. V. Davidov photograph of ball lightning	5
1.3	1978 W. Burger photograph of ball lightning	6
2.1	Magnetic field direction around a wire	28
2.2	Charge distribution within a cumulonimbus cloud	31
2.3	Schematic representation of an electromagnetic knot	40
2.4	Model of polymer-composite ball lightning.	43
3.1	A pinhole camera	51
3.2	The basic raytracing method	52
3.3	Diffuse Lambertian lighting model	53
3.4	Aliasing artifacts	54
3.5	A regular voxel volume representation	57
3.6	Descartes' raindrop	61
3.7	Rainbow properties	62
3.8	Kruszewski's electrification process	70
3.9	Glassner's process of adding tortuosity	71
4.1	2D plot of ball lightning motion	82
4.2	3D plot of ball lightning motion	83
4.3	Ball lightning approaching a circular hole in a screen	84
4.4	Advecting voxel volume for ball lightning simulation	88
4.5	Varying the field parameter of the "blob" function	90
4.6	A "blob" function convolved around the z-axis	91
4.7	The definition of viscosity	94
4.8	Extending the hole into the new ball lightning	96
5.1	Deformation of a ball lightning	102
5.2	GUI used to configure visual ball lightning properties	103
5.3	Increasing the number of particles in a ball lightning	104
5.4	Increasing the opacity of a ball lightning	104
5.5	Varying the "blob" function field parameter	105
5.6	Varying the glow width parameter	106

5.7	Glow width parameter used with a deforming ball lightning	107
5.8	Number of particles vs. simulation time	110
5.9	Number of particles vs. rendering time	112
5.10	Simulation rendering pipeline	112
5.11	Artifacts generated from lack of adaptation	114
5.12	Proposed rendering pipeline	116

List of Tables

5.1	Memory requirements for various voxel densities	109
5.2	Effect of increasing number of particles on rendering time	111

List of Abbreviations

§	subsection
&	et (and)
etc.	et cetera (and on)
et al.	et alii (and others)
μ s	microsecond
3D	three-dimensional
C	Coulomb
CG	cloud-to-ground lightning
cm	centimeter
CPU	Central Processing Unit
CT	computed tomography scan (i.e. CAT scan)
dc	direct current
dm	decimeter
GUI	Graphical User Interface
i.e.	id est (that is to say)
I/O	input/output
J	Joule
K	Kelvin
m	meter
MB	megabyte
MJ	megaJoule
MRI	magnetic resonance imaging
mm	millimeter
ms	millisecond
p.	page
pp.	pages
pixel	picture element
RGB	red, green, and blue
s	second
TEM	transmission electron microscopy
V	volt
voxel	volume element
vs.	versus

Chapter 1

Introduction

Computer Graphics is a wide field with many avenues open for exploration. The variety of topics in computer graphics include rendering techniques, geometric modelling, data visualization, simulation of phenomena, graphics hardware design, and many others. Each field has a different focus, and different goals; but for many members of the computer graphics community, the generation of photorealistic¹ images is the ultimate goal.

This work will focus on the simulation of *natural phenomena*. Rendering images of outdoor scenes is an important area of computer graphics that needs more attention. Some excellent images have been created, but much more work needs to be done in order to really capture the magnificence of the natural world. The captivating exhibitions of natural phenomena are also not generally well appreciated by physicists. Thus the interface between physics and computer graphics offers opportunities for realistically modelling natural phenomena. It is essential that phenomena be studied and modelled so that convincing images of the outdoor world can be created. One natural phenomenon that has received no attention in the field of computer graphics and scarce attention in physics is ball lightning. It is likely the most scarce and poorly understood aspect of physics today. A computer graphics simulation of a rare feature

¹Photorealistic images are purportedly indistinguishable from photographs.

such as ball lightning would greatly improve animated sequences of thunderstorms. Also, a physical model of ball lightning might also aid physicists in discovering the *true* nature of ball lightning.

This thesis presents the first attempt at a computer graphics simulation of ball lightning. It is based on observations and physical theories which have described the properties of ball lightning. A purely physical simulation cannot be implemented since the nature of ball lightning is not well understood. In particular, little is known about the internal structure of ball lightning. As such, common computer graphics techniques that are efficient and easy to implement are used to approximate the deformations of a ball lightning as it passes through small openings. An emphasis is placed on clearly defining a set of parameters that affect the visual qualities of the animation. In this way, the final output can be adjusted to suit the variety of observations that have been documented.

1.1 What Is Ball Lightning?

Ball lightning is a rare natural phenomenon that is usually, but not always, associated with thunderstorms and foul weather. It often assumes a nearly spherical form, but has also been observed to be ring-, rod-, and teardrop-shaped. It seems to move independently of the environment, even against the wind and through glass panes. Most observations report that it is somewhat larger than a grapefruit, and is about as bright as a 120 Watt light bulb. It has been observed to deform so that it may pass through small openings and walls. It has even been seen aboard aircraft and dangling from aircraft wings. Sometimes it decays silently; other times it explodes violently. There is evidence to suggest that it can contain a considerable amount of energy, since it has damaged objects and killed people. On the other hand, some people have been struck by ball lightning without injury or harm. Ball lightning is likely a plasmoid²

²A plasmoid is an object that is in the fourth state of matter — the plasma state. Plasma is the break down of gaseous matter from a molecular or atomic form into free ions and electrons[41].

of some sort. There are many ball lightning theories whose explanations range from simple combustion to nuclear fusion. In his 1971 book, Stanley Singer described ball lightning as:

a luminous globe which occurs in the course of a thunderstorm. It is most often red, although varying colors including yellow, white, blue, and green have also been often reported for the glowing ball. The size varies widely, but a diameter of one-half foot is common. Its appearance is in striking contrast to ordinary lightning, for it often moves in a horizontal path near the Earth at a low velocity. It may remain stationary momentarily or change course while in motion. Unlike the rapid flash of ordinary lightning, ball lightning exists for extended periods of time, several seconds or even minutes[116].

Since ball lightning is such a rare phenomenon, very few photographs have been taken of it. There are two types of photographs that are available. The most common type is one where the camera's shutter is left open to expose the film for several seconds. With this type of photograph, one sees a long streak which represents the path taken by the ball lightning. The validity of this type of photograph is often difficult to determine, since a moving light source or a moving camera could be used to mimic the motion of ball lightning. The second type of photograph is one where a short shutter speed is used (approximately $\frac{1}{8}$ th of a second) and a still image of ball lightning is captured. This type of photograph rarely turns out well since the high contrast between the bright fireball and the dark background of foul weather conditions is not captured well on film. It should be noted that photographic evidence is most reliable when the ball lightning has been witnessed by the photographer during the exposure of the film[118].

Early reproductions of ball lightning were sketches. Figure 1.1 was done in 1868 by W. von Haidinger for the scientific journal *Sitzungsberichte. Akademie der Wissenschaften in Wien. Mathematisch-Naturwissenschaftliche Klasse*. He witnessed the



Figure 1.1: 1868 sketch of a ball lightning observation by W. von Haidinger. Permission to reproduce this image provided by Kluwer Academic/Plenum Publishers.

bright red and yellow ball through a window, where it remained directly before him for two or three seconds. Long reddish-yellow rays shot toward the right, while short rays shot toward the left. The long rays on the right were blinding white at their ends[116].

Figure 1.2 is a long exposure photograph that traces the path of a ball lightning until it struck the window of a house. The photographer claimed to be in another room while the camera shutter was left open. After noticing a lightning flash and hearing a “crackling noise” he returned and closed the shutter. He did not witness the event personally. The validity of this photograph has been disputed, but the report of the event indicates that burn marks were left on a 3.5–4 cm length of the wooden window frame, and that soot was found on the glass[116].

One of the most recent and convincing photographs of ball lightning was taken in 1978 in Austria by W. Burger. (See Figure 1.3.) It was taken during the summertime in the mountainous region of Sankt Gallenkirch. Herr W. Burger reported that he was taking photographs of an approaching storm squall when this “fireball fell down” in front of him[125]. Since he witnessed the ball lightning that was photographed, the photo’s validity is difficult to dispute. Many alternative explanations have been

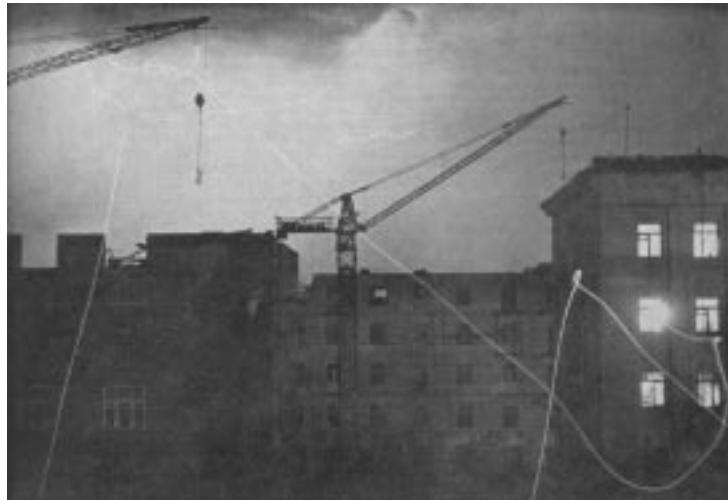


Figure 1.2: 1957 long exposure photograph showing the path taken by a ball lightning. The report of the incident indicated that a soot-like residue was found on the window. Photo taken by B. V. Davidov in Kharkov on 27 August, 1957. Reproduced from the original[36].

given for the photograph (pyrotechnics, for example), and experts in the respective fields have discussed the alternatives at great length[74][75].

It should be noted that there is some dispute about the frequency of ball lightning events. In Stanley Singer’s recent publication[118], he discusses this conundrum. The tally of ball lightning reports has reached approximately 10’000, most of which are kept in a Russian data bank. This is a fairly large number of reports for a topic that has only been given attention for approximately 200 years. Furthermore, most of these reports were collected in Russia, Japan, and Europe, which leaves out Africa, much of Asia, and the Americas. A 1966 survey of 4400 NASA employees produced by Warren D. Rayle provided 112 detailed accounts of ball lightning observations[102]. Rayle did not define ball lightning as a “rare” phenomenon. He noted that the number of ball lightning witnesses was 44% of the number of witnesses of regular cloud-to-ground lightning impact points. It should be further noted that Rayle defined ball lightning *lexicographically*, hence any phenomenon labeled by the observer as “ball lightning”



Figure 1.3: 1978 colour photograph of ball lightning taken in Sankt Gallenkirch in Austria by W. Burger. Originally published in [74]. Copyright photograph supplied by Fortean Picture Library.

was considered to be valid. Another survey performed by Dr. J. Rand McNally, Jr. of the Oak Ridge National Laboratory found that 110 people in a sample size of 1962 had seen ball lightning[108, pg. 8]. That's more than one in twenty people.

Probably one reason why it is more easy to study cloud-to-ground lightning impacts is because it can be induced by a launched rocket which carries a grounded wire upward. Still, scientific studies of non-induced cloud-to-ground lightning have been successful[136], whereas similar studies of ball lightning have not[118]. Perhaps it is only the unpredictability and insignificance of size and luminescence which makes ball lightning difficult to study?

1.1.1 Characteristics

The most recent (and perhaps the most accurate) survey of ball lightning characteristics can be found in the first chapter of Mark Stenhoff's book[125]. He uses the data published in several studies to describe the modal properties of ball lightning.

Certainly this summary must contain some level of bias, but it will suffice as a guide for the purpose of this work.

Unless otherwise cited, the information from this section was obtained from *Ball Lightning: An Unsolved Problem Atmospheric Physics* by Mark Stenhoff[125].

Most ball lightning events occur during thunderstorms of at least average violence, with medium to heavy rainfall just before the incident. In about three quarters of the reports, ball lightning was seen following a lightning flash — usually a cloud-to-ground flash. Ball lightning has been observed outdoors, indoors, within aircraft, and outside of aircraft. Ball lightning observations within aircraft consistently report that the ball moved with a moderate speed along the center of the aircraft from the nose to the tail of the aircraft.

About nine out of ten reports state that ball lightning is spheroidal, with a modal diameter of 10-20 cm. Other shapes such as ellipsoids, rings, and rods have also been reported. At one 1987 event a ball lightning with a diameter of approximately 100 m was photographed [3, §1(q)].

Usually a ball lightning is witnessed for 2 to 5 seconds. Note that this number refers to the time which the event was in sight, not the lifetime of the ball. Not uncommonly do observations reach the 20 to 50 second range. Usually the ball is described as being “bright enough to be clearly visible in daylight.” The luminosity and size usually remain constant throughout the viewing time of the ball.

Statistically there is a poor correlation for colour, though Stenhoff points out in §3.3.7 of his book that “the perception and memory of colours also has inherent uncertainties,” and that approximately 10% of people suffer from colour-vision defects. Yellow, orange, white, red, and blue have been regularly reported. Often a mixture of colours have been reported, and sometimes green is also stated as the colour of the ball.

Often ball lightning moves horizontally. Barry[18] lists the following types of motion:

- cloud to cloud
- Earth, or near Earth, to cloud
- cloud to Earth
- near Earth to Earth
- horizontally, near Earth
- stationary, above the Earth

Recently, there has been a report of ball lightning moving vertically from the Earth to a height of several tens of meters[3, §2(g)]. Ball lightning has been observed to rotate, bounce, and fit through small openings.

Sometimes odour and sound are associated with ball lightning. Odours are commonly described as acrid. The sounds associated with ball lightning are described as a hissing or a buzzing noise. Explosive decay of ball lightning is sometimes accompanied by a *bang*.

Less than one half of ball lightning reports state that there was some resulting damage, or evidence left behind from the incident. Evidence of ball lightning include damaged window frames, clothing, heated water, and loss of life.

Barry[18, p. 36][17] states that there have been three different types of structure observed for ball lightning. The first type has a solid appearance that is either dull or reflecting. This type is opaque and may also appear to have an enveloping translucent layer. The second type is a rotating structure with internal motion and stress. The final type looks like a burning sphere or ellipsoid.

Recently, reports have surfaced which describe the structure of ball lightning from a close vantage point. One observer described the internal structure as “writhing within a contained area.” He could observe that this movement was contained by some sort of surface tension[3, §1(p)]. An other report describes the structure of ball lightning as being a “tangle of woolen threads, as if blue threads covered a warp of red threads[3, §2(f, u)].” An encounter with the burning-sphere type described the ball as “rolling over the ground like a wheel.” It had a dense core that was covered with “shaggy fire strips.” An 80 cm train of these strips was following the ball[3,

§2(j)]. Several reports from the same collection describe ball lightning as having a cotton-wool or a poplar-fluff structure[3, §2(l, n, o, q)]. One report stated that a ball lightning was “composed of a vast number of smaller balls, in fact dots”[60].

1.1.2 Ball Lightning Reports

The tally of recorded ball lightning events is well into the thousands. In 1923, Brand[21] collected some 600 reports, 215 of which were detailed enough to be considered instances of ball lightning. Though he was a skeptic, Humphreys collected 280 reports[68] in 1936, which he mostly dismissed as optical illusions. In 1971, Singer approximated his tally to have about 1000 reports[116], and Barry claimed to have more than 1100 reports in his 1980 monograph[18]. In the last two decades many more reports have surfaced. (See [3] for an example.) Singer recently stated[118] that some 10000 reports have been collected in a Russian “databank.”

Accounts of ball lightning are often grouped by reliability. If a single untrained observer witnesses the event, then the report is not very reliable. Though if several witnesses observed the event, then reliability increases. Reliability also increases with the credentials of the observer. If the event was witnessed by an expert in meteorological phenomena, then it is considered to be a strong report. Singer says that there are perhaps 15 published events where the witness was a scientist[118]. For example, see Mr. A. B. Mallinson’s comment on p. 46 and Mr. R. H. Rawll’s comment on p. 48 of [58], as well as Gold[55], Brown[24], Jennison[69], Covington[32], Bromley[23], Felsher[45], Wittmann[142], and Pippard[97].

In this section some interesting accounts of ball lightning will be *briefly* described. The purpose is *not* for scientific evaluation of the reports, but to inspire interest and provide motivation for creating a simulation. Therefore, several details have been omitted.

In a letter to the editor of an English newspaper called *The Daily Mail*, W. Morris described a bright red ball which descended from the sky and struck the house. It

damaged the house by cutting telephone wires and burning a window frame. It then descended into a tub of water which boiled for minutes[58]. This is one of the most frequently cited ball lightning events. Several people have used this description to estimate that the energy contained in a ball lightning is greater than 1 MJ[18].

On 8 August, 1975 in England, a severe thunderstorm that damaged many buildings began at 6:00 PM. A lady was in her kitchen when a 10 cm diameter ball lightning appeared close to an open door and a ventilation shaft. The ball moved toward her and she attempted to brush it away with her left hand. It exploded with a bang that was loud enough to be heard by a neighbour. After the one second incident was over, she found that a hole had been burned in her dress and her tights. Though she suffered no serious harm, her legs were reddened and numbed, and her wedding ring on her left hand felt as though it was burning into her finger. She had to force it off under cold, running water. The damage done to her dress has been reproduced in photographs[125, pp. 83–85].

In 1960, a pilot of a USAF tanker aircraft carrying fuel for B-47 bombers was en route to a refueling rendezvous in a KC-97 aeroplane. The aircraft was in clouds at 18,000 feet with light precipitation and above freezing temperatures. St. Elmo's fire (a commonplace observation for pilots) was "dancing around the edges of the aircraft windows." Suddenly, an 18 inch diameter ball lightning "emerged through the windshield center panels." It was yellow-white in colour, and moved at a rate of a "fast run" toward the rear of the aircraft. The pilot, worried for the safety of the crew since the cargo consisted solely of jet fuel, ignored the ball lightning to prepare for an emergency. Three seconds later, the boom operator who was stationed at the rear of the craft called forward and described the path that the ball lightning took through the rear and exited over the right wing[135]. Lilienfeld[84] suggests that the antenna may be a point of entry for a ball lightning into an aircraft, but this is likely not the case with this detailed account.

Not only has ball lightning been observed within aircraft, it can also attach itself

to the exterior of an airplane. In 1985 an airplane was landing during a foul weather system with lightning. The observer, who is a high temperature materials chemist, did not notice lightning striking the aircraft, but suddenly a ball lightning appeared on the wingtip and lasted for 10–15 seconds. It decayed with an explosion. The observer suspects that the size of the ball was similar to that of a soccer ball[3, §§1(b)]. Felsher’s account[45] is similar.

A chemist named Dmitriev, who had performed some studies on plasma, experienced ball lightning while camped on the bank of the Onega River in Russia. He first saw the ball after an intense flash of lightning. The ball did not appear at the point of impact of the lightning, but over the river. The ball passed over him and he was able to take samples of the air shortly afterward with evacuated bulbs. The ball moved more slowly over land than over the river, while slowly ascending. The ball lightning disappeared after a total of 60–65 seconds of witnessing. The event took place in 1967[116, pp. 30–32].

Sometimes ball lightning is reported to be observed in a location multiple times, and with multiple instances of the lightning. Such is the case reported by C. F. Talman in 1930[126]. An inn at the summit of the Faulhorn in the Swiss Alps experienced ball lightning on two occasions within seven years of each other. The second occasion was witnessed by the woman in charge of the inn, along with her sister and six guests. The group was in the dining room at 5:00 PM when they noticed an approaching thunderstorm. Neither rain, snow, nor hail had fallen, but the dark cloud was seen. All at once, a “large number of very bright round balls of various colors” came from out of the wood burning stove, which was lit. The largest was about the size of a person’s head. A “dreadful deafening explosion” occurred and the balls vanished. No damage was done, nor was anybody injured, though the guests closest to the fireplace felt an electric shock.

Though often no damage nor injury is caused by ball lightning, sometimes an unfortunate case is reported. After a period of rain with no thunderstorm a woman

went outside to fan a flatiron. A glowing ball with a diameter of less than 10 cm was observed at a distance of 2–3 m from her. The ball seemed to be attracted to the iron. When she raised the flatiron up behind her neck the ball lightning flew at it. The woman collapsed and died shortly thereafter. The ball lightning event lasted for only one or two seconds[3, §2(o)]. Ball lightning might also have caused the death of the physicist G. W. Richman in 1753[98].

1.1.3 Similar Phenomena

Due to the rarity of the phenomenon the study of ball lightning has been greatly hindered over the centuries. In fact there are still skeptics in the scientific community which doubt the existence of the phenomenon, despite thousands of eyewitness reports[18, pg. 3, ch. 6][125, ch. 10][68][110]. One source of the skepticism is due to the confusion between ball lightning and other phenomena. In centuries past, very general terms were used to describe a wide variety of phenomena. For example, the words “thunderbolt” and “fireball” were used to describe a number of phenomena[125, §1.3]. Only since the 20th century has the distinction between various phenomena become more clear.

St. Elmo’s fire is a type of corona discharge which occurs on top of tall metal structures that are grounded such as church spires, flag poles, masts on ships, and rocky ridges in the mountains. It is similar to ball lightning in shape, it often has a diameter of about 10 cm, and it is usually blue or white in colour. It is also observed during periods of high electrical activity. Since its energy source is the intense electric field generated by a thunderstorm, it can last for several minutes which is uncharacteristically long for ball lightning. Also unlike ball lightning, *St. Elmo’s Fire* cannot move independently. It must remain attached to the grounding source. Many reports of ball lightning are actually instances of *St. Elmo’s Fire*, or some other corona discharge[68]. Most scientists believe that ball lightning and *St. Elmo’s fire* are distinct phenomena[18][116][125], but there is some dispute about this

fact[134]. Powell and Finkelstein suggest[98] that some ball lightnings are formed as St. Elmo's Fire and become detached when a direct current field provides the power to do so.

Bead lightning, also known as *pearl lightning* and *chain lightning*, occurs after an ordinary lightning stroke. After completion of the return stroke, short, separated segments of the original lightning channel remain for a short duration — sometimes for up to one or two seconds. Usually these segments are almost spherical[18]. On some occasions only a single ball is left at the bottom of a typical cloud-to-ground lightning stroke, instead of a string of beads. This is considered to be ball lightning by some, though most experts disagree.

Strange lights seen before, during, or after an earthquake are commonly deemed *earthquake lights* or *EQLs*. One easily accessible study of earth quake light sightings in the Saguenay region of Québec can be found in the journal *Nature*[94]. Three different types of luminescence were observed by the inhabitants of the region during a period of seismic activity in the late 1980's. These are: fireballs, who's description resembles that of ball lightning; diffuse light, which occupies the same portion of the sky as a sunrise or sunset would; and horizontal, aurora-like, bands in the air. The description of the fireballs bears a close resemblance to many ball lightning reports. Marcel Ouellet says that:

fireballs a few meters in diameter often popped out of the ground in a repetitive manner Others were seen several hundred meters up in the sky, stationary or moving.

This description sounds *remarkably* similar to some ball lightning reports. For example, there is one account of ball lightning where the observer witnessed six sequential balls appear in the grass and fly up to a height of several tens of meters, where they exploded[3, §2(g)]. Perhaps this experience was in fact due to some small amount of seismic activity that was undetectable to the human observer? Perhaps the "fireball" observations associated with earthquake lights would be more appro-

riately identified as ball lightning? Or perhaps there is an unknown connection between seismic activity and ball lightning, the understanding of which would ultimately give the scientific community a firm grasp on the nature of ball lightning *and* earthquake lights? Barry discussed this possibility as well as other natural forces that have produced ball lightnings[17]. Ohtsuki et al.[93] describe two occasions where ball lightning has coexisted with seismic activity.

There is one more phenomena which is similar in description to ball lightning. The rare phenomenon known as a *will-o'-the-wisp* can sometimes be found in wet, marshy, terrains. Anaerobic decay of organic matter will produce luminous objects, which may take an ellipsoidal form. They are usually seen on or near the ground and can be blown around by the wind. Will-o'-the-wisps can have a similar lifespan as ball lightning, but they have also been reported to last for hours. The visual similarity of this phenomenon with ball lightning can lead to misinterpretation of a report given by an observer that is uneducated in such matters. Will-o'-the-wisps are also known as *jack-o'-lanterns*, *specter lights*, *swamp gas*, or more properly *ignis fatuus*[125, §3.1.3].

Optical illusions may also hinder ball lightning research. Positive images are sometimes seen after a bright flash. If an observer viewed the impact point of a regular lightning stroke, then the extreme contrast between the bright flash and the dark sky will create an afterimage on the eye. If this afterimage is off center, then the eye will naturally try to center it. The result will appear as a bright spot which appears to move. Positive afterimages may last for 2–10 seconds, which is similar to the duration of many ball lightning events[11][18, §6.2][125].

1.1.4 Ball Lightning as a Category of Phenomena

The descriptions of ball lightning found in the reports vary considerably. This fact has hindered ball lightning research since most ball lightning models are unable to account for all characteristics. The wide range in ball lightning characteristics might be due to two different reasons. First, other phenomena may have been mistaken for

ball lightning and accidentally included in the statistical analyses of ball lightning properties. (See §1.1.3 for descriptions of such phenomena.) Second, the term “ball lightning” has been applied to almost any luminous ellipsoidal form that moves independently. Therefore, it may be that a number of different physical mechanisms produce such an object, and the term “ball lightning” would be more accurately used as a categorical heading for a set of similar phenomena.

Ball lightning has been observed before a stroke of cloud-to-ground lightning, shortly after such a stroke, as a result of such a stroke, and also when no lightning stroke has been observed at all. It has been observed falling from the sky, and forming on the ground. It could be that ball lightning formed in the sky differs from ball lightning formed on the ground, and from ball lightning formed from a lightning stroke.

Barry[18, pp. 9, 39] and Stenhoff[125, §1.4.14] both suggest that there are possibly several different types of ball lightning. Barry goes so far as to say that laboratory experiments have provided evidence of this. This belief is supported by the present author. Therefore for this work, only a subset of the known ball lightning characteristics will be chosen for the purposes of simulation, which will be discussed in detail in Chapter 4.

1.2 Rendering Physical Phenomena

Following the general descriptions of the ball lightning phenomenon, a discussion of how natural phenomena can be rendered is now given.

There are two common techniques used to render images with a computer. The most modern technique uses specialized hardware to create simple but realistic scenes, which can be manipulated by an individual while the scene unfolds. The more classical technique uses expensive computations in main memory in an attempt to produce very realistic images. The end result of this technique is usually a series of static images

which can be combined to create an animation, that can not be manipulated while being viewed.

Modern, interactive 3D rendering is performed with special pipelined hardware that is accessed by an application programming interface such as OpenGL[®][143]. This is the case with most modern video games and interactive 3D applications. The graphics hardware is specialized so that triangles, and groups of triangles can be rendered quickly. Only simple lighting models are implemented since images must be produced within a fraction of a second. Recently, some flexibility has been added to graphics hardware so that custom shaders can be implemented, though the above limitations still exist.

The purpose of 3D graphics hardware is to render animations in real-time³ so that a user can manipulate a scene as it is being displayed. Interactive rates are usually around 30 frames per second or faster. The entire scene must be rendered for each frame, therefore this specialized hardware must be very fast, and many sacrifices in image quality must be made.

Although the performance of real-time 3D graphics hardware is increasing, the resulting images are still generally lower in quality to those generated with the classical raytracing technique.

The basic raytracing algorithm is simple. A 3D scene is first developed using standard geometric objects and collections of triangles. The eye point of the viewer is defined with respect to the 3D scene. Between the scene and the eye is an *imaginary screen* that is divided up into rectangular picture elements, commonly called *pixels*. For each pixel, a ray is cast from the eye in the direction of that pixel. The ray is then intersected with the objects in the scene. The closest object is selected (since it occludes the objects behind it) and lighting calculations are performed in order to determine the colour of that pixel. After iterating over each pixel, the imaginary

³Real-time systems are implemented such that input is processed and output is given with very strict time constraints. The system responds to the inputs so quickly that it appears as though no processing has been done.

screen is output as the resulting image[63][113][138].

The idea of tracing rays is not new. Although computer graphics is a young field that has only made use of the raytracing technique since 1968[10], René Descartes used raytracing to determine the physical properties of rainbows as early as 1637[37], as discussed later.

The raytracing algorithm is very computationally expensive for computer graphics. The intersection calculations of each ray with the scene are costly. In addition, computing the colour of the struck object requires casting several more rays. When using the most simple type of light source, one ray is cast for each light in order to determine shadows. Unfortunately, such a simple lighting model will not generate very realistic images — the shadows will look too harsh. Complex lighting models increase the realism, but they dramatically add to the computational cost. Transparent and translucent objects also require more rays. In addition to all this, complicated models are developed to simulate the interaction of light with the various surfaces in the scene. Generally, the quality of an image is proportional to the computational cost required to make the image.

So far only a brief overview of how basic objects can be rendered has been given. One can imagine how much more complicated it is to render intricate phenomena, whose physical properties are not completely understood. For motivational purposes, consider the complexity of a rainbow. Rainbows are formed in nature by the refraction of light through countless drops of water. Each tiny drop of water acts as a prism which splits sunlight up into the colour spectrum[59]. Since countless raindrops are required to produce a rainbow, the problem becomes computationally intractable. The rendering of rainbows was addressed by F. Kenton Musgrave[89]. He used the ray tracing method of Descartes on a single, ideal, raindrop to build a table of values. More details of this solution will be discussed in §3.3.1.

The subset of phenomena considered to be *natural* is quite large. It includes obvious phenomena such as rainbows, lightning, tornadoes, the aurora borealis (more

commonly known as the Northern lights), and rain and clouds. There are also many lesser known phenomena such as earthquake lights, will-o-the-wisps, sprites, and ball lightning. The category of *natural phenomena* also includes many things that are easily taken for granted, such as light intersecting with paint drying, plants, sunlight, dust, human skin, and sand dunes.

As one would expect, a number of attempts have been made to simulate natural phenomena. Since lightning is a very powerful yet common phenomenon, simulating it in computer graphics has been attempted and improved upon by several researchers[38][52][53][54][77][103][124]. A very good simulation of rainbows has been done by F. Kenton Musgrave[89]. Variation in sky colour and aerial perspective (the blue-shifting of distant objects) has been modelled at the University of Utah by A. J. Preetham et al.[99]. Plants have been studied quite extensively in the past[9][122][19][100]; and new work in this research niche is continuing today[80]. Recently, soap bubbles[78], drying paint[95] and mud[44] have been studied. The list is ever growing.

To the knowledge of the author, none of the more rare phenomena have been reproduced by the graphics community. Even within the scientific community these phenomena are generally not studied in as much depth. This is likely due to their unpredictability and low frequency of occurrence. For example, it is much easier to find books and papers on typical lightning strokes than earthquake lights — even though the understanding of earthquake lights may aid in the prediction of earthquakes and hence prevent disasters[94].

It is understandable that uncommon and poorly understood phenomena are neglected by the graphics community. How can one create a *photorealistic* image of something that has rarely been seen, let alone photographed? Why should something that is so mysterious be simulated? There are several answers, three of which are given here in the context of the study of ball lightning.

First, the nature of ball lightning has thus far eluded the scientific community.

There are dozens of theories that range from simple combustion to nuclear fusion to antimatter meteorites. Using an existing model which describes the motion of ball lightning can be very valuable to the scientific community. If the implementation successfully describes the predicted motion, and if the results can be verified by eyewitnesses to the phenomenon, then a strong argument for the validity of the model has been made.

Second, ball lightning is such an uncommon phenomenon that many eyewitnesses don't even know what it is they are seeing, until they've read about it after the fact[130]. (See [3, §1(p), 2(a)] for well archived accounts.) For such cases it might be useful to first ask the eyewitness to describe the event, either with a personal letter or via questionnaire, and then present a video of a ball lightning in motion, to determine if what they saw was similar. Since no video footage of a ball lightning in motion exists, a computer simulation would be the next best thing. This would have the secondary benefit of validating (or invalidating) the model used in the simulation. If all eyewitnesses consistently agree that there is a flaw in the simulation, then the model needs to be updated.

Finally, a graphical representation of ball lightning would also be useful for the computer graphics industry. When animating suspenseful sequences in movies etc., a rare feature such as ball lightning would increase the drama of thunderstorms and foul weather. Artists could make use of such a phenomenon with their creative intent. Ball lightning has also been associated with aircrafts in flight[3]. Such a feature could be used in a flight simulator to test the response of a new pilot to an unexpected and mysterious event. Already, real-time renderings of foul weather are being attempted by members of the graphics community[38]. Eventually, a real time simulation of ball lightning may be possible.

Chapter 2

Ball Lightning Research

This chapter discusses some of the modern scientific models of ball lightning. The intent of this chapter is *not* to provide a detailed analysis of these scientific models, but to give an overview of the various theories that are being researched today. High level descriptions of some ball lightning models are provided along with the resulting characteristics that the ball lightning would possess.

The ultimate purpose of this thesis is to render an animation of ball lightning which has its roots in the physical world. Since there are several working theories which attempt to explain various characteristics of ball lightning, this can be a difficult task. Some theories well explain certain ball lightning characteristics, while completely ignoring other observed properties. The trend in ball lightning research is to attempt to create a model which explains as many of the ball lightning observations as possible[2]. Unfortunately, there is still no model which satisfactorily describes every observation.

An overview of the various types of ball lightning theories is provided in §2.1. A selection of the various pitfalls for ball lightning models is presented in the following section. Such a list is provided so that the models discussed in §2.5 can be analyzed. In order to appreciate some of the ball lightning models, some knowledge of plasma physics and typical lightning is required. These two topics will be discussed in §2.3

and §2.4 respectively.

When determining which ball lightning characteristics are important for the purpose of rendering an animation, there are two things to consider. First, invisible features such as magnetic fields and certain types of radiation will not affect the rendering of an image. These properties may however influence the shape and movement of a ball lightning and should be considered in a model which describes its motion; but they do not have an influence on the final colour attributes stored in the resulting image. They are only used to determine the position of the ball lightning.

Second, no one ball lightning model completely describes all the observed features of the phenomenon such that it can be considered to be positively correct. There may also be several “correct” models which describe various phenomena that are *categorized* as ball lightning. (See §1.1.4 for a brief discussion of *ball lightning as a category of phenomena*.) This makes choosing the model (or models) which will become the foundation of this work an important task that cannot be taken lightly.

Due to these two considerations, some properties of ball lightning are more important for computer graphics than others. Those properties that are important will be discussed in Chapter 4.

2.1 Overview of Ball Lightning Research

Ball lightning has been a topic of research for almost two centuries. Unfortunately there has been no widespread and systematic effort to formulate and test ball lightning theories. Only for the past 15 years has there been seven symposia dedicated to the study of ball lightning. This haphazard approach is probably due to the the obscurity of the phenomenon and the inability to make scientific measurements of ball lightning attributes. According to Singer[118], no attempt to measure the properties of ball lightning has been successful.

Even though ball lightning has been difficult to study, it has been acknowledged to

exist by several renowned scientists such as Arago, Faraday, Arrhenius, Kelvin, and Kapitsa[118]. When an individual proposed that ball lightning does not exist since the reported characteristics are so varied and inexplicable, Arago replied: “Where would we be if we decided to deny everything that we can’t explain[116, pg. 77]?”

Ball lightning papers can be categorized in many ways. Typically, a ball lightning paper will have one of the following foci.

1. It will be a publication of a new ball lightning observation.
2. It will propose a new ball lightning model. Usually such a paper will attempt to explain formation, long lifetime, and decay at a high level, however a complete theory is usually not developed.
3. It will refine or criticize a previous ball lightning model.
4. It will attempt to calculate some aspect of a ball lightning theory, such as the energy content of a ball lightning event.
5. It will provide an experimental validation of some aspect of a ball lightning model.
6. It will review previous efforts to explain the ball lightning phenomenon.

Of course one paper may touch on several of these aspects. One should expect that most ball lightning papers fit into type 3. Indeed this seems to be the case.

In §2.5 of this chapter, a few of the important ball lightning models (papers of type 2) will be discussed. Criticisms and refinements (type 3) and experimental validations (type 5) will be noted in some cases. Observational papers (type 1) and calculations (type 4) are cited as evidence. It is sometimes necessary to use review papers (type 6) to fill in missing details from hard to locate papers.

As stated above, ball lightning has interested scientists for centuries, though no focused effort has been made to come up with a solution. Up until the 1950’s occasional publishings were made, many of which were singleton efforts. In 1955 Kapitsa[71] developed a new and influential theory which described how ball lightning might be produced by an external energy source. This paper had two effects: first, it resurged interest in ball lightning research[64]; second, it created a continental divide between ball lightning researchers — those who favoured the concept of an external energy

source in nature, and those who believed that the entire energy content is stored within the lightning ball upon formation.

The aftermath of Kapitsa's paper resulted in a new enthusiasm for ball lightning study. Shortly after the anti-communist McCarthy era, but still during the cold war between the Eastern and Western countries, Ritchie published an article entitled "Reds May Use Lightning as Weapon" in the journal *Missiles and Rockets*[107]. This paper purports that Russian scientists were developing a mechanism to generate lightning balls which could be directed toward incoming missiles and aircraft. This certainly had some effect since it is not difficult to find papers that deal with ball lightning in the major Western scientific journals of the 1960's. This interest prompted the republishing of several key Russian ball lightning papers in book form[108].

During the the late 1960's and 70's, ball lightning ceased to be regarded as a weapon. Turner states that ball lightning has not been reproducible with any control or regularity[134], which perhaps has affected the funding of research projects. Nevertheless, the phenomenon is still being investigated and new ideas are being published in major journals. Occasionally, whole issues of a journal are dedicated to the phenomenon (such as *Physics Reports*[119][120] and *Philosophical Transactions*[2]) and there has been a special feature in *Nature*[66] on the topic.

Today there is little doubt to the existence of ball lightning, even though skepticism exists[68][110]. In the last 50 years the phenomenon has received mention in several books that deal with natural phenomena[28][70][87][105][110][136] and there are an incredible number of eyewitness reports (which includes several by members of the scientific community)[117][118]. The present author has had verbal communication with two ball lightning witnesses (one has even provided a written account [130]), and has heard of two more events through hearsay. Perhaps a future generation will indeed reveal the *true* nature of ball lightning.

2.2 Typical Pitfalls in Ball Lightning Theory

Physical models which attempt to explain the nature of ball lightning usually only focus on a subset of the observed ball lightning characteristics. In this sense the models are inadequate. This inadequacy arises because of the extremely varied observations of the phenomenon. Ball lightning has been seen indoors, outdoors, and aboard sealed aircraft. Sometimes it is seen falling from the sky; other times it is traveling horizontally along a road. Often it emits sparks and other times it does not. Ball lightning can decay with an explosion or disappear silently. There is evidence to suggest that some ball lightnings contain a great amount of energy, while other reports provided evidence to the contrary. The reported colours of ball lightning also vary, yet the colour of each ball lightning instance usually remains constant. With all these variations in the phenomenon, it is an extremely difficult undertaking for physicists to develop one model that provides a complete explanation.

Sometimes the unexplained characteristics are willed away as being inappropriate or due to other phenomena. This is not necessarily invalid since almost all ball lightning data come from chance observations. There have been attempts to set up apparatuses which will scientifically measure the characteristics of ball lightning, though none have been successful[118]. Therefore some anomalous and infrequently reported characteristics may be attributed to observational error.

Following is a list of ball lightning characteristics that have been reported on a number of occasions. A modern ball lightning theory should attempt to explain each of them. Any unexplained attribute could be considered a deficiency in the model. This list does not attempt to include every fault that could be found in a ball lightning model. Only characteristics which are commonly used to challenge the validity of ball lightning models are listed.

1. long lifetimes (several seconds)
2. preventing convection due to heat
3. stability in size, colour, intensity, etc. until decay

4. explosive *and* quiet decay
5. occasional vertical motion (usually downward)
6. horizontal motion (often in a straight line)
7. change of direction
8. potential risk of damage, injury, and death
9. presence in sealed containers such as houses and aircraft
10. trailing sparks on occasion
11. energy source
12. energy of some reports exceeds the virial theorem (explained on p. 26)
13. containment mechanism that is stable
14. decay of the containment mechanism
15. passage through window panes, without causing damage

Explaining the long lifetime (item 1) of ball lightning with a model is difficult. If ball lightning is composed of a plasma (see §2.3), then the lifetime should be about the about the same as that of a lightning channel, which is also composed of plasma. If ball lightning is composed of a burning filament, then how is the combustion of the fuel slowed down so that it has a lifetime of a few seconds or longer?

A problem with a some ball lightning models is convection (item 2). If a gaseous body is warmer than the surrounding atmosphere, it may have a lower density and convective forces will cause it to rise.

When a fuel is slowly exhausted it tends to change intensity and colour. When the interface between the atmosphere and a ball lightning erodes, the ball lightning should change shape. Yet these changes have only rarely been observed. Therefore the constant appearance of a ball lightning (item 3) can be difficult to explain.

Items 5, 6, and 7 should all be explained by a ball lightning theory. Ball lightning has been observed to move in all directions, though upward motion is by far the least common. It has also been observed to be motionless. Occasionally, ball lightning has been seen moving against the wind[17][21][117], though clear reports are difficult to find. A ball lightning theory is incomplete if it leaves any type of motion unaccounted for.

The type of decay (item 4) and the potential risks (item 8) from ball lightning

may be related points. Related to the decay are items 10, 13, and 14. Somehow the ball lightning must be contained for a length of time. There may possibly be a breakdown of the containment interface, which allows sparks to form. This, in turn may create an explosive or quite decay. Ball lightning theories need to address these issues so that all combinations of these parameters are addressed.

Ball lightning has also been observed inside sealed compartment aircraft (item 9). In these observations the ball is usually first seen in or near the cabin and slowly makes its way down the fuselage to the rear of the airplane where it disappears silently[69] or exits the aircraft[135]. Many ball lightning models do not account for such behaviour since they require that the lightning be formed outdoors and then enter through an opening.

The energy source of ball lightning is a big question (item 11). There are two basic categories of models: internal energy models where “fuel” is consumed; and external energy models where forces in the atmosphere provide the necessary energy to sustain the ball lightning.

The virial theorem limits the quantity of chemical potential energy that a ball lightning can contain. Many ball lightning reports are witness to extreme amounts of energy release. This energy can be estimated and has been found to exceed the limits of the virial theorem (item 12). Therefore these reports are false, the virial theorem is incorrect, or something else has been misunderstood.

Ball lightning has been reported to pass through glass window panes and other solid objects. Sometimes the ball lightning will damage the window, other times it will leave the window glass unscathed[60]. Some theories attempt to explain both types of passage through windows, while others ignore the possibility all together. Despite the eye-witness evidence, there has been some argument as to whether ball lightning does in fact pass through window glass[132][29][131][30][133].

2.3 Plasma

In order to understand many ball lightning theories, it is helpful to know a little bit about plasma physics. For a very good introductory book see *The Fourth State of Matter: An Introduction to Plasma Science* by S. Eliezer and Y. Eliezer[41]. Most of the information in this section was derived from their book.

Students in elementary school science classes learn the three states of matter. First (and coldest) is solid, then liquid, and finally gas. Plasma, not included in the three states, is often described as the fourth state of matter.

When atoms or molecules in the solid state are heated sufficiently (i.e. energy is added to the system), the bonds between the molecules begin to break down. When a sufficient number of molecules become free to move, the matter is said to be in the liquid state. With further application of energy, individual atoms or molecules are energetic enough to leave the liquid state and enter the gaseous state.

Up until this point the substance still keeps its chemical and electrical properties. It is electrically neutral. When more energy is added to the system ionization occurs and some negatively charged electrons are freed from the atoms, leaving the remainder of the atom with a positive charge. The positive remnant is called an ion. This mixture of free electrons and ions is called the plasma state. Despite losing some electrons, the nuclei of the atoms are unchanged and so they retain their chemical properties. Since the matter has changed from a volume of gaseous, neutral, atoms to a volume of charged particles, there is a change in the electrical and magnetic properties of the system.

Usually, only a small number electrons leave an atom. Since most of the electrons remain on the atom to balance out the positivity of the free nuclei, the entire system is *quasineutral*. An effect of quasineutrality is that free electrons and photons¹ can collide with the positive ions. When such a collision occurs an electron attached to

¹The concept of a photon was introduced by Albert Einstein in 1905. A photon is a particle with zero mass and charge. It moves at the speed of light and is one quantum (or unit) of radiant energy.

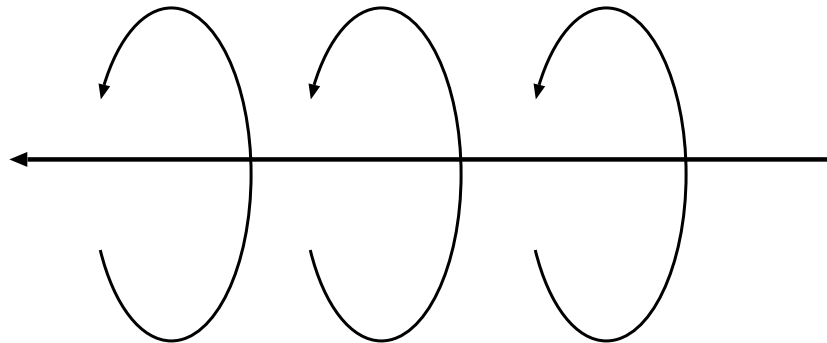


Figure 2.1: The direction of a magnetic field around a current in a wire.

the atom is raised to a higher energy level. An electron in a high energy level of an atom will tend to lose energy and fall to a lower level if there are no other electrons in the way. When this happens, it releases some energy in the form of a photon, which may be seen as visible light.

If ball lightning is in fact a free-floating plasmoid, then the luminosity is easily explained. There are unfortunately many other difficulties introduced in the ball lightning model if it is indeed based on a plasma structure.

One major problem with using plasmas in a ball lightning model is that positive ions and negative electrons tend to attract and recombine. In other words, plasma cools very quickly and will return to the gas state in less than a millisecond[125, pg. 184].

Another problem with using plasma in a ball lightning model is diffusion. Left uncontained in the atmosphere, a plasma will diffuse just as a perfume sprayed from a bottle would. Some models of ball lightning describe a containment mechanism that does not require the understanding of the properties of plasma, while other theories use the electromagnetic properties.

Plasmas are electrical in nature. The charged ions and electrons are in continual motion. With any electrical force there is also an associated magnetic force. For example, if a direct current is flowing through a wire then its magnetic field moves in

a circular motion around the wire. (See Figure 2.1.) Therefore plasmas are affected (and can potentially be contained) by electric and magnetic fields present during a thunderstorm.

Gas particles are typically neutral in charge. Therefore these free particles are very unlikely to collide with one another. When a gas enters the plasma state, the free electrons and ions are electrically charged. These electrically charged objects exert forces of attraction and repulsion on each other. Therefore their area of influence is much greater than the area of influence of a neutral atom. As such, plasma particles tend to oscillate collectively in an orderly manner. Since the positively charged ions are far more massive than the negative electrons, the ions have a much smaller frequency of motion than the electrons. Although the motion of electrons and ions is orderly, plasmas suffer from many instabilities, which renders the plasma into a state of disorder. Different instabilities are caused by different variations of the plasma properties, and have been given names such as “kink,” “sausage,” “banana,” and “ion-acoustic.” These instabilities are a fundamental aspect to many ball lightning plasma theories.

Using the basic laws of motion to statistically analyze the motion of the plasma particles, along with the electromagnetic properties of the plasma, physicists can model the motions of the particles and count their collision frequency. This is not a simple task since the electrical field of the ions and electrons has a much larger effect than geometric size. Also a large group of ions or electrons can *shield* one particle from other particles. Understanding the motion and electrical properties can lead to better models of confinement.

The only natural sources of plasma on Earth are lightning channels[136], aurorae[16] (better known as the Northern and Southern lights), and potentially ball lightnings. Man-made plasmas are more common. They are visible in neon signs and electric arcs. Although plasmas may not be common on our planet, more than 99% of the universe is in the plasma state. The sun, for example, is an ellipsoidal mass of plasma.

2.4 Lightning

In order to understand many ball lightning theories it is essential to have a working knowledge of other forms of lightning. Uman[136] has provided an excellent summary of lightning research, which is the primary resource for this section.

Lightning is a awesome force which has thrilled and terrified people all throughout history. Its powerful force has had an impact on religion and mythology. Jove (or Jupiter) used “thunderbolts” as retribution, and to warn against bad behaviour. A clap of thunder is still used this way in modern drama as an audible clue. The fierce god of the Norsemen, Thor, produced lightning as his hammer struck an anvil. Thunder was believed to be the sound of his chariot. Church bells in Europe were sometimes inscribed with the saying “Fulgura Frango” (I break up lightning). During storms the bells were rung to chase away the storm. This sometimes led to the unfortunate death of the bell ringers.

A lightning stroke sends a considerable amount of electrical charge to the ground, which at times have caused great damage. Often churches were stuck since they were built at the highest point in a town and were usually the tallest building. In the 18th century it was common to store munitions in church vaults. In 1769, the church St. Nazaire in Brescia Italy was storing gunpowder when its steeple was struck. One sixth of the city was destroyed and 3000 people were killed. Ships were also struck often due to their high masts. The British ship *Resistance* was destroyed by a lightning stroke in 1798. As Uman points out, the name of the ship was “an unwary symbol of its electrical susceptibility.” Franklin had suggested that the lightning rod be used to prevent such destruction in 1749. The news of this discovery was unfortunately slow to be spread. Preventing damage to aircraft, spacecraft, and sensitive ground-based electronics has motivated lightning research since the 1970’s.

Lightning usually comes from cumulonimbus clouds. Cumulonimbus clouds are very large and have a impressive vertical dimension. The charge distribution of a cumulonimbus cloud is divided into three regions: The **N**, **P**, and **p**. regions. (See

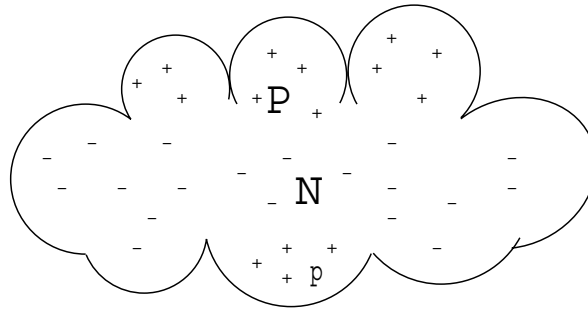


Figure 2.2: Charge distribution within a cumulonimbus cloud. The P-region contains a highly positive charge; the N-region contains a highly negative charge; and the p-region contains a small positive charge.

Figure 2.2.) Typically, the P-region contains about 40 Coulombs (C) of charge and is approximately 10 km above the Earth's surface. The N-region is about 5 km high, and contains about -40 C of charge. The p-region is about 2 km high and contains only 10 C of charge.² The charge in the N-region of the cloud is not uniformly distributed. There are localized pockets of high space-charge concentrations.

Most strokes occur within the cloud itself. These strokes transfer charge from region to region. Most often these stroke can not be viewed directly since they are within the cloud itself. The visual effect is an illumination of the cloud which is called *heat lightning* or *sheet lightning*. Sometimes the stroke travels along the edge of the cloud and hence is visible as a stroke in the sky. This type of lightning is very difficult for experts to study, though understanding it is important for aircraft safety and some ball lightning models.

The most rare type of cumulonimbus lightning stroke is a cloud-to-cloud discharge. These strokes can be many kilometers long and they transfer charge from one cloud to another. They are even more difficult to study because of their relative rarity.

The most dangerous and most studied type of lightning is that which connects a

²These approximations come from South African data where the ground is 1.8 km above sea level.

cloud with the ground. These can be divided up into four sub-categories:

1. negative charge lowered
2. positive charge lowered
3. negative charge raised
4. positive charge raised

Types 1 and 2 are often called cloud-to-ground (CG) lightning. They are initiated within the cloud and the majority of the charge is lowered to Earth. Types 3 and 4 are sometimes called ground-to-cloud lightning. They are usually initiated atop tall man-made structures or mountain peaks. They are relatively rare. Often in literature the distinction is not made between cloud-to-ground and ground-to-cloud lightning. This work will attempt to keep the distinction.

More than 90% of lightning strokes are negative cloud-to-ground strokes (type 1). Less than 10% of strokes lower positive charge (type 2). The physical processes of a lightning stroke are very complicated and not fully understood. Therefore the statement “negative charge is lowered” means that overall, the *effective* result is a lowering of negative charge.

At this point, some terminology must be clarified. A *flash* of lightning is defined to be the entire event. A flash of the common type 1 CG lightning will last for about a half a second. This flash of lightning is usually made up of several distinct *strokes*. A stroke of lightning typically lasts 1 ms. The pause between strokes is on the order of several tens of milliseconds.

The complete process of a typical CG lightning flash is as such. Once sufficient charge is built up within the cloud electrical breakdown of the air will occur and a *stepped leader* will advance toward the Earth. This electrical breakdown is indeed “stepped.” Leader steps usually advance for one microsecond and have a pause of 50 μ s between them. They can be from 10–200 m in length. As this negatively charged leader approaches the Earth, it induces a charge equidistant below the Earth’s surface. (The Earth’s surface resembles an electrical mirror.) Once the leader is sufficiently

close to the Earth, positive streamers start to form from protruding objects. These positive *streamers* move upward toward the negative *leader*. Once a positive streamer connects with the negative leader, the circuit is complete, and a single *return stroke* occurs, and it is believed that one of the localized pockets of negative charge in the N-region of the cloud is neutralized. Return strokes have a speed of approximately 10^8 m/s. Peak temperature occurs within the first $10 \mu\text{s}$ and is approximately 30,000 K. After only $20 \mu\text{s}$, the temperature has been cut down by a factor of two thirds to 20,000 K. Compare the peak temperature to the surface of the sun, which is 5800 K[72]. The average electron density over the first $5 \mu\text{s}$ of the stroke is 10^{18} per cm^3 . The average pressure for this duration is 8 atmospheres. Photographic evidence and investigations of physical damage suggests that the lightning channel radius is between 1.5 and 11.5 cm.

Some 50 ms after the first stroke, another pocket of negative charge initiates a leader. Since there already exists a partially ionized channel to the Earth, it is relatively easy for the new leader to progress downward. Thus, this second leader is called a *dart leader*. Once the dart leader makes contact, a second return stroke will occur and another pocket of charge is neutralized in the N-region of the cloud. The dart leader return stroke process repeats several times until a sufficient amount of charge is lowered in the cloud so that a new leader is not formed and the channel is destroyed through recombination of the ions and diffusion accelerated by wind.

Sometimes, a strong wind will blow the partially ionized remnant of a stroke. If the channel remains intact long enough for several strokes despite the strong wind, then the lightning flash may look like a ribbon to an observer. This is commonly called *ribbon lightning* and is rather rare.

Sometimes a stroke will transfer current for an unusually long time. This is called continuous current. A flash with at least one long continuing current stroke is called a *hybrid flash*. Flashes with continuous current strokes cause the most damage because of the prolonged heating.

Positive CG lightning is very similar to what has just been described, except that the P-region of the cloud is neutralized. Geographical locations with high elevations, or extreme latitudes experience a higher ratio of positive to negative CG lightning. This is because the freezing point in the atmosphere is closer to the Earth and hence the P-region is also closer to the ground. Also, heavy winds can distort the cloud so that the N-region is on the windward side of the cloud and hence no longer below the P-region. Thus leaders can progress from the P-region to the ground, without having to pass through the N-region. Positive lightning commonly occurs at the end of a storm when the N-region has been largely neutralized and hence provides little shielding.

Positive CG lightning is interesting because the flashes can be much more powerful than negative lightning. The electric fields from positive CG lightning are two times stronger than that of the negative counterpart. More charge is transferred and long continuing current is common. The continuing current is one order of magnitude greater than that which occurs with negative lightning. Finally, there is usually only one powerful return stroke for positive lightning, as opposed to several weaker return strokes associated with negative lightning.

With upward lightning (ground-to-cloud) a positive or negative stepped leader moves upward toward the sky from the top of a high mountain, tall building, or radio tower. They are often preceded by a cloud discharge which provides the electric fields needed to initiate the leader. The visual distinction is that the forks of the lightning (if any) are in an upward direction. Subsequent dart leaders usually move downward as they would with downward cloud-to-ground lightning, and the second and later return strokes are the same as they would be with cloud-to-ground lightning.

This type of lightning can be initiated with a model rocket that carries a grounding wire upward. An interesting point for ball lightning theory is that *beaded decay* has been observed with this type of lightning initiation — especially when there has been a long duration of continuing current. For a discussion on bead lightning, see §1.1.3.

2.5 Ball Lightning Models

Theoretical ball lightning models are discussed in this section. It is important to recall that Kapitsa[71] suggested that ball lightning's long lifetime is provided by an external energy source. Most external energy source models are a derivative of this influential paper and are grouped together in §2.5.1 in this discussion. The most difficult point for these models is to demonstrate that the energy source exists, and is consistent.

The subsequent section discusses the model of ball lightning where the fundamental structure is a fine, particulate, *skeleton*. Particulate matter is formed when a flash of lightning strikes soil or an object. This model has a completely contained energy source which is consumed slowly. A common difficulty with these models is explaining how the consumption of the fuel is contained and retarded so that the phenomenon will last for several seconds.

The next subsection describes some models that suggest the containment mechanism is a vortex. Countering convective forces is often a challenge for this approach. Also, entrapment of the fuel source needs to be explained.

Finally, in §2.5.4 some very unique models are briefly examined.

2.5.1 External Energy Source Models

In 1955 Kapitsa authored a paper[71] which described at a high level how ball lightning could be powered by an external energy source. This paper was very influential and divided ball lightning research into two primary categories: internal and external energy sources.

Kapitsa argues against internal energy models after a simple calculation of an nuclear explosion. He reasons that the largest possible amount of electromagnetic radiation would be emitted from such a blast. Since a 150 m diameter nuclear cloud is completely radiated in less than 10 seconds, a 10 cm ball lightning would only last

0.01 seconds at most. Henceforth an internal energy source model of ball lightning must contradict the first law of thermodynamics³.

(There is an argument in response to Kapitsa's reasoning. The material involved in the nuclear reaction may disperse because of the violence of the nuclear reaction; whereas with ball lightning fuel dissipates via exhaustion or recombination. A stabilizing or confining mechanism could therefore further increase the life of a lightning ball. Some ball lightning observers report that the internal structure seems to rotate, which provides some evidence for this argument[115].)

Kapitsa reasons that thunderstorms must produce intense radio waves which provide a power source for ball lightning. Initially, there must be a very small, weakly ionized, ball of plasma at the formation site. Radiation reflects off the Earth's surface and creates a series of nodes and anti-nodes — similar to the nodes and anti-nodes created in the wave-pool experiments that are performed at the highschool level of education. If this small ball of plasma is located at the one of these interference anti-nodes, then the intensified electromagnetic radiation will act as a power source and grow the ball lightning. The ball lightning's diameter increases due to the increase of kinetic energy of the plasma, which in turn increases the pressure.

The period of the oscillations of the plasma (see §2.3) must coincide with the radiation being absorbed. Resonance characteristics of highly ionized plasmas which emit visible radiation are determined by their geometric properties. Kapitsa provides the following formula for a sphere:

$$\lambda = 3.65d \tag{2.1}$$

where λ is the radiation wavelength and d is the diameter of the sphere. The units are both a linear measurement of length.

Therefore, the absorption process is eventually balanced by the geometric dimen-

³The law of conservation of energy.

sion of the ball lightning. For when the diameter of the ball lightning increases too much, the oscillations of the plasma will not coincide with the oscillations of the power source, and hence the radiation will no longer be able to power the plasma. Thus the ball lightning reaches a stable size.

Equation 2.1 enables us to predict the wavelength necessary for typical ball lightning observations. Kapitsa calculates that ball lightnings in the range of 10–20 cm require electromagnetic radiation wavelengths of 35–70 cm, which is in the radio wave frequency range.

With this theory, Kapitsa is able to explain the motion of ball lightning against wind, etc., since the ball will follow the anti-node of the standing wave. This also explains the lack of convection and suggests how ball lightning would enter a building. He is able to explain both decay types with the decay of the energy source. A suddenly terminated energy source will cause the ball lightning plasma to recombine quickly which will generate a shock wave. An energy source which extinguishes slowly would create a silently decaying ball lightning. One item *not* explained is the source of the radiation within the electrical storm.

Shortly after Kapitsa's paper, Kogan-Beletskii[76] applied the theory to explain how ball lightning could form outside of an aircraft, and potentially follow the outside surface of the aircraft. Kogan-Beletskii provides some evidence for his results by relating two eyewitness accounts of aircraft being struck by ball lightning. In one of these accounts there was reported damage.

Kapitsa's paper[71] was a high-level description of a *new* mechanism which could produce a ball lightning event. It proposed an avenue of research which propelled a resurgence in the understanding of the ball lightning phenomenon. It *did not* provide sufficient detail to either accept or dismiss the idea.

Shafranov[111][112] was quick to support Kapitsa's work with some more detailed theory concerning plasmas in magnetic fields. He studied the equilibrium configurations for such conditions by taking into account gravitational forces, external pressures

from surrounding gasses, and the external magnetic fields. Ladikov[79] added even more detail to this work. Yankov[145][146] also provided some theory to support the external energy source paradigm. He investigated how small perturbations[145] and oscillations[146] would affect the stability a homogenous plasma sphere.

Watson[137] was also quick to support the external energy source model. He endorses Kapitsa by attempting to show how a polarized electromagnetic standing wave can provide a containment mechanism for charged particles in the neighbourhood of the electric nodes. Near such nodes there is high ionization due to electron collisions which set up an electron avalanche pattern. Surface absorption causes the lightning to have a spherical shape because it has a minimum surface area to volume ratio. Watson provides some more detailed calculations for the ball lightning formation which provided similar results for the expected wavelength. His theory differs from Kapitsa's in that he suggests that ball lightning would form at the node, as opposed to the anti-node of the standing wave.

Silberg[114] also considered Kapitsa's theory in more detail. He calls the electromagnetic energy source model "interesting but somewhat controversial." He agrees that much more work is necessary in order to validate it. Silberg argues that a continuous radio frequency field would not create the necessary interference for Kapitsa's model. He also notes that it has never been proven that either inter- or intra-cloud discharges produce the discrete radiation fields necessary to produce ball lightning, but there is some evidence that they exist.

There have also been several experiments which give credit to the feasibility of the external energy source model. Babat[13] had already performed some electrodeless discharge experiments before Kapitsa's model was published. He found that in some of his experiments a "greenish milky mist" persisted for several seconds after the power was turned off. Hamilton[61] used pulsed microwave discharges to create luminous bodies at lower pressures. More recently, Ohtsuki and Ofuruton[92] produced fireballs with microwave interference. They claimed to be able to direct the balls to move

against air currents and through walls intact.

Of course, not everyone agrees with the prospect of external energy models. In 1960, Lewi Tonks[129] criticized Kapitsa's work. He discusses some of the difficulties of his theory. For example, Tonks claims that ball lightning should form at a node (which is agreement with Watson[137]), but that it would persist at an anti-node. Therefore there must be a shift in its placement along the electromagnetic field interference patterns. He also suggests that the power required to maintain a ball lightning in this state is too high to be found in nature. Overall, Tonks seems to have the opinion that even if ball lightning can be reproduced in a laboratory with an external energy source, it would still be difficult for Nature to create the phenomenon.

In 1970, Powell and Finkelstein[98][65] argued that the radio frequencies required by Kapitsa's theory don't exist in nature. On the other hand, direct current (dc) fields of 1000 V/cm do exist, and these could power a ball lightning. They suggest that the phenomenon is either a remnant of a lightning stroke (either cloud-to-ground or intra-cloud) or that it begins as an occurrence of St. Elmo's Fire. Without the external dc field, the lifetime would be short (approximates 0.5 seconds for a lightning stroke remnant; or the typical duration of a St. Elmo's fire). If by chance, this remnant sphere of plasma were to form inside a $1000 - 2000\text{ V/cm}$ dc field, then the lifetime would be extended — or an instance of St. Elmo's Fire could escape its electrical ground. Powell and Finkelstein argue that if the dc field is directed downward, then this force would counteract buoyancy. With this model, they are able to explain how ball lightning would pass through glass without damaging it, how it would enter buildings, and how it would be attracted to electrical conductors. They fail to explain extended lifetimes within aircraft since any dc power source would be shielded.

A more modern external energy source model was proposed by Rañada and Trueba[101]. They do not cite Kapitsa's paper directly, but they do suggest that an electromagnetic knot may be the the source for a ball lightning event. An electromagnetic knot is an electromagnetic field where a pair of magnetic lines (or electric

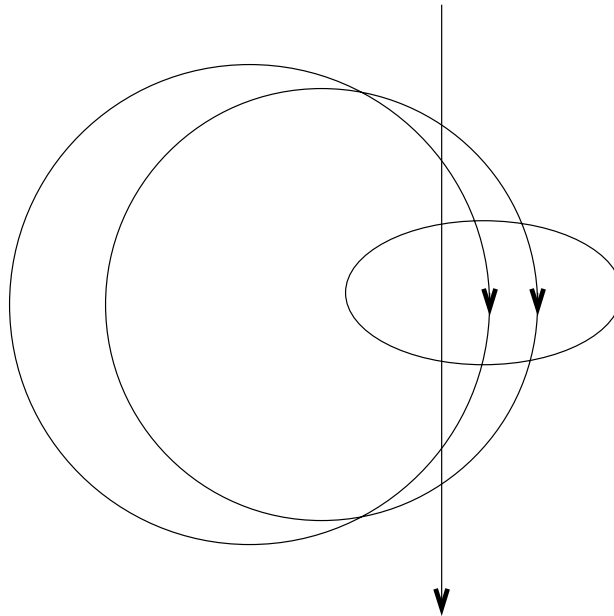


Figure 2.3: Schematic representation of magnetic field lines which form an electromagnetic knot. Redrawn from Rañada and Trueba 1996[101].

lines) form a pair of linked curves. (See Figure 2.3.) They assume infinite conductivity in their calculations which requires a temperature of at least 30,000 K, which is not an unreasonable temperature for a lightning channel. (See §2.4.)

2.5.2 Erosion Discharge and Particulate Models

Hill[64] did not think that the material composition of ball lightning was sufficiently ionized to become a plasma, since a pure plasma would recombine within one millisecond. If ball lightning was a plasma, then it would require an external energy source. This mechanism is feasible, but unnecessarily complicated. Instead, Hill believes that ball lightning is just a highly ionized gas *in molecular form* with relatively *few free electrons*. Molecular recombination is more slow than plasma recombination. He also suggested that impurities such as dust, water vapour, and combustible gasses may be necessary for the formation of ball lightning. Such impurities would sufficiently

complicate the mechanism to make it very difficult to reproduce.

Andrianov and Sinitsyn[5] developed the impurity model further. They suggest that ball lightning could be related to the fulgurite formation process. Fulgurites are formed when a typical cloud-to-ground lightning flash strikes sand. The sand in the discharge path of the charge is heated to an intensity great enough to cause the sand to fuse into a glass-like structure. The structure resembles a hollow tube a few centimeters in diameter and up to 2.5 m in length. Andrianov and Sinitsyn suggest that the extreme pressures in the fulgurite vessel force an expulsion of material which contains particulate matter from the fulgurite cavity walls. They developed an experiment to simulate such cavity walls, since reproducing fulgurites requires a strong discharge which tends to blow away the sand in the laboratory environment. They managed to create glowing balls and rings which lasted approximately 100 times the expected recombination rate of plasma, but still for only a few milliseconds.

Several papers have been published that describe how various sub-micron sized filament particles can model ball lightning. Aleksandrov et al.[6] describe how such particles can form an aerosol⁴ structure, which can be reproduced in the lab. Such structures cannot be seen since the particle diameters are smaller than the wavelength of visible light. Formation of the spherical shape may be due to atmospheric electrical fields. The structures themselves are very stable and have been maintained in labs for long durations. Since the density is similar to that of air, this model can avoid convective problems. A satisfactory explanation of the illumination escapes Aleksandrov et al., but several ideas are considered.

Smirnov considered combustible fractal structures similar to those formed from a lit candle as a candidate for ball lightning illumination[119][120][121]. A rigid skeleton would form as a tangle of interwoven fractal fibers, of nanometer size. Such a structure provides an explanation for several ball lightning properties.

The personal experience of Graham K. Hubler is documented in his 2000 news

⁴The dictionary definition of an aerosol is any suspension of fine solid or liquid particles in gas.

column[66]. He gives credit to the ball lightning model proposed by Abrahamson and Dinniss[4] for their ability to describe his experience with theory. Abrahamson and Dinniss proposed another nanoparticle model where oxidation reactions are the source of illumination. They credit the previous work with fulgurites[5] for the mechanism to form ball lightning, but they formalize the chemical processes involved differently. They believe that silicon metal (and other silicon-based compounds found in soil) are the key to explaining the oxidation reactions. They would form an aerogel⁵ which oxidizes slowly and lasts for the lifetime of a ball lightning. Abrahamson and Dinniss have simulated a lightning stroke on various types of soil and have found that nanometer-sized particles were in fact created. A transmission electron micrograph (TEM) of their results shows that these nanoparticles accumulate into chains. With this model they can explain many ball lightning properties. They even include a proposal to explain the passing of ball lightning through window panes. They can explain how this would either cause damage or would not cause damage. There are several ball lightning properties that they openly admit they can't explain. For example, the model doesn't include a solution for ball lightnings formed in the atmosphere or in airplanes. Some of these missing details have been addressed in Abrahamson's further work[1][26]. As with most ball lightning models, there is still work to do.

The last model to discuss for this section is the polymer-composite variant[27]. This model attempts to account for a very high energy density. The energy density of ball lightning is a much disputed factor. Estimations of energy content based on qualitative reports sometimes result with ball lightning having very high energy concentrations. (See [26] and [147] for examples.) While Abrahamson says the calculations should be performed with a particular model in mind[26], the polymer-composite[27] model tries to account for potentially high energy in general.

The polymer-composite model assumes that ball lightning is a tangle of polymer-

⁵An aerogel is a silicon-based material, that is mostly empty space.

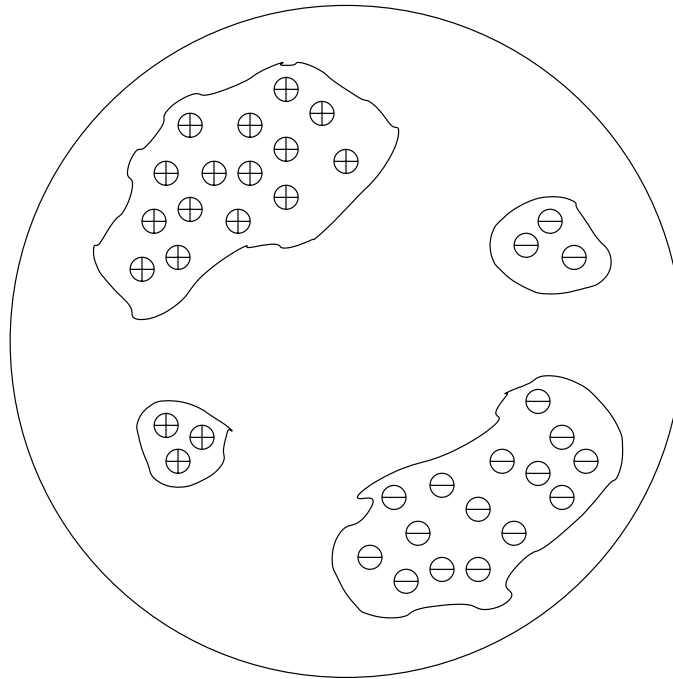


Figure 2.4: Model of polymer-composite ball lightning charge distribution. The distances between the charge regions are greater than the sizes of the charge regions themselves. Redrawn from V. L. Bychkov 2002[27]

dielectric⁶ threads with regions that are positively and negatively charged. (See Figure 2.4.) The key to this model is that the distances between the charged regions is greater than the size of the regions themselves. This allows for a high energy concentration. The polymers in this model eventually form a fractal structure similar to Smirnov's[121]. They are not necessarily linked to each other, so that the ball lightning can pass through screen doors without causing damage. Bychkov has also performed erosion discharge experiments to validate his model. He has been able to produce luminous objects with a long life that can penetrate through small holes and damage electric films.

⁶I.e. insulating.

2.5.3 Lightning Impact Models and Vortex Containment

One of the earliest ball lightning models is the impact model. Since ball lightning is associated with storms and electrical activity, it is only natural to predict that it forms as a direct consequence of a cloud-to-ground lightning stroke. Such is the case with W. M. Thorton's 1911 paper "On Thunderbolts"[128]. Thorton believes that on occasion there is not quite enough charge remaining in a cloud after a "flash" of lightning to create a second "flash." (It is the belief of this author that what Thorton calls a "flash" would be properly called a "stroke" in modern day, as per §2.4 of this work.) Ionization will occur "on a great scale" within the cloud and ozone will be formed. If this is localized, then it will form into the shape of a ball. It's luminosity comes from the same source as St. Elmo's fire (see §1.1.3) and it will fall from the cloud since ozone is more dense than the atmospheric gasses. When it reaches the ground it may have a like charge similar to that induced by the thundercloud on Earth. Hence it will remain buoyant and seem to move freely.

Wooding[144] also believes that ball lightning is formed by the impact of a cloud-to-ground stroke. He suggests that a ball lightning is a plasma vortex ring and is formed in a similar manner as a smoke ring. It would be formed in the rare occurrence that a CG stroke impacts with a solid object that has an aperture, such as a chimney. Several ball lightning properties are explained, but plasma recombination rates could be considered a problem.

Bruce[25] suggests that ball lightning is not formed directly from an impact of a CG lightning stroke with a solid object, but that a hole is pierced at a "joint" in the channel where it changes direction. An instability like this that has a 1 cm diameter would easily eject several liters of plasma that could easily fill a lightning ball. Some 10^3 – 10^4 J of energy would be stored in a lightning ball with a diameter of 10 cm. This theory would explain both ball lightning events, and bright points of luminosity that have been photographed during the stepped leader propagation phase of a CG stroke.

Endean[42] disagrees with the idea that ball lightning is a trapped plasma. Instead he suggests that it is electromagnetic radiation that has been trapped and contained by an ionized sheath in the form of a vacuated sphere. The formation process of a rod-shaped (i.e. cylindrical) ball lightning is as such:

1. A stepped leader descends in the normal fashion of a CG stroke.
2. A positive streamer charge attempts to greet the negative leader in the usual way.
3. A misalignment occurs and a rotating dipolar mass of charge is created.

In order for the charges to remain separated, the “peripheral speed of the . . . rotating field pattern” should be greater than the speed of light, which he says is “quite possible” since individual charged particles need not exceed light-speed. Endean argues that the principles behind the spherical case are the same, except that an extra velocity is required.

Though the idea of ball lightning forming from a lightning stroke is certainly one of the older theories, it is certainly not dead. In 1969 Lowke et al.[86] performed some calculations to determine the feasibility of such models, and abstractly consider ball lightning events that are initiated from a lightning stroke. Lowke et al. imagine that the formation would resemble a sphere of heated air with various chemical compositions. They propose three models and test them with calculations for validity. These models are:

1. cooling spheres of air
2. cooling spheres of air containing sodium vapour
3. cooling spheres of mixtures that are:
 - (i) 7/8 carbon vapour and 1/8 air
 - (ii) 3/4 copper vapour and 1/4 air

Lowke et al. showed that models 1 and 2 should rise because of convection, and as such, were not good candidates for ball lightning. Model 3 should not rise, but

there is insufficient light emission. They suspect that the model may still be feasible if other, unconsidered, chemical reactions emit visible light. One interesting point regarding the carbon vapour variant of model 3 is that they predict it will have a “shell” structure, which is not uncommonly reported by ball lightning witnesses. Lowke et al. don’t consider the external energy source models (discussed in §2.5.1) to be of value, since there is no evidence that such energy sources exist.

In 1986, Karl Nickel[91] proposed another model where ball lightning is produced directly by the result of a lightning stroke. He presents the argument that ball lightning may be related to the slightly less rare phenomenon, bead lightning. (See §1.1.3 for a description of bead lightning.) Contrary to Wooding’s work[144], Nickel suggests that the discharge of a lightning stroke creates a very fast jet of air which strikes the solid earth. This jet of air plumes and on occasion forms a vortex structure. He has experimented with ring-shaped vortices called Hill vortices and has shown that they can contain charged particles that are completely separated from the outside air with an interface. A spherical Hill vortex could perhaps be a configuration of fluid flow that is associated with ball and bead lightning. Nickel suggests the luminosity of ball lightning is due to a localized:

1. burning of combustible gases; or
2. heating process of vapourized materials; or
3. excitation of air molecules leading to energy storage.

All of which can be confined by the interface of a vortex.

2.5.4 Other Models

There have been many theories proposed to explain the nature of ball lightning. In the previous subsections some of the most popular and actively researched theories were discussed. Here, a few singleton, yet viable theories are described.

One idea[90][46] suggests that quantum mechanical exchange forces could be used

to explain ball lightning. Neugebauer[90] computes that if the density of electrons is about the same as the number of molecules of air per volume, then cohesion can be explained. This theory does suggest that ball lightning forms upon lightning impact, but its focus is upon the plasma recombination calculations. He suggests that the recombination process is slowed because of its high temperature and also because the electrons are held together by exchange forces. A recent publication[51] suggests that cohesion can be explained with *photon exchange forces*. Experimental data from plasmas that are formed as a result from detonating explosives are compared with the ball lightning phenomenon.

A thermonuclear model has been proposed by Dauvillier[35]. He reports that previous experiments with thermonuclear reactions produced oscillating plasmas. He postulates that the same nuclear reactions may occur in lightning strokes of high intensity. The result may be a stable reaction that is the source of the ball lightning phenomenon. Altschuler et al.[7] took the stance that certain high-energy ball lightning events could not be explained through contemporary ball lightning theories. They also proposed a mechanism by which a self-contained nuclear reaction could be triggered by a lightning stroke. Although they admit there are many difficulties with their proposed model, Altschuler et al. suggest that the nuclear model could be validated experimentally. These experiments were performed by Ashby and Whitehead[12] for a period of about 12 months. Four spikes in radiation were observed as predicted by the Altschuler model, but these intense radiation periods could not be correlated with storm activity. Ashby and Whitehead incorporated the concept of antimatter meteorites into their theory of ball lightning formation.

A maser-caviton model of ball lightning was proposed by Handel and Leitner[62]. In the words of Handel and Leitner, “the plasma caviton is a localized nonlinear quasi-stationary electric field and plasma configuration in oscillation, also described as soliton.” They propose that an atmospheric maser⁷ is the energy source for such

⁷A maser is a coherent beam of microwave energy similar to a laser.

a plasma caviton. Many ball lightning properties can be explained with their model. They cite Ohtsuki and Ofuruton's experiments[92] as evidence to back up their theory.

An interesting idea was presented by Lowke where ball lightning is a corona discharge that follows the motion of current slightly below the Earth's surface[85]. Close to where lightning strikes soil charge moves quickly through air, fulgurites, etc.. Far from the lightning stroke charge moves slowly through various mediums such as water and soil. The motion of charge creates an electric field which supplies the power and directs the motion of the ball. This theory could only explain ball lightnings which form and decay quietly near Earth, and tend to move horizontally.

It is possible that ball lightning can be produced by several different mechanisms which give rise to the same manifestation. This is certainly the belief of Golka, who claims to have explained the submarine variant of ball lightning[57]. He is able to routinely reproduce a ball lightning like phenomena which has been reported in submarines and on aluminum-skinned aircraft. The ball lightning he creates consists of a liquid metal core that is surrounded by a metal vapour boundary layer. They last from 2–5 seconds and are about 6 mm in diameter. They are created by short-circuiting alternating currents of 1200 amperes across copper and aluminum electrodes. They can be produced under water or in the air, though the underwater variant is more safe to observe.

Chapter 3

Simulating Phenomena

Roughly speaking, the field of computer graphics can be subdivided into two sub-fields. These are rendering and modelling. There are many volumes of work dedicated to both of these areas, and both can be divided into more and more detailed categories.

Two rendering techniques were used to produce the results in this work. These are *raytracing* and *splatting*. Raytracing was briefly introduced in Chapter 1. It is a computationally expensive technique which is used to generate high quality images. Splatting is just one technique used in the discipline of *volume rendering*. Volume rendering attempts to render a scene that is created from volumetric data. Another rendering technique uses hardware to project basic primitives onto a screen. (This was briefly discussed in comparison to raytracing in §1.2.) While most techniques strive to achieve realistic images, other researchers concentrate on non-photorealistic rendering techniques.

Modelling is another diverse category. *Geometric modelling* is a very mathematical field which investigates the properties of curves, surfaces, and many other mathematical objects. Geometric modelling has applications in manufacturing and computer-aided design[43], as well as in the more creative and artistic endeavors of computer graphics. Much of the modelling research attempts to reproduce the visual quality of our everyday surroundings. Light sources, shadows, surface materials,

natural phenomena, etc. can all be modelled.

The intent of this chapter is to introduce the computer graphics concepts that are necessary to model and render realistic images of ball lightning. Since visual realism is a primary concern a more classical approach to producing images has been taken. Therefore, in §3.1 of this chapter an elaboration of the raytracing technique will be provided. Splatting is also important to this work and will be discussed in §3.2.

Various natural phenomena have been modelled with some degree of success. Some of these will be examined in at the end of this chapter, in order to detail some of the various approaches that have been used to model phenomena.

3.1 Basic Ray Tracing

Many graphics texts discuss raytracing at length[63][138], and some are completely dedicated to the subject[113]. The basic raytracing algorithm (raytracer) is very simple. There are three concepts to simulate when raytracing a scene: (a) light sources; (b) a camera; and (c) the scene itself. Each of these three concepts have been researched extensively since the first raytracers were produced.

The most simple camera to simulate is a pinhole camera. (See Figure 3.1.) The image formed by a pinhole camera is projected through the pinhole, so it appears upside-down and inverted horizontally on the screen. Usually, when a raytracer is implemented, the eye point is located at the pinhole, and the screen is placed at an arbitrary point between the eye and the scene without any loss of generality. In this way, the scene is rendered without being inverted.

There are many types of light sources that can be simulated. One of the more simple types, which yields satisfactory results, is a point light source. A point light source emanates an equal intensity of light in all directions. Usually, point light sources are specified as a location and an intensity. Sometimes the intensity is specified with red, green, and blue components, in order to simulate a coloured light source.

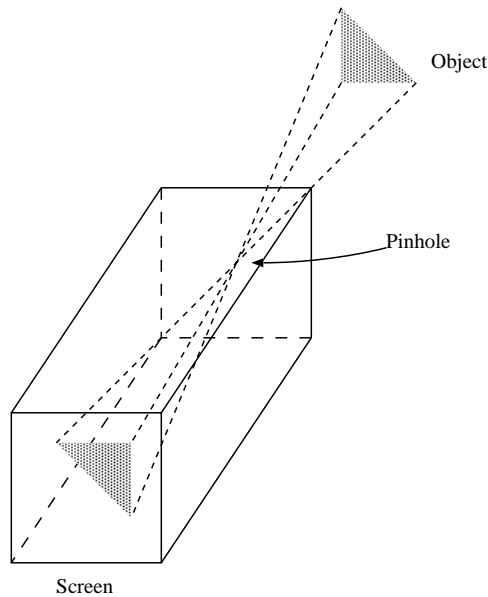


Figure 3.1: A pinhole camera.

A simple scene can be created from basic geometric primitives. For example: boxes, spheres, triangles, other polygons, etc.. More complicated surfaces such as Bézier patches are often implemented as well. Usually, complicated scenes are modelled with a separate software component that outputs the scene to be rendered with the raytracer.

The raytracing method makes use of these three devices to create an image. Algorithm 1 describes the basic process, and Figure 3.2 provides a visual representation.

The principle desire of raytracing is to accurately simulate the complex interaction of light with the environment and its projection onto camera film. Goldstein & Nagel[56] were the two pioneers to suggest that photorealism can be achieved. They explained that the brute-force method of tracing rays through a scene from each light source until a sufficient number of rays struck the screen (or film) of the camera would be inefficient. To decrease the number of rays required they reversed the process so that *primary* rays are directed from the eye-point through the location of the screen to be sampled. (See Figure 3.2.) If an object in the screen is struck, then *secondary*

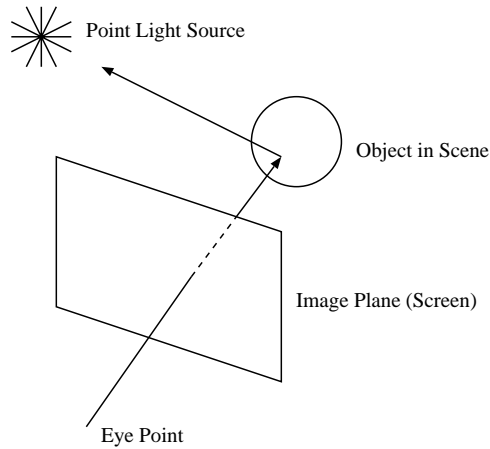


Figure 3.2: The basic raytracing method. A ray is cast from the eye point through the pixel location to be shaded. The sphere is struck. A colour for the sphere is determined using its properties and the light source. The pixel is shaded.

rays are directed from the intersection point to each light source to determine if the object lies in shadow. Shading calculations make use of the surface normal and the user-defined material properties of the object to compute the final colour to be stored at the location of the screen being sampled.

Algorithm 1 The basic raytracing algorithm

- Step 1.** For each pixel (i, j) in the output image.
 - Step 2.** Create a ray with origin **eye** and direction $(\mathbf{pixel} - \mathbf{eye})$
 - Step 3.** Intersect the ray with the scene, and store struck objects in a list.
 - Step 4.** Compute the colour of the closest struck object and assign pixel (i, j) .
 - Step 5.** Iterate.
-

The screen being intersected is divided into (usually) square pixels. In Step 1 of Algorithm 1, each pixel is iterated over yielding an $\mathbf{O}(n^2)$ algorithm with respect to sampling.

A ray is created in Step 2. The eye-point is the ray origin. To compute the

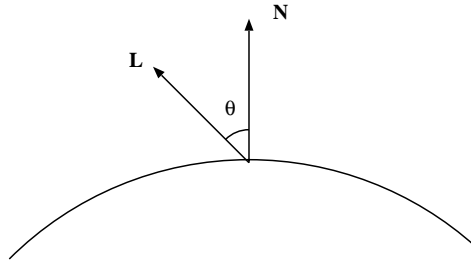


Figure 3.3: Diffuse Lambertian lighting model. Redrawn from Hearn & Baker[63].

direction of the ray, the (i, j) coordinates of the screen-space must be converted into \mathbf{R}^3 world-space coordinates. The vector resulting in the subtraction of these two points is normalized and used to intersect the scene.

It is Step 3 which is often the most computationally expensive. The naïve method of intersecting the ray with every object in the scene can be very costly. Various spatial partitioning methods have been examined so that the number of objects to be tested is minimized. A discussion of such techniques was recently provided by Smits[123], who added some of his practical experience to the discussion. Intersection techniques for individual primitives are also being improved upon regularly. A fast triangle intersection method was recently presented by Möller and Trumbore[88].

Step 4 can also be a very expensive step in the rendering process. For opaque, matte, objects, Lambert’s cosine law can be used to effectively shade the surface[63]. Lambert’s law states that the intensity is proportional to the cosine of the angle between normal of the surface and a vector pointing toward the light source. (See Figure 3.3.)

$$I = k_d \cos(\theta) \quad (3.1)$$

In Equation 3.1, I is the final intensity, k_d represents the diffuse colour components for the surface, and θ is the angle between the normal to the surface and the light source. If vectors **L** and **N** (from Figure 3.3) are both unit vectors, then Equation 3.1 can be rewritten to use the inner product of the two vectors to efficiently compute

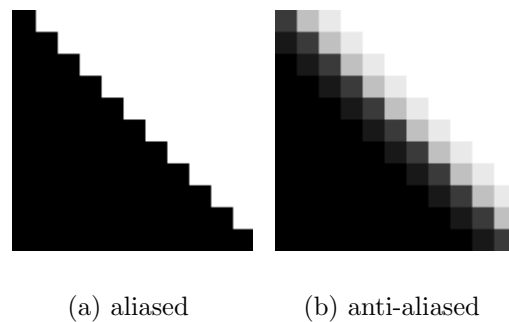


Figure 3.4: Aliasing artifacts are demonstrated in (a). The result of applying an anti-aliasing technique is shown in (b).

the cosine.

The basic ray tracing algorithm is very simple and many enhancements can be performed. One of the most common problems arises because only one ray is shot through the center of each pixel. The result of this *under-sampling* will be a very jagged edge. To correct this problem more rays are shot through pixels that are at a boundary between colours, and the average colour is chosen. This is often called *super-sampling*. Figure 3.4 demonstrates the difference between an aliased and an anti-aliased image. Figure 3.4(a) is a close up an image that contains a black object on a white background. Notice the jagged edge. Figure 3.4(b) has been super-sampled near the boundary. The difference is often perceptible to the human eye, even when the image is viewed without zooming.

Phong[96] introduced an illumination model and a shading mechanism that can yield very convincing results inexpensively. Phong shading interpolates the viewing lightning parameters over the surface of flat triangles which approximate curved surfaces. The Phong illumination model extends Lambert's law and adds a specular component which depends upon the viewing location, as one experiences in real life.

Implementation of transparent objects causes further difficulties. *Secondary* rays may need to be cast in order to effectively simulate refraction, which adds to the computational costs. A discussion of the some methods for efficiently implementing

transparency are discussed by Kay & Greenberg[73].

A more expensive mechanism for implementing Step 4 of Algorithm 1 is presented by Whitted[141]. He suggests the use of a tree structure to model transparency and inter-reflection between objects in the scene. Anti-aliasing can be easily incorporated into his ray-tree model by super-sampling each pixel.

The raytracing rendering method is a natural extension to classical geometry. In fact, Descartes[37] used the geometry and optics that were well known in his time to raytrace an ideally spherical raindrop. With this method he was able to determine quite accurately the properties of both primary and secondary rainbows.

Computer rendering of solids has only been investigated since the 1960's. Appel[10] used a technique which he called "point-by-point shading" to render three-dimensional images on a digital plotter. This would evolve into the raytracing algorithm described above. Instead of progressing pixel-by-pixel in the space of the output image, Appel projects the vertices of the solid to be rendered onto the image plane¹. He then creates a "roster" of points within the limits of this projection. Rays are cast through the points in this roster and intersected with the scene. Simple shading and shadow calculations are performed to determine the intensity of the point to be plotted.

As mentioned above, Goldstein & Nagel[56] were two of the first researchers to report an attempt at simulating the photographic process and to synthesize realistic images. They discuss a "combinatorial geometry method" for modelling objects (which is very similar to the constructive solid geometry methods used today). They also present the basic raytracing algorithm discussed above. Finally, they propose the possibility of applying such technology to the entertainment industry.

¹I.e. the plane defined by the output screen.

3.2 Splatting

Technology advances since the 1970's have provided mechanisms to extract three-dimensional (3D) volumetric data for many applications. Perhaps the most well known applications are *computed tomography* (CT) scans² and *magnetic resonance imaging* (MRI). These two technologies are have diagnostic applications in the medical field. Another application that may yield 3D volume data is *transmission electron microscopy* (TEM). TEM was used by Bychkov[27] to show that nanometer-sized particles are eroded when an electrical discharge is applied to a polymer tube. A third 3D data source is the seismic data which results from oil exploration.

Volume data is often represented by a set of intensity values that are stored at locations defined by (i, j, k) -tuples. The (i, j, k) -tuples act as indices into the volume. In this scenario, the samples are regularly spaced along each axis. To obtain the world-space coordinates of the intensity stored at a tuple, one merely takes the element-by-element product of the (i, j, k) vector with a vector of appropriate displacement values. For example:

$$\begin{aligned}(x_w, y_w, z_w) &= (i, j, k) \times (dx, dy, dz) \\ &= (i \ dx, j \ dy, k \ dz)\end{aligned}$$

For 3D data sampled at regular intervals, one can easily divide the volume into volume elements, or *voxels*. (See Figure 3.5.) The sample data is usually considered to be at the center of each voxel.

Volumes can, of course, store information other than scalar intensities. Fluid simulations store velocity and acceleration vectors at each sample location. Sometimes volume data isn't sampled regularly, which is a more difficult situation to work with since each (x_w, y_w, z_w) world coordinate must be stored separately.

3D data can be viewed by projecting it onto a two-dimensional (2D) screen, such

²Often abbreviated as "CAT scan."

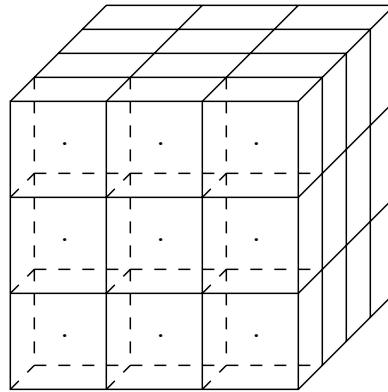


Figure 3.5: A regular voxel volume representation. The sample points for the closest *slice* are shown.

as a computer monitor. There are several approaches to this task. Westover[139] divides the various algorithms into two categories: *backward mapping* and *forward mapping*.

Backward mapping algorithms project the image plane onto the volumetric data. These algorithms commonly employ raytracing techniques to retrieve the data samples which affect a particular pixel. A ray is cast through the volume and is tested for intersection with each voxel. The pixel colour contribution for each sample point along the ray is usually a linear interpolation of the intensities of the neighbouring voxels.

The forward mapping technique uses the opposite approach. The volumetric data is projected forward onto the image plane, and clipped to the extent of the screen. This projection can be either *back-to-front* or *front-to-back*. With the back-to-front approach, the volume elements furthest from the screen are mapped onto the screen first. With front-to-back forward mapping, the closest voxels have their contributions added to the image raster first.

Shading calculations can be approached in many ways. One basic conundrum is that normals have to be extracted from the data. A simple approximation to finding

the normal (reviewed by Drebin et al.[39]) is to perform a simple subtraction from the neighbouring voxels.

$$N_x = I_{x+1,y,z} - I_{x,y,z}$$

$$N_y = I_{x,y+1,z} - I_{x,y,z}$$

$$N_z = I_{x,y,z+1} - I_{x,y,z}$$

Here $\mathbf{N} = (N_x, N_y, N_z)$ is the resulting normal. $I_{x,y,z}$ is the intensity of the corresponding (i, j, k) voxel.

A common method to extract surfaces from volumetric data is to associate opacity levels with intensity ranges. For example, if it is known that bone tends to have a particular intensity, then the voxel samples within a range of intensities are assigned a high opacity. Voxel samples far outside of this range are given a low opacity so that the bone surface will dominate the image. Lenz et al.[82] performed some of the early experiments with various display mechanisms.

Recent forward mapping algorithms are sometimes called *splatting* algorithms. Elements of splatting are relevant to this work, so a short history of the work leading up to the modern splatting ideas will be given. A good summary of earlier volume rendering work is presented in [39].

Frieder et al.[47] developed a simple back-to-front method for rendering volume data. Their method traverses the volume, voxel-by-voxel, along an axis-aligned route. It is a very simple method which traverses the entire volume instead of doing extra computation to determine which voxels are visible. For the machines available at the time, they claim their method was very fast because of its simplicity. They could also render the volume from an arbitrary viewpoint whereas some of the other algorithms forced the user to choose from a list of specific views.

The rendering volume data is prone to artifacts appearing on the output image. Drebin et al.[39] discuss the reason for such artifacts and present a mechanism to

eliminate them. They believe the artifacts arise because (in previous work) the voxel samples are classified by material based on a set of thresholds. Instead of using thresholds to determine which material the sample represents, Drebin et al. use filters to approximate the percentage of each material that would be contained within the voxel volume. The algorithms for such filters are specific to each data type. They compute several volumes of data from the output of the the filters such as colour, opacity, gradient vectors, density, “surface strength,” etc.. They also allow the specification of “matte” volumes that contained weights which can be used to slice the data or slowly change opacity in the view direction. They then transform combinations of these volumes to output the desired scene. Their rendering algorithm is of the backward mapping flavour.

Westover[139][140] provided volume rendering methods which approached interactive rates. He used the forward mapping technique which he called “splatting.” For every sample point, Westover evaluated the “footprint” that the sample point would produce upon the image plane. He used probabilistic/weighed rendering decisions like Drebin et al. to render his final images. Westover states that the major difference between forward mapping and backward mapping is how the reconstruction of the 3D signal from the sample points is performed. The backward mapping method tends to reconstruct the 3D signal interpolating from the nearest data samples, whereas forward mapping spreads the sample data over the affected pixels in the image plane.

With the advent of accelerated graphics hardware, Laur and Hanrahan[81] decided to approximate the footprint of Westover’s splats with shaded polygons. They stored a hierarchy of these polygons in an octree data structure so that varying levels of detail could be rendered. At each node in the hierarchy, an estimation of the error was also stored. In this way, the error tolerance could be elevated to ensure interactive rates persisted while the the user of the application changed viewpoints, etc..

3.3 Modelling of Phenomena

Modelling natural phenomena for computer graphics is a very diverse topic. The category is quite large and many approaches have been developed to suit the expansive list of phenomena. This section will present a brief survey of only a few of the natural wonders that have been examined thus far.

3.3.1 Modelling Rainbows

Rainbows are a beautiful natural phenomenon that can significantly improve a rendering of an outdoor vista. Rainbows are also commonly seen in fountains, in the mist-covered lakes, and various other locations where water droplets are suspended in air[59]. Rainbows are created by the dispersion³ of sunlight through innumerable water droplets. Therefore a brute force technique which simulates dispersion of sunlight through billions of water droplets is not an acceptable mechanism for simulation. Simulating dispersion through a single prism is expensive process[127]; simulating dispersion through countless raindrops is intractable.

It is helpful to understand the nature of a simple rainbow before discussing its simulation. Descartes[37] provided one of the first explanations of the phenomenon, and Greenler[59] has provided a modern, high-level description.

It has been known for several centuries that the rainbow is created by the dispersion of sunlight into monochromatic components by water droplets. Descartes observed that rainbows occur in fountains and in similar situations, as well as after a rainstorm. He theorized that the size of the water particles was not important to its creation and decided to investigate the interaction of light with a single, idealized “raindrop” that he manufactured from a spherical vial filled with water. (See Figure 3.6.) He also validated his results with the known theory of his day.

³Dispersion is the splitting of light into its monochromatic components via refraction. Each wavelength of light has a slightly different index of refraction.

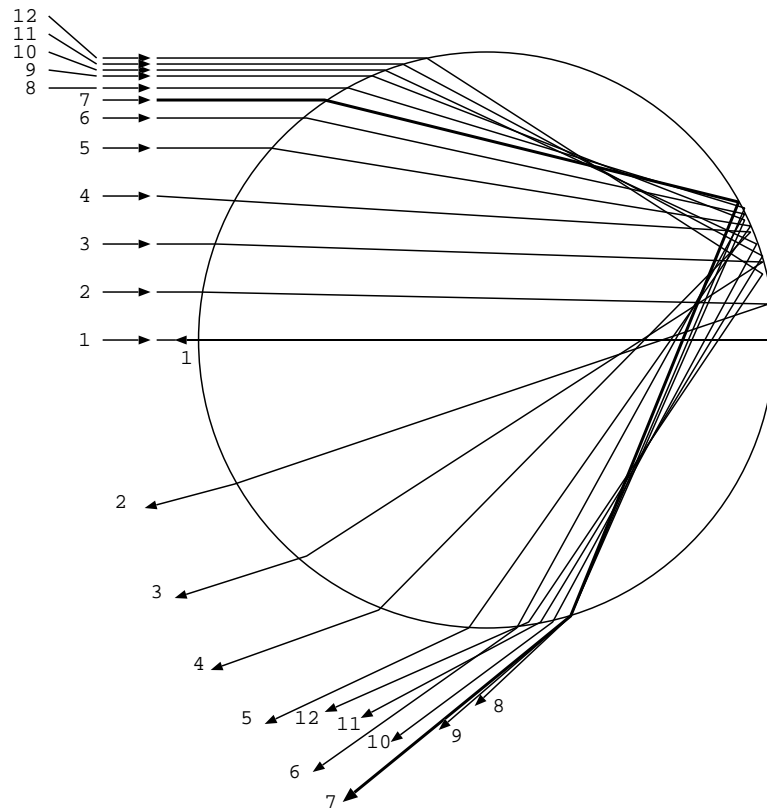


Figure 3.6: An ideal raindrop, raytraced by Descartes in 1637. Redrawn from Greenler[59].

Examining Figure 3.6, one will notice that twelve parallel rays lying in a plane have been traced through a sphere. The plane intersects a sphere through the center (by assumption). Thus the intersection curve is a circle. Each ray enters the raindrop on or above the horizontal axis. Each ray is refracted into the water drop, internally reflected once, and then refracted again when exiting. Only a fraction of the light entering the drop follows the ray paths shown in this figure, but these paths produce the primary rainbow⁴.

Ray 1 is directed so that it strikes the sphere perpendicular to the surface. There

⁴The secondary rainbow is the result of the first refraction, then *two* internal reflections, and then a final refraction.

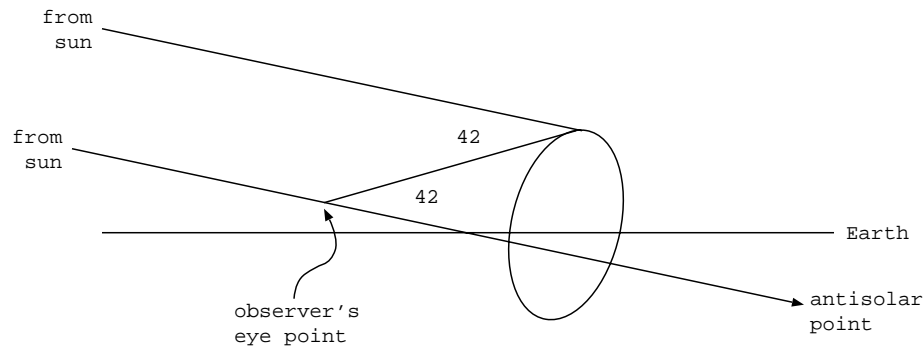


Figure 3.7: The view cone which defines the shape of a rainbow. Redrawn from Greenler[59].

is no refraction in this case and the portion of light that is internally reflected is redirected toward the light source. The exit angle of rays 2–7 steadily increase away from ray 1. Ray 7 is known as the *Descartes Ray*. It is special because the exit angles for all other rays are smaller than that of the Descartes Ray. Notice how rays 8–12 tend once again toward ray 1. Descartes determined experimentally, and verified analytically with this method, that the angle between ray 1 and ray 7 is approximately 42° . Descartes determined that a large number of rays exit at the 42° point, so this is the reason why rainbows form at a 42° angle away from the direction of the sunlight from the observer. (See Figure 3.7.)

Light from the sun has traveled such a long distance so that the rays are effectively parallel. The ray passing through the eye point of the observer (if that were possible) would lead to the anti-solar point⁵. If a rainbow is present in the sky, it will be located where a volume of raindrops lies within a cone shape whose apex is at the observers eye. The axis of the cone will start at the eye and go in the direction of the anti-solar point. The angular distance of the cone from the axis is 42° . It is interesting to note that each observer of a rainbow (and in fact each eye observing the rainbow) has

⁵The anti-solar point is any point that is in the opposite direction of the sun from the point of observation. To find the approximate anti-solar point on a sunny day, one simply looks where the head of one's shadow lies on the ground.

a slightly different set raindrops within the view cone, and will thus will perceive a slightly different rainbow.

One of the first attempts to render a rainbow was performed by Cook[31]. The focus of Cook's work was to describe a generic mechanism to specify shading parameters on a surface-by-surface basis. He used a *directed acyclic graph* to store the shading model to be used for each surface. In this way, some surfaces could be rendered with a complex algorithm while simple diffuse surfaces could use an inexpensive shading model. Keeping with this theme, Cook suggests that atmospheric properties such as fog and rainbows could be rendered using similar trees. The outputs of a shade tree would be the input to an atmospheric tree. Explicit details about the rainbow simulation are not provided since the focus of the paper is on shading algorithms, but Cook does suggest that a simple model based on the viewing angle was used.

In an attempt to capture the brilliant specularly of gems, Thomas[127] developed a model for dispersive refraction. Each material that transmits light has its own *dispersive function*, which relates the index of refraction to the monochromatic wavelength of light. The dispersion functions are usually curved; and for many materials are not readily available in the physics literature. Therefore, Thomas' model linearly interpolates the dispersive function given the overall index of refraction and a dispersion value. He used an adaptive approach to subdivide incident rays so that the newly spawned rays (those transmitted) would cover a portion of the spectrum.

Musgrave[89] developed a similar model for dispersion, which he used to render prisms and rainbows. To render rainbows, Musgrave provides two models. The first, "empirical" model is similar to the work of Cook[31], though Musgrave gives far more details. The second model attempts to be more physically-based.

The total illumination of an object over all monochromatic colours of a point on

a surface can be described by the following equation.

$$\int_{380}^{800} I(\lambda) d\lambda \quad (3.2)$$

where $I(\lambda)$ is the intensity of the monochromatic colour of wavelength λ . Clearly, this is expensive to compute.

For his “empirical” model, Musgrave chose to linearly interpolate the dispersive function for each transmissive material for computational efficiency reasons. Therefore, equation 3.2 is approximated with sample wavelengths that are summed. Musgrave chose 13 uniformly distributed sample wavelengths which are converted into the best possible red, green, and blue (RGB) components, and stored in a table. Based on the angle between the view direction and the direction of the suns rays, Musgrave looks up an appropriate value from this table and adds it to the intensity of the ray, as though it were a fog. To give a smooth looking transition between rainbow colours, the index into the table is jittered.

Musgrave’s physical model is more elaborate, but yields better results. For this model Musgrave returned to the work of Descartes and computationally raytraced a raindrop. Again he used 13 sample wavelengths to approximate Equation 3.2; but this time he used a slightly more accurate interpolation for the dispersion function. Musgrave traces 50,000 parallel rays in the range between rays 1–12 of Figure 3.6 for each sample. If modelling both primary and secondary rainbows, then the rays can emerge from almost anywhere out the front of the raindrop. Therefore Musgrave uses 1800 “buckets” (one bucket per $\frac{1}{10}$ th of a degree) to sum the output intensities from each ray. This table need only be computed once and stored in an auxiliary data file. When rendering an outdoor scene with a rainbow, this data can be used to compute the colours of the rainbow in a manner similar to Musgrave’s “empirical” model and Cook’s model.

3.3.2 Modelling Aurora

In [16] Baranoski et al. present a method for modelling the aurora borealis, which is more commonly known as the Northern lights⁶. In their model, they attempt to incorporate as many known auroral physics concepts and data as possible. The algorithm they present is expensive since it attempts to model the paths electrons follow into the atmosphere, but it can be parallelized easily[15].

The physics behind the driving mechanisms of the aurora borealis is not yet totally understood, but enough details are known to facilitate graphical simulation. The basic process begins with the sun ejecting a constant stream of subatomic particles known as the *solar wind*. Particles from the solar wind strike the Earth's magnetosphere, which is a large electromagnetic envelope that protects the planet from such radiation. Many of the particles are caught by the magnetosphere and are focused toward the Earth's polar regions where our magnetic field lines converge. Due to an hitherto unknown mechanism the electrons in the magnetosphere are ejected into the atmosphere. These electrons precipitate in a spiraling motion down through the layers of atmosphere. When an electron strikes an atmospheric particle (usually at an elevation in the 100-300 km range) some of its energy is transferred into the struck atom which puts its own electrons into an excited state. The precipitating electron is deflected and continues with its remaining momentum. After a certain length of time, the excited atom returns to its normal state and emits a photon⁷. Different atoms prevail at different altitudes and emit photons of different wavelengths, which produces the array of colours seen when viewing the aurora.

The shape of the aurora borealis is determined by the energy and density of the electrons that permeate into the atmosphere, and the electric field variations of the Earth. A simple auroral display looks like a curtain of light emissions with folds and curls. The curtain formation results from the sheets of electrons entering the

⁶Their model does not exclude modelling aurora australis, the less visible Southern lights.

⁷See §2.3 for more.

atmosphere. The bends and folds create bright visible streaks.

To render aurora, Baranoski and Rokne combine techniques from particle systems and volume rendering. Each particle in the system represents a number of electrons falling through the atmosphere. When a simulated collision occurs, the particle becomes emissive and contributes to the final rendering. This emissivity is rendered using the ideas from the splatting technique discussed in §3.2. The shape of the precipitating electron sheets are modelled with a trigonometric sine wave. Several parameters are used to determine phase shift, end points, width, etc.. They also add parameters to model small folds which are observed as bright streaks in the auroral display.

It is too computationally expensive to represent every electron that is captured by the Earth's magnetosphere and accelerated toward the poles. The set of collisions for the countless number of particles that create the aurora is immense. Thus the model of Baranoski and Rokne makes use of electron beams to represent large collections of electrons. The model diverges from reality slightly when an electron beam is impacted with an atom. Instead of modelling the distance travelled by an atom that has been struck, they consider the initial point of collision to be the emission point of the photon. A Gaussian distribution is used to blur the image slightly to compensate for this inaccuracy.

Atoms emit different monochromatic spectral lines when moving out of the excited energy state. The emission lines also vary with altitude. The model uses observed emission curves to determine the colour and intensity at emission points. Though realistic, this detail is not explicitly modelled.

The rendering process is performed in three steps. First, light emissions from the struck atoms are mapped onto the view plane. This forward mapping is similar to the forward mapping splatting technique. Second, the intensities of the different wavelengths are converted to RGB values. Finally, an antialiasing technique is used to simulate the auroral temporal and spatial variations. This last step is implemented

by applying a colour channel dependent filter on the final image.

3.3.3 Modelling Lightning

Lightning is another phenomenon that can be challenging to simulate. In §2.4 the physical properties of the phenomenon are discussed. The important aspects for computer graphics of the most common type of lightning are repeated here.

Most lightning strokes occur within the cloud itself. These strokes neutralize portions of the cloud. Since the cloud obscures the path of the lightning stroke, observers on the ground perceive it as a constant flash in the sky. This type of stroke is commonly called *heat lightning* or *sheet lightning*.

Of the lightning strokes that transfer charge between the cloud and the ground, about 90% of these *lower*⁸ negative charge to the Earth, and are formed by downward moving stepped leaders. Less often, lightning lowers a positive charge to Earth. This is the type of lightning that is typically simulated in computer graphics.

The shape of the lightning stroke is determined by a step leader which slowly maneuvers from the base of the cloud to the Earth in incremental steps. This leader is generally not seen by observers of a lightning stroke, but has been photographed using special equipment, and is important here only because it determines the shape of the lightning stroke. The leader typically starts from an elevation of 2–3 km, and each section is typically 10–200 m in length.

When the stepped leader is sufficiently close to the ground it will make contact with an upward moving streamer. These streamers are typically formed from objects that protrude from the Earth by the induced charge of the stepped leader. When contact is made it is similar to the flicking of a light switch. The circuit is closed and a lightning stroke occurs. The typical duration of a lightning stroke is 1 ms. Often there are several such strokes in a *flash* of lightning. A *flash* of lightning is the set of

⁸The physical process of charge transfer is very complex. The *lowering* of charge is taken here to mean the overall effective lowering of charge. Some positive charge could be *raised*.

strokes that occur consecutively from one channel which is formed by a step leader. A flash can last up to a half a second.

Another type of lightning that is important to simulate for graphics, but is not often discussed in the graphics literature, is lightning formed by an upward moving stepped leader. This type of lightning often forms from tall buildings or mountain tops. It is characterized by a V-shape, whereas the lightning discussed above tends to be mostly linear and will have several faint branches extending out so that they form an upside-down V in the sky. After reading much of the computer graphics literature, an animator would incorrectly assume that the stepped leader that strikes a tall building would have moved downward from the cloud, instead of upward from the building.

The first graphical simulation of lightning was done by Reed and Wyvill in 1994[103]. In their paper, they describe a very simple method to generate a stroke of lightning, and render it with a raytracer. This paper does not develop a physical model, but instead describes how a particle system can be used to randomly generate a realistic looking lightning stroke. Their method accurately shapes the lightning based on statistical data. It is the path of the stepped leader which is simulated by Reed and Wyvill. An initial “seed” segment of this leader is first chosen. More segments are recursively generated by rotating around the seed segment. By always generating new segments that have their direction based on the seed segment direction, Reed and Wyvill ensure that the path of the lightning will be more or less straight. Branches are created probabilistically.

Reed and Wyvill also describe how to render the lightning stroke. This includes the channel, its branches, and the glow often observed around the lightning channel. They used a raytracer to render their results, so intersection between rays and the line segments which make up the lightning channel is highly improbable. Therefore an extra lightning contribution is added to every primary ray. The contribution is determined by the formula.

$$I_{total\lambda} = \sum_i I_{i\lambda}, \quad \text{where} \quad I_{i\lambda} = m_{i\lambda} \exp\left(-\left(\frac{d_i}{w_{i\lambda}}\right)^{n_{i\lambda}}\right) \quad (3.3)$$

Here λ represents one of the three colour channels — red, green, or blue. $I_{i\lambda}$ is the contribution from the i^{th} segment of the lightning channel. $m_{i\lambda} \in [0, 1]$ is the maximum contribution of $I_{i\lambda}$. d_i is the shortest distance between the ray and the i^{th} segment. $w_{i\lambda}$ is the half-width (i.e. radius) of the i^{th} lightning channel segment. $n_{i\lambda} > 1$ is used to control the contrast of the lightning channel. For $n > 8$, the lightning channel will look sharp.

A similar exponential formula is used to generate a “glow” around the lightning channel. This glow is often recorded on photographs of lightning. Reed and Wyvill also discuss how to animate the statistically generated lightning bolt. This is a little unrealistic since a typical lightning stroke lasts for a single millisecond, which is $\frac{1}{40}$ th of the duration of a frame in an animation. They also discuss a simple method which allows the generated lightning bolt to act as a light source in a rendering. Effectively, a line segment light source is placed along each segment of the stroke.

Five years later, Kruszewski improved upon the method for generating a stroke of lightning[77]. Like Reed and Wyvill, Kruszewski’s goal was to present a practical model for generating a realistic lightning stroke instead of implementing a physical simulation. He used random binary tree theory to generate a 3D mesh which spans space between two electrodes which are specified as inputs to the model. Kruszewski introduced the idea of creating a basic skeleton which consisted of straight cylindrical segments which are then subdivided into smaller subsegments. He calls this process *electrification* of the segments. Glassner[52][53][54] uses a similar process to add detail to a skeleton which he describes as *adding tortuosity*.

The model of Reed and Wyvill suffered from one problem that Kruszewski specifically addresses: the branching pattern was difficult to control due to the nature of their algorithm and the erratic behaviour of the pseudo-random number generator. This was fixed by using three parameters. The parameters are *number of segments*,

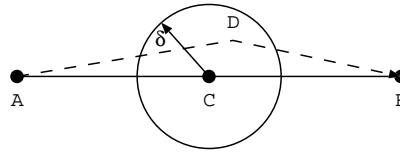


Figure 3.8: Electrification of a skeleton segment by recursively breaking up line segment AB into two subsegments. D is a random point within the disk centered at C with radius δ . Redrawn from Kruszewski[77].

amount of forking, and *amount of randomness*. By using these three parameters, Kruszewski was able to statistically control the look of the skeleton, irregardless of the seed used in the random number generator.

The *electrification* process described by Kruszewski uses a midpoint replacement algorithm to subdivide each segment recursively. Figure 3.8 demonstrates the 2D case. A disc of radius δ is created at the midpoint of line segment AB. A random point, D, within this disc is chosen and the new subsegments are then created as AD and DB. The natural extension of this algorithm into three dimensions is to use a sphere instead of a disc. Kruszewski found this to give erratic results and instead chose to rotate each subsegment around its axis by 11° .

In the early 1980's an accurate 3D model of a lightning the stroke was developed using Monte Carlo methods[109][106] at the University of Toronto. The model was developed so that the acoustics of thunder could be studied, and not for computer graphics. This very simple model generates a basic lightning stroke *without branching* using statistics and known properties of lightning strokes. From the acoustic properties of thunder, it is determined that the entire length of a lightning channel should be subdivided into 3 m segments. This is, however, too small of a resolution to be observed in photographs, which are limited to 40–60 m lengths.

In order to keep the shape of the lightning bolt approximately linear, Ribner and Roy[106] developed a technique that they call *memory smoothing*. Memory smoothing is a simple concept that works effectively. When choosing a direction for a new

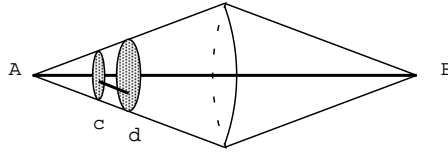


Figure 3.9: Adding tortuosity to a skeleton segment by iterating over the line segment and adding smaller segments which are contained within a cone. Redrawn from Glassner[53].

segment the average direction from the last k segments is used as a basis. A random direction is chosen within a solid angle centered on this average direction.

Glassner used the work of Ribner and Roy[106] as a foundation to his own lightning model[52][53]. He also discussed how to implement the generation of thunder from his model[54] as per Ribner and Roy[106].

Glassner splits Ribner and Roy’s model up into a two phase process that is similar to that of Kruszewski. The primary segments define the basic shape of the lightning, while tortuosity (electrification) is added in the second phase.

For Glassner, the basic lightning shape creation is similar to that of Ribner and Roy. Glassner does add a probability distribution function which varies the the length of the segments depending upon altitude. He developed this function from measured data taken from lightning photographs.

It has been stated above that Glassner’s second refinement step is similar to that of Kruszewski. Instead of recursively subdividing a segment with a rotating disc, Glassner iterates though a cone-shaped containment volume for each segment. Referring to Figure 3.9, one can see how the tortuous details are added by iterating over the segment length. The new segments are contained within an enclosing cone-shape. The point on disc d is chosen by perturbing the location of of the previous point on disc c .

Sosorbaram et al.[124] note that all previous efforts to simulate lightning have produced results which only describe one type of lightning — the typical cloud-to-ground

discharge. They attempt to model all four forms of lightning (intracloud, cloud-to-cloud, cloud-to-ground, and ground-to-cloud) by basing their model on charge locations. Although he focuses on cloud-to-ground lightning flashes, Kruszewski[77] does account for different types of lightning and electrical discharges by defining a source and a destination for the current flow. Sosorbaram et al. extend this by adding initial space charge and electrical potential distributions that are associated with cloud growth.

Sosorbaram et al. also add more realism to their model by dividing space up into *cells*. These cells are analogous to the voxels discussed in §3.2. They have two parameters to their model which are used to physically determine the shape and the branching structure of the generated lightning. These two parameters control the number of branches at each cell based on the electric field properties.

To render a lightning, Sosorbaram et al. have developed two methods. The first is used for a visible lightning stroke, such as a cloud-to-ground stroke. They use cylindrical solid textures and to represent the segments of a lightning stroke and sum their contributions. The density of the texture increases toward the center of the cylinder. Thus the contribution to the image of a ray intersection with the cylinder can be implemented using the backward-mapping volume rendering techniques discussed briefly in §3.2.

Intracloud discharges are rendered by placing light sources along the segments of a lightning channel. These light sources are assumed to attenuate quickly to keep computational costs down. These light sources cause reflections within clouds that are implemented as particle systems.

A less expensive rendering mechanism to render lightning and its interaction with clouds was presented by Dobashi et al.[38]. They use the method of Reed and Wyvill[103] to generate their lightning strokes because of its simplicity and efficiency. Line drawing in OpenGL[®] is used to render the actual lightning stroke. Point

light sources are placed at segment endpoints to produce the illumination. Metaballs⁹ are used to represent the clouds. Intensity calculations which determine atmospheric glow and cloud illumination are described, and a mechanism to render the results with graphics hardware is presented.

⁹Bloomenthal[20, pg. 26] compares metaballs to implicit surfaces which can be blended together to form a single surface.

Chapter 4

Simulating Ball Lightning

Simulation of the ball lightning phenomenon can be approached from a variety of angles. An accurate physical model is desired, but efficiency must also be considered. A model with too much detail would be difficult to implement. Furthermore, the physical nature of the phenomenon is not fully understood (as was demonstrated in Chapter 2), therefore it is not possible to implement a model that is entirely based on physics. As a result, a hybrid model has been developed whereby the incompressible motion of a ball lightning is modelled by a fluid dynamical implementation, but deformations are approximated using common computer graphics techniques.

The ball lightning simulation is broken down into two distinct parts. First, motion of a non-deformable ball lightning through air is simulated physically by numerically solving a system of partial differential equations derived by Gaǐdukov[48][50]. This will be discussed in §4.1. Second, the deformation of a ball lightning through a small opening is approximated by computing the tangent planes of a convoluted “blob” function at discrete intervals. The blob function provides control over the shape of the ball lightning deformation and is simple and efficient to implement. Fluid dynamical properties are also considered during this phase of the simulation, which is discussed in §4.2.

Note that the purpose of studying fluid dynamics for this work was *not* to develop

a thesis that would further fluid dynamics research. Only a basic understanding of fluid dynamics terminology is necessary in order to use it as a tool with which one can accurately describe the motion of ball lightning.

Once the ball lightning is simulated, it must also be rendered. The internal physical properties of the phenomenon are still disputed, so a stochastic particle system is used to create the impression of internal motion for the ball lightning. Adjusting the parameters of the particle system allows for different effects to be produced. Each particle in the system is considered to be an emissive unit of plasma. It is however computationally inefficient to model each particle as a light source in a raytracer, therefore a forward mapping technique is borrowed from the volume rendering discipline. The ball lightning images must be composited onto a scene which is rendered via another method — in this case, a simple raytracer. The details of this process are discussed in §4.3.

4.1 Non-deformable Motion

Gaǐdukov[48][50] decided that the problem of ball lightning should be broken down into small, manageable pieces. Instead of concentrating on the internal structure of ball lightning he chose to validate a few of its properties from a fluid dynamics perspective. In order to explain how a ball lightning will pass through a hole in a wall, there are four steps to consider: the ball lightning’s approach to the wall from a distance; the ball lightning’s motion as it nears the wall; the motion of the ball lightning’s internal plasma into the wall; and the ball lightning’s reformation on the other side.

Gaǐdukov’s work describes a ball lightning’s motion from a fluid dynamics perspective. His work disregards the aspect of Kapitsa’s[71] work which describes how ball lightning motion follows the direction of electromagnetic energy fields. §2.5.1 discusses external energy source models, which often try to explain the motion of ball

lightning, and it's ability to move independently of the wind direction.

Gaidukov makes a few assumptions to simplify the problem of describing a ball lightning's approach to a wall. He assumes that there is an interface between the ball lightning and the surrounding environment which prevents air particles from adhering to the surface. (See §2.5 for ball lightning theories which describe various interfaces.) Second, when the ball lightning is more than one radius in distance away from the hole, a point source is used to attract the ball lightning instead of a disk or jet. The point source is specified as a single value, γ , which has units of intensity per unit solid angle.

Spherical coordinates, i.e. (r, θ, φ) -tuples, are used to specify the location of the ball lightning. Similarly, rates of change with respect to time are also specified in spherical coordinates. Gaidukov's equations use the standard physics notation where $\frac{dx}{dt} = \dot{x}$, and $\frac{d^2x}{dt^2} = \ddot{x}$, hence, the same notation will be used here. The equations of motion of an incompressible ball lightning toward a point source are:

$$\ddot{r} - r(\dot{\theta}^2 + \dot{\varphi}^2 \sin^2 \theta) = -\frac{2\gamma^2}{a^5} \left[\left(\frac{a}{r}\right)^5 + 2\left(\frac{a}{r}\right)^7 \right], \quad (4.1)$$

$$\frac{1}{r} \frac{d}{dt} (r^2 \dot{\theta}) - r \dot{\varphi}^2 \sin \theta \cos \theta = -\frac{\gamma \dot{\theta}}{r^2}, \quad (4.2)$$

$$\frac{1}{r \sin \theta} \frac{d}{dt} (r^2 \dot{\varphi} \sin^2 \theta) = -\frac{\gamma \dot{\varphi} \sin \theta}{r^2}, \quad (4.3)$$

where a is the ball lightning radius.

Equations 4.1–4.3 describe the motion of a ball lightning in the air moving toward a point source. The point source approximates the force of the air current through an open window or door. While moving toward such an opening, the ball lightning does not change shape, and does not appreciably interact with the surrounding air. Notice that there are no \dot{a} (i.e. $\frac{da}{dt}$) terms in Equations 4.1–4.3; therefore, the radius of the ball lightning is assumed to be constant. Further note that it is assumed that the point source, γ , is also constant, and is located at the origin of the spherical coordinates.

The next section will describe how these equations can be solved numerically, and what initial conditions are required to obtain a solution.

4.1.1 Numerical Solution to Non-deformable Motion

A numerical solution is required to Gaídukov's equations since there is no known analytical solution. A fixed-step, fourth order, Runge-Kutta integration method is employed as per [33] in order to obtain the results. A fourth order approximation yields results which are sufficiently accurate for computer graphics. Optimizations such as implementing a variable step size would certainly improve the efficiency of the algorithm, however they are not needed since the forthcoming examples (provided in §4.1.3) were all computed in less than five seconds on a modern desktop computer.

Discussing the details of how to implement a Runge-Kutta solution to a set of ordinary differential equations (such as Equations 4.1–4.3) is not in the scope of this work. Instead, the interested reader is referred to Crenshaw's book[33]. The title of Crenshaw's book reflects his experience with real-time systems, but the book is actually a very general, step-by-step guide, to implementing state-of-the-art numerical methods.

It is important to mention that numerical methods for solving ordinary differential equations generally operate on first order equations of the form

$$\dot{x} = f(x, t)$$

Unfortunately, most equations that describe the motion of physical bodies include an acceleration term. Such is the case with Newton's second law of motion

$$\ddot{x} = \frac{F}{m}$$

In order to use the Runge-Kutta method on this system, a change of variable is required[33]. Simply let $v = \dot{x}$ to eliminate the second derivative term. The following

system is first order.

$$\begin{aligned}\dot{v} &= \frac{F}{m} \\ \dot{x} &= v\end{aligned}$$

This step is required in order to obtain a numerical solution to Equations 4.1–4.3. In addition, notice that Gaidukov's equations still contain the derivative operator. For example, the first term of Equation 4.2 is $\frac{1}{r} \frac{d}{dt} (r^2 \dot{\theta})$. Such operators must be expanded in order to find a numerical solution. Recall that the ball lightning position is a (r, θ, φ) -tuple, and that r , θ , and φ are all functions of time.

To solve the system the following variable changes are used.

$$u = \dot{r} \tag{4.4}$$

$$v = \dot{\theta} \tag{4.5}$$

$$w = \dot{\varphi} \tag{4.6}$$

From Equation 4.4, we get $\dot{u} = \ddot{r}$, etc.. Notice how u , v , and w take on the role of the ball lightning velocities. Substituting Equations 4.4–4.6 into Gaídukov's original equations, expanding the derivative operators, and solving for the velocity terms, yields the following equivalent system of six differential equations.

$$\dot{u} = r(v^2 + w^2 \sin 2\theta) - \frac{2\gamma^2}{r^5} \left(1 + 2 \left(\frac{a}{r} \right)^2 \right) \tag{4.7}$$

$$\dot{v} = \frac{\gamma v}{r^3} - 2 \frac{uv}{r} + w^2 \sin \theta \cos \theta \tag{4.8}$$

$$\dot{w} = -\frac{\gamma w}{r^3} - 2 \frac{uw}{r} - 2 \frac{vw \cos \theta}{\sin \theta} \tag{4.9}$$

$$\dot{r} = u \tag{4.10}$$

$$\dot{\theta} = v \tag{4.11}$$

$$\dot{\varphi} = w \tag{4.12}$$

Here is a system of six first order, ordinary differential equations that can be solved numerically. To do so, starting values for r , θ , φ , $u = \dot{r}$, $v = \dot{\theta}$, and $w = \dot{\varphi}$ must be chosen. These initial values are then substituted into Equations 4.7–4.12 in order to compute the differentials. Then using a fourth order Runge-Kutta method, the next value for a time step can be computed. Time steps are computed sequentially until the ball lightning is within one radius of the point source.

4.1.2 Initial Conditions for Non-deformable Motion

Choosing initial conditions for the ball lightning position and velocity is a mandatory requirement for finding a numerical solution to Gaídukov's equations. It was convenient for Gaídukov to derive Equations 4.1–4.3 using spherical coordinates, but it is more convenient for computer graphics to use a Cartesian coordinate system. Therefore, a conversion from Cartesian coordinates to spherical coordinates is necessary to facilitate their use. The conversion factor for position is well known. It is

$$\begin{pmatrix} r \\ \theta \\ \varphi \end{pmatrix} = \begin{pmatrix} \sqrt{x^2 + y^2 + z^2} \\ \tan^{-1}\left(\frac{y}{x}\right) \\ \cos^{-1}\left(\frac{z}{\sqrt{x^2 + y^2 + z^2}}\right) \end{pmatrix} \quad (4.13)$$

The initial velocity must also be specified in spherical coordinates. To convert from Cartesian to polar velocities, the derivative of the (r, θ, φ) -tuple must be computed with respect to time in terms of Cartesian coordinates. The derivation for $\frac{dr}{dt}$ is the most simple. Start by employing the chain rule in three dimensions.

$$\begin{aligned} \frac{dr}{dt} &= \frac{\partial r}{\partial x} \frac{dx}{dt} + \frac{\partial r}{\partial y} \frac{dy}{dt} + \frac{\partial r}{\partial z} \frac{dz}{dt} \\ &= \frac{\partial}{\partial x} \sqrt{x^2 + y^2 + z^2} \frac{dx}{dt} + \frac{\partial}{\partial y} \sqrt{x^2 + y^2 + z^2} \frac{dy}{dt} + \frac{\partial}{\partial z} \sqrt{x^2 + y^2 + z^2} \frac{dz}{dt} \\ &= x(x^2 + y^2 + z^2)^{-\frac{1}{2}} \frac{dx}{dt} + y(x^2 + y^2 + z^2)^{-\frac{1}{2}} \frac{dy}{dt} + z(x^2 + y^2 + z^2)^{-\frac{1}{2}} \frac{dz}{dt} \end{aligned}$$

$$= \frac{1}{\sqrt{x^2 + y^2 + z^2}} \left(x \frac{dx}{dt} + y \frac{dy}{dt} + z \frac{dz}{dt} \right)$$

$\frac{d\theta}{dt}$ is obtained similarly.

$$\begin{aligned} \frac{d\theta}{dt} &= \frac{\partial\theta}{\partial x} \frac{dx}{dt} + \frac{\partial\theta}{\partial y} \frac{dy}{dt} + \frac{\partial\theta}{\partial z} \frac{dz}{dt} \\ &= \frac{\partial}{\partial x} \tan^{-1} \left(\frac{y}{x} \right) \frac{dx}{dt} + \frac{\partial}{\partial y} \tan^{-1} \left(\frac{y}{x} \right) \frac{dy}{dt} + \frac{\partial}{\partial z} \tan^{-1} \left(\frac{y}{x} \right) \frac{dz}{dt} \\ &= \frac{-y}{x^2} \cdot \frac{1}{1 + \left(\frac{y}{x}\right)^2} \cdot \frac{dx}{dt} + \frac{1}{x} \cdot \frac{1}{1 + \left(\frac{y}{x}\right)^2} \cdot \frac{dy}{dt} + 0 \\ &= \frac{1}{1 + \left(\frac{y}{x}\right)^2} \left(\frac{-y}{x^2} \frac{dx}{dt} + \frac{1}{x} \frac{dy}{dt} \right) \end{aligned}$$

Finally, we derive a formula for $\frac{d\varphi}{dt}$.

$$\begin{aligned} \frac{d\varphi}{dt} &= \frac{\partial\varphi}{\partial x} \frac{dx}{dt} + \frac{\partial\varphi}{\partial y} \frac{dy}{dt} + \frac{\partial\varphi}{\partial z} \frac{dz}{dt} \\ &= \frac{\partial}{\partial x} \cos^{-1} \left(\frac{z}{\sqrt{x^2 + y^2 + z^2}} \right) \frac{dx}{dt} + \frac{\partial}{\partial y} \cos^{-1} \left(\frac{z}{\sqrt{x^2 + y^2 + z^2}} \right) \frac{dy}{dt} \\ &\quad + \frac{\partial}{\partial z} \cos^{-1} \left(\frac{z}{\sqrt{x^2 + y^2 + z^2}} \right) \frac{dz}{dt} \end{aligned}$$

Let $m = \frac{z}{\sqrt{x^2 + y^2 + z^2}}$, so we get

$$\begin{aligned} \frac{d\varphi}{dt} &= \frac{-1}{\sqrt{1-m}} \cdot z \left(-\frac{1}{2} \right) (x^2 + y^2 + z^2)^{-\frac{3}{2}} (2x) \frac{dx}{dt} \\ &\quad + \frac{-1}{\sqrt{1-m}} \cdot z \left(-\frac{1}{2} \right) (x^2 + y^2 + z^2)^{-\frac{3}{2}} (2y) \frac{dy}{dt} \\ &\quad + \frac{-1}{\sqrt{1-m}} \cdot \left(\frac{(1)(x^2 + y^2 + z^2)^{\frac{1}{2}} - (z) \left(\frac{1}{2}\right) (x^2 + y^2 + z^2)^{-\frac{1}{2}} (2z)}{(x^2 + y^2 + z^2)^1} \right) \frac{dz}{dt} \\ &= \left(\frac{1}{\sqrt{1-m}} \right) \left(\frac{1}{(x^2 + y^2 + z^2)^{\frac{3}{2}}} \right) \left(xz \frac{dx}{dt} + yz \frac{dy}{dt} \right) \\ &\quad - \frac{1}{\sqrt{1-m}} \left((x^2 + y^2 + z^2)^{-\frac{1}{2}} - z^2 (x^2 + y^2 + z^2)^{-\frac{3}{2}} \right) \frac{dz}{dt} \end{aligned}$$

$$\begin{aligned}
&= \left(\frac{1}{\sqrt{1-m}} \right) \left(\frac{1}{(x^2 + y^2 + z^2)^{\frac{3}{2}}} \right) \left(xz \frac{dx}{dt} + yz \frac{dy}{dt} \right) \\
&\quad - \frac{1}{\sqrt{1-m}} \left(\frac{(x^2 + y^2 + z^2)}{(x^2 + y^2 + z^2)^{\frac{3}{2}}} - \frac{z^2}{(x^2 + y^2 + z^2)^{\frac{3}{2}}} \right) \frac{dz}{dt} \\
&= \frac{1}{\sqrt{1-m}} \cdot \frac{1}{(x^2 + y^2 + z^2)^{\frac{3}{2}}} \left(xz \frac{dx}{dt} + yz \frac{dy}{dt} - (x^2 + y^2) \frac{dz}{dt} \right)
\end{aligned}$$

Therefore, our final conversion for rates of change in position from Cartesian to spherical coordinates is given by

$$\begin{pmatrix} \frac{dr}{dt} \\ \frac{d\theta}{dt} \\ \frac{d\varphi}{dt} \end{pmatrix} = \begin{pmatrix} \frac{1}{\sqrt{x^2+y^2+z^2}} \left(x \frac{dx}{dt} + y \frac{dy}{dt} + z \frac{dz}{dt} \right) \\ \frac{1}{1+\left(\frac{y}{x}\right)^2} \left(\frac{-y}{x^2} \frac{dx}{dt} + \frac{1}{x} \frac{dy}{dt} \right) \\ \frac{1}{\sqrt{1-m}} \cdot \frac{1}{(x^2+y^2+z^2)^{\frac{3}{2}}} \left(xz \frac{dx}{dt} + yz \frac{dy}{dt} - (x^2 + y^2) \frac{dz}{dt} \right) \end{pmatrix} \quad (4.14)$$

where $m = \frac{z}{\sqrt{x^2+y^2+z^2}}$.

If we use Equation 4.13 to compute the (r, θ, φ) -tuple before evaluating Equation 4.14, then we can make use of the fact that $r = \sqrt{x^2 + y^2 + z^2}$ to simplify Equation 4.14. This leads to

$$\begin{pmatrix} \frac{dr}{dt} \\ \frac{d\theta}{dt} \\ \frac{d\varphi}{dt} \end{pmatrix} = \begin{pmatrix} \frac{1}{r} \left(x \frac{dx}{dt} + y \frac{dy}{dt} + z \frac{dz}{dt} \right) \\ \frac{1}{1+\left(\frac{y}{x}\right)^2} \left(\frac{-y}{x^2} \frac{dx}{dt} + \frac{1}{x} \frac{dy}{dt} \right) \\ \frac{1}{r^3 \sqrt{1-\frac{z}{r}}} \left(xz \frac{dx}{dt} + yz \frac{dy}{dt} - (x^2 + y^2) \frac{dz}{dt} \right) \end{pmatrix} \quad (4.15)$$

Using Equations 4.13 and 4.15, it is possible to specify the initial conditions in the familiar Cartesian coordinate system, and then convert them to the spherical coordinate system required by the Gaídukov equations.

4.1.3 Example Solutions to Gaídukov's Equations

Figure 4.1 is a plot of a ball lightning starting at a position 4 m to the right and 3 m away from a hole in a wall, which has a point source of intensity $\gamma = 50$. The

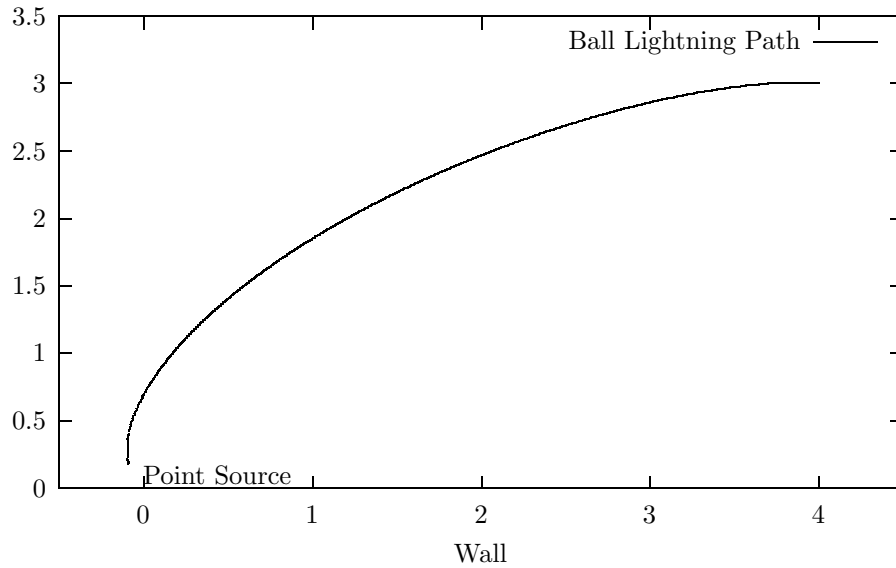


Figure 4.1: 2D plot of ball lightning motion computed from Gaǐdukov’s equations. The lightning starts a position $(4, 3)$ and is drawn toward a point source at the origin.

ball lightning has a radius of 20 cm which is a typical ball lightning radius[125]. The ball lightning is initially traveling with a velocity components of -1.0 m/s in the x-direction (along the wall toward the hole) and 0.1 m/s in the y-direction (perpendicular to the wall). As discussed earlier, the hole in the wall is at the origin. Since the ball lightning is located on the xy-plane, and since there is no initial vertical motion, the motion can be plotted in 2D. Using Equations 4.13 and 4.15, the initial conditions in spherical coordinates are computed. They are

$$\begin{aligned} r &= 5.000 & \theta &= 0.6435 \\ \frac{dr}{dt} &= -0.7400 & \frac{d\theta}{dt} &= 0.1360 \end{aligned}$$

Figure 4.2 is a 3D example. Here the ball lightning starts at the same (x, y) position, but this time it is located 1 m above the hole in the wall. The initial component velocities are 2 m/s toward the hole in the direction of the wall, and 3 m/s upward. There is no initial motion away from the wall. The point source

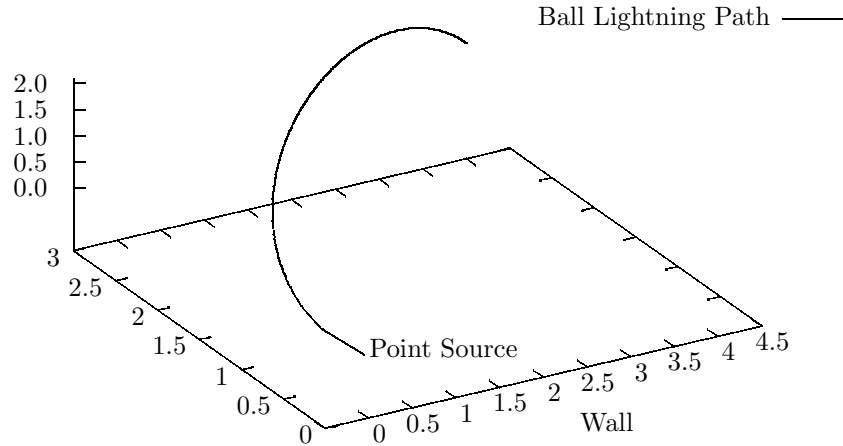


Figure 4.2: 3D plot of ball lightning motion computed from Gaídukov’s equations. The lightning starts a position $(4, 3, 1)$ and is drawn toward a point source at the origin.

intensity is set to 100 and the ball lightning radius is 15 cm. In terms of spherical coordinates, the initial conditions are

$$\begin{aligned} r &= 5.099 & \theta &= 0.6435 & \varphi &= 0.1974 \\ \frac{dr}{dt} &= -0.9806 & \frac{d\theta}{dt} &= 0.2400 & \frac{d\varphi}{dt} &= 0.6983 \end{aligned}$$

4.2 Deformation Through an Opening

Implementing a true fluid dynamical simulation of ball lightning is a difficult problem. Many approximations were necessary to mathematically model the motion of a ball lightning through a circular hole with a radius greater than the ball lightning’s radius[49]. Modelling deformation through a small opening is even more challenging. Gaídukov describes the mathematical difficulties of this problem as “insurmountable”[50].

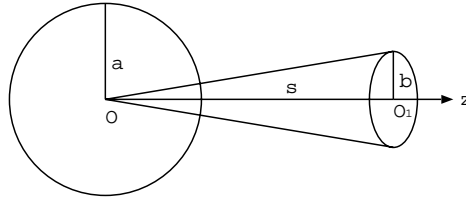


Figure 4.3: Ball lightning approaching a circular hole in a flat screen. Redrawn from Gaídukov 1989[49].

To simplify the model, Gaídukov breaks the problem down into four sub-problems. First, non-deformable motion of ball lightning as it approaches the hole is described by a set of three ordinary differential equations. (See §4.1 for details.) Second, the motion of ball lightning along an axial line toward the hole can also be described mathematically in terms of force. Newton's law, $F = ma$, coupled with Gaídukov's equations[49], predicts that the ball lightning will slow down as it approaches the wall[50]. Third, the motion of a ball lightning as it transforms from a ball into a cylindrical jet of plasma can be described. Finally, the physics describing the transformation from a cylindrical jet of plasma back into a spherical ball is described.

Gaídukov's second subproblem models the approach of a ball lightning toward a circular hole in a flat screen (i.e. a thin wall). The force equations are given in [49] and [50]. They are:

$$F_s = F_1 + F_2, \quad (4.16)$$

$$F_1 = -\frac{2\pi a^3 \rho \gamma^2 s (2s^2 - b^2)}{(s^2 + b^2)^4} \left(1 + \frac{(2s^2 - 3b^2)a^2}{(s^2 + b^2)^2} \right), \quad (4.17)$$

$$F_2 = -\frac{d}{dt} \left(\frac{2}{3} \pi a^3 \rho \dot{s} \right). \quad (4.18)$$

Here, F_1 is the resulting force of the ball lightning interacting with air flow in the hole, and F_2 is the drag force of the ball lightning. The sum of these two forces F_s is the total amount of force on the ball lightning.

Figure 4.3 describes the independent variables. In these equations the hole has radius b which is at least one order of magnitude smaller than the ball lightning's radius, a . γ is the intensity of an annular source per unit solid angle, which is located at origin O_1 . $s > b$ is the distance of the ball lightning from the origin. The ball lightning's velocity is therefore $-\dot{s}$, since it is moving toward the hole. The acceleration of the ball lightning is given by

$$\ddot{s} = -\frac{F_1}{2\pi a^3 \rho} \quad (4.19)$$

In order to physically describe the process of the the ball lightning entering the circular hole, a detailed understanding of the internal structure is required[50]. Since Gaídukov does not intend to determine the internal mechanisms with his work, he again makes assumptions about the internal forces that occur within the ball lightning. The main assumption is that the internal forces of the plasma are sufficiently small and can be neglected when compared to the body forces of the ball lightning interacting with the wall. Gaídukov constructs equations to describe the pressure gradient on the ball lightning which can be used to numerically determine the radius as a function of time. Another system of equations describes the center of mass of a ball lightning with respect to time.

Modelling the outflow from the hole is the final problem that Gaídukov tackles. This process is analogous to that of the ball lightning entering the hole. The center of mass is determined for the outflow. Internal stresses of the ball lightning cause it to reform its spherical shape near the hole with a growing radius.

4.2.1 Graphical Approximation

The physical computations required of Gaídukov's work as a graphical model are tedious, costly, and difficult to implement. The physical description discussed in §4.1, illustrates how solving a simple set of equations can become too cumbersome for

the purpose of computer graphics simulation. Computing an accurate shape for the passage of a ball lightning through a hole in a screen would not be easy. Therefore tools from computer graphics are used to achieve a plausible visual representation, without the deep physical understanding required for a more accurate solution.

It should be noted here that ball lightning is a very rare phenomenon[116]. Since it has not been witnessed by very many people, convincing animations are more easy to generate. Compare this simulation with something commonplace such as a person talking. People communicate with each other every day and the human cognitive system is very attuned to the motion of the facial expressions. Even the slightest error will be perceptible since a lifetime has been spent watching other individuals talk. Watt and Watt[138, p. 412] point out that “the closer the facial model resembles that of an actual human head the more critical is our perception of it.”

Ball lightning is a rare phenomenon. This means that most people have no pre-conceived notion of what it should look like. If it is observed it is a unique experience in most cases. The range of plausible simulation is therefore relatively large and there is room to waver when deciding exactly how physically accurate a ball lightning simulation should be. For this work, it has been decided to forgo some of the accuracy in exchange for ease of implementation, lower simulation time, and simplicity.

From eye-witness reports[60] and physical descriptions[50], it is understood that ball lightning can pass through a narrow hole that has a radius much smaller than that of the ball lightning. The basic description is as such. A spherical ball lightning moves independently through the air until it reaches the hole which it is to penetrate. The lightning ball will slow down when it comes within a distance of two of its radii from the hole. A protrusion will form that extends toward the hole. The ball lightning’s material will form a jet of plasma that flows through the hole. The remainder of the lightning will slowly collapse until all the matter has been exhausted. On the outflow side of the hole, the ball lightning’s internal forces keep the material from dispersing. The ball lightning will slowly increase in radius until it has reached its original radius

and all matter has passed through the opening.

The ball lightning is simulated as a particle system[104]. Each particle is a free-moving, emissive, unit of plasma. For the non-deformable motion of the ball lightning (see §4.1), the particles are free to move within a spherical bounding volume defined by the ball lightning's radius. To model deformation, such a bounding volume is not so easy to define. Therefore a voxel-volume (see §3.2) is instantiated which encompasses the ball lightning, the hole in the wall, and the volume of space where the ejected ball lightning will form. The particles of the ball lightning are then advected through the voxel volume in the same way that fluids would be with a physical simulation. *Determining the direction vectors for each voxel of this volume is the focus of this simulation.* This is very important since the plausibility of the simulation is entirely dependent upon it.

4.2.2 Voxel Volume Initialization

This section discusses how to initialize the voxel volume that will be used to advect an emissive particle system that represents the plasma of a ball lightning. The voxel volume initialization is broken down into four steps or *segments*, which are further discussed below. The first segment pushes the ball lightning slowly toward the hole along an axial line that has its origin at the hole's center. The second segment deforms the ball lightning so that it's plasma will flow into the hole. The third segment advects the plasma through the hole to the other side. Finally, the fourth segment reshapes the plasma into a ball.

Figure 4.4 is a schematic of the voxel volume. The ball lightning starts at the left of the diagram and is forced through the shown bounding volume. Note that the third and fourth segments overlap slightly. The reason for this will be explained below.

When initializing the voxel volume, two opposing corners in world space are provided, as well as a voxel density. From the opposite corners the minimum and maxi-

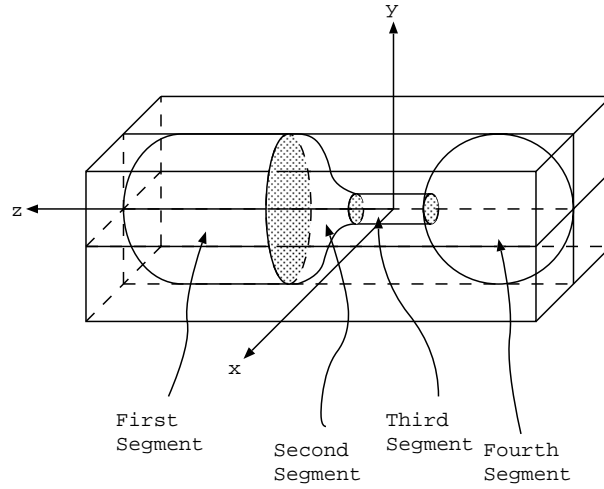


Figure 4.4: Advecting voxel volume for simulating the passage of a ball lightning through a small hole.

imum values are stored in the variables $VVmin$ and $VVmax$.

$$VVmin = (min_x, min_y, min_z)$$

$$VVmax = (max_x, max_y, max_z)$$

The dimensions of the voxel volume are also computed and stored, these are

$$VV_i = VVdensity \cdot (max_x - min_x)$$

$$VV_j = VVdensity \cdot (max_y - min_y)$$

$$VV_k = VVdensity \cdot (max_z - min_z)$$

For this project, linear measurements are specified in decimeters (dm), so the density parameter ($VVdensity$) is specified in voxels per decimeter. Decimeters are a convenient unit since a typical reported ball lightning radius is in the range of 1–2 dm.

The hole start and end points must be defined for the voxel volume. The hole

radius must also be specified. For implementation simplicity, it is assumed that the origin is placed at the center of the hole and that the z-axis runs through the length of the hole.

Voxels within the volume are indexed as (i, j, k) -tuples. Conversion from a point, p , in world coordinates to voxel element indices is done by computing the scalar-vector product of $VVdensity$ with the vector $(p - VVmin)$. The result will be the appropriate (i, j, k) -tuple. To convert from voxel volume indices to world coordinates is also simple. The desired result is achieved by dividing the (i, j, k) -tuple by $VVdensity$ and adding $VVmin$.

The voxel volume is divided into *slices* from left to right in Figure 4.4, or from greatest to smallest z value. Initialization of the advection vectors is done *slice-by-slice*, iterating over k . Each voxel of a slice is visited by iterating over i and j .

First Segment of the Voxel Volume: Forward Motion

For the first segment, the advection vectors are all initialized to $(0, 0, -s)$, where s is the desired speed of the ball lightning per frame. In this way, the ball lightning is slowly pushed toward the hole in the wall. The ball lightning's deceleration to its minimum speed is not explicitly modelled in this simulation.

The number of slices to initialize for the first segment is determined by multiplying the length of the segment (units: dm) by the voxel density (units: voxels/dm). For this implementation, the length of the first segment is chosen to be equal to the diameter of the ball lightning. Iterate from $k = 0$ to the number of computed slices. Then iterate over all (i, j) in each slice and assign the advection vector $(0, 0, -s)$.

Second Segment of the Voxel Volume: The Blob Function

It is desirable to control the shape of the ball lightning when it deforms to fit through a hole. One class of functions that are designed for this purpose are known as *field* functions or “blob” functions. These functions are valid in the domain of $[-1, 1]$ and

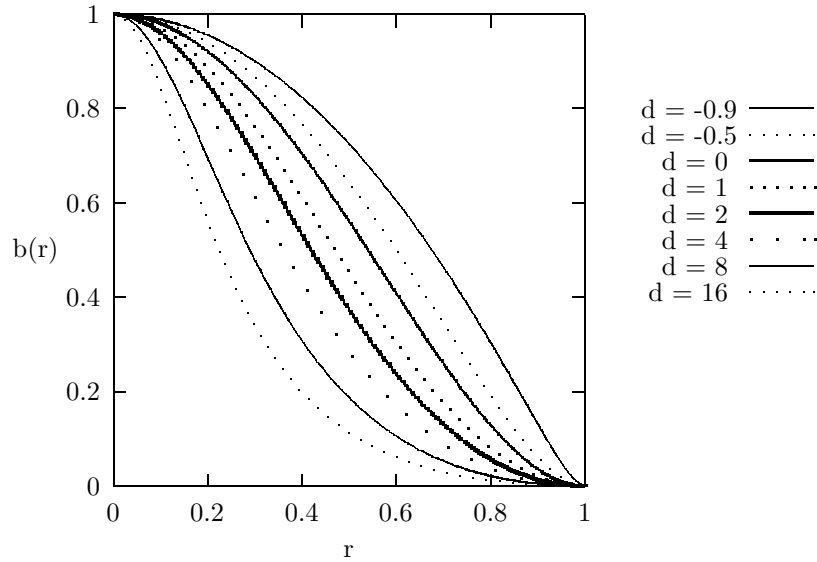


Figure 4.5: Varying the field parameter of the “blob” function provides control over how a ball lightning will flow into a hole in a wall.

have a range of $[0, 1]$. They are monotonically increasing in $[-1, 0]$ and monotonically decreasing in $[0, 1]$. For a blob function $b(r)$, $b(-1) = b(1) = 0$, and $b(0) = 1$. Finally, blob functions have the property that $b'(-1) = b'(0) = b'(1) = 0$.

For this work, the blob function introduced by Baranoski and Rokne[14] was used because it is both efficient and controllable. Efficiency is a concern since the function will be called once for each voxel that is initialized in the second segment. More importantly, their blob function is controllable by specifying a field parameter. Figure 4.5 is a plot of Baranoski and Rokne’s blob function with several values of the field parameter, d . ($r \in [0, 1]$ is the domain that useful for this work.) For their blob function, acceptable values for d are $d \in (-1, \infty)$.

To control the shape of a ball lightning, Baranoski and Rokne’s blob function is used as a curve in the yz -plane — i.e. $y = b(z)$. $b(z)$ is scaled, translated, and then convolved around the z -axis in order to form the shape shown in Figure 4.6. For this project, the domain is scaled to fit one ball lightning radius. The range is

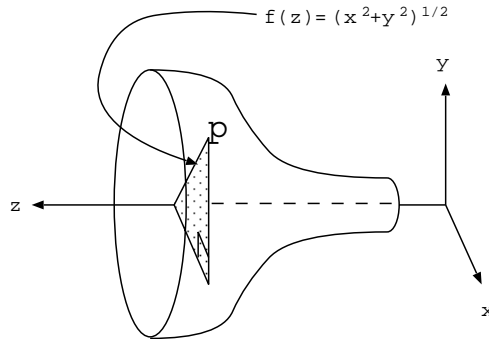


Figure 4.6: A “blob” function that has been scaled, translated, and convolved around the z -axis. This is the desired shape of the ball lightning when it enters a hole in a wall.

scaled and translated to $[r, R]$, where R is the ball lightning’s radius, and r is the hole radius. This modified blob function is very convenient to use, since the current z -axis coordinate is passed in as a parameter, and the range fits the desired shape.

For convenience, the scaled and translated blob function will be referred to as $f(z)$. To convolve $f(z)$, an implicit function $F(x, y, z)$ is defined in the following way.

$$F(x, y, z) = \sqrt{x^2 + y^2} - f(z) \quad (4.20)$$

When $F(x, y, z) = k$, an implicit surface is defined. For different values of k , different concentric surfaces are implicitly defined. Refer to Figure 4.6 to understand the derivation of this implicit function. For any point p on the desired surface, the length of the hypotenuse is given by the Pythagorean theorem. In this case, $h^2 = x^2 + y^2$. Furthermore, $h = f(z)$ by construction. Thus the following equality is obtained.

$$\sqrt{x^2 + y^2} = f(z). \quad (4.21)$$

If $f(z)$ is subtracted from both sides of Equation 4.21, then the obtained implicit

surface is identical to letting $F(x, y, z) = 0$ in Equation 4.20.

$$\sqrt{x^2 + y^2} - f(z) = 0 \quad (4.22)$$

It is convenient to use the name $F(x, y, z)$ to identify the the implicit surface shown in Figure 4.6, because elementary calculus can be used on F to compute the normal at any point p . Recall that the gradient of G , denoted ∇G , yields the desired normals for any implicitly defined surface $G(x, y, z) = k$. Note that $\nabla G(x, y, z)$ is the same no matter what value of k is chosen, since the derivative of a constant is zero. Therefore, $\nabla F(p)$ is the normal of F at the point p , for any $F(x, y, z) = k$.

To create the advection vectors for segment two, the concentric surfaces defined by letting $F(x, y, z) = k$ are used. Algorithm 2 is used to compute the correct direction vector for each voxel in the second segment (which are indexed as (i, j, k) -tuples).

Algorithm 2 Algorithm to compute direction vectors for voxels in segment two

Step 1. Compute the location of the voxel, p , in world coordinates as described at the beginning of this section.

Step 2. Compute the normal vector $\mathbf{n} = \nabla F(p)$.

Step 3. Create a vector $\mathbf{t} = O - p$, where O is the origin.

Step 4. Compute the direction vector $\mathbf{d} = \text{proj}_\pi \mathbf{t}$, where π is the plane defined by the normal \mathbf{n} and the point p .

Step 5. Let $\mathbf{d} = s \frac{\mathbf{d}}{\|\mathbf{d}\|}$, where s is the desired speed per frame.

The projection of a vector \mathbf{t} onto a plane, π , is denoted $\text{proj}_\pi \mathbf{v}$. The only unexplained idea in Algorithm 2, is this projection which is used in Step 4. Informally, the world coordinate system defines a vector space that is labelled \mathbf{R}^3 . Any plane in \mathbf{R}^3 defines a proper subspace. Introductory linear algebra texts such as [8] or [83] will provide an algorithm for projecting a vector onto a subspace. The only problem is to find two basis vectors in \mathbf{R}^3 which define the plane.

To find such a basis, choose an arbitrary vector, \mathbf{i} , whose inner product (or dot product) with \mathbf{n} is 0. This is easy to achieve since the inner product is defined as $\langle \mathbf{i}, \mathbf{n} \rangle = i_x n_x + i_y n_y + i_z n_z = 0$. Simply choose two of \mathbf{i} 's components randomly and solve for the third. Now compute the cross product of \mathbf{i} and \mathbf{n} to find the second basis vector \mathbf{j} . Normalize \mathbf{i} and \mathbf{j} , and the basis has been found. There is one small detail left to consider: \mathbf{i} and \mathbf{j} form a basis for the plane that contains the origin of the world coordinate system, and not the point p as desired. Either a translation must be introduced, or a quick check can be performed to determine if the computed direction vector is in the correct direction. To implement the “quick check,” simply test the sign of the d_x . If it is positive, let $\mathbf{d} \rightarrow -\mathbf{d}$.

One final note must be made with respect to segment two. The discussion above describes how to advect plasma particles toward the hole. Particles that are close to the z-axis need not be redirected. Therefore, voxels that are within one hole radius of the z-axis are assigned the advection vector $(0, 0, -s)$.

Third Segment of the Voxel Volume: Through the Hole

The third segment describes the hole in the voxel volume. Since the wall is a physical boundary for the plasma particles, it is necessary to contain the particles within this boundary with vectors that point to the z-axis. For a small radial distance further than the hole radius, the advection vector should be computed as

$$\mathbf{d} = (0, 0, z) - p,$$

where z is the z-coordinate of the current slice and p is the coordinate location of the current voxel, relative to the origin of the voxel volume. \mathbf{d} should be normalized and scaled appropriately.

Within the hole itself, plasma particles are pushed in the direction of $\mathbf{d} = (0, 0, -1)$. Unlike the first segment, the velocities through the hole are scaled based on their dis-

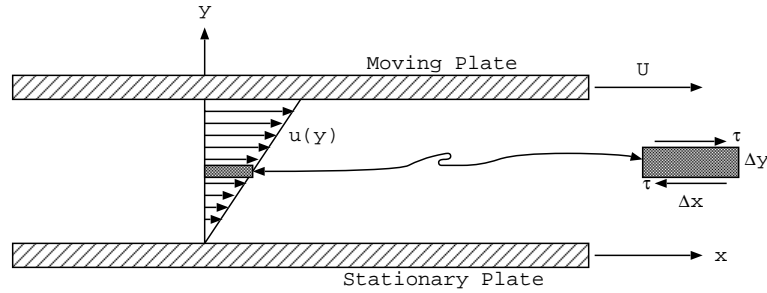


Figure 4.7: Fluid flow between parallel plates is used to illustrate viscosity. The velocity function $u(y)$ is linear across the channel. It is $\mathbf{0}$ across the bottom and \mathbf{U} at the top. The shear stress is illustrated with the enlarged element. Redrawn from William F. Hughes & John A. Brighton 1999[67].

tance from the wall of the hole. This is an approximation to the fluid dynamic principle of viscosity[67]. Viscosity is demonstrated in Figure 4.7. The bottom plate is stationary while the top plate moves with a velocity \mathbf{U} . The fluid moves with a velocity of \mathbf{U} near the top plate and with a velocity of $\mathbf{0}$ at the bottom plate. The change in velocity for every simple fluid is linear, thus the velocity differential is a constant. The stress from shear is also constant and the following statement can be made.

$$\tau = \mu \frac{\partial u}{\partial y} \quad (4.23)$$

In Equation 4.23, τ is the shear stress, and μ is the viscosity. $u(y)$ is the linear function shown in Figure 4.7, thus $\frac{\partial u}{\partial y}$ is also a constant.

The principle of viscosity causes the fluid to move faster at the center of a pipe than near the walls. This is simulated by computing a scaling factor for $(0, 0, -1)$ based on the distance from the pipe wall. For this work, the scaling factor was determined with the following calculation.

$$scale = c \frac{r - \sqrt{x^2 + y^2}}{r} + 1.0, \quad (4.24)$$

where $0 \leq c \leq 1$ is a control constant, r is the radius of the hole, and (x, y) is the point in a plane perpendicular to the z -axis which runs through the center of the hole.

Fourth Segment of the Voxel Volume: Ball Lightning Reformation

The fourth segment does not advect the plasma particles like the other segments do. It is possible to implement advection here as well, but it is unnecessarily expensive. A simpler stochastic process will work. According to Gaídukov[50], the plasma ball should grow in radius as material is ejected from the hole in the wall. To contain the plasma particles within a growing ball lightning, it is only necessary is to check that the randomly moving plasma particles are kept within the current radius.

Although, implementation of a time-dependent radius would not be difficult, this physical detail was ignored in this project. Instead a static radius was implemented and the plasma particles propagate through the new volume with random direction vectors.

Notice in Figure 4.4, that segment three is extended into the final sphere radius. This is necessary for implementation reasons. The plasma particles must be advected sufficiently far into the new ball lightning volume in the third segment so that they end up in the containment sphere that bounds the new ball lightning location.

Figure 4.8 illustrates how to compute the length of the extension. The geometry is simple when projected into the plane. R is the ball lightning radius, and r is the hole radius. When projected, they form a circle and a rectangle respectively. The dashed line is the extension required so that the plasma will reach the ball lightning circle. By construction, the length of the extension is

$$l = R - \sqrt{R^2 - r^2}.$$

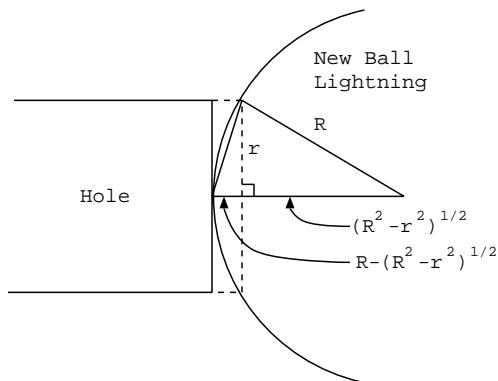


Figure 4.8: Extending the hole into the new ball lightning volume is necessary in order to transport the plasma particles. This figure illustrates how to compute the length of the extension. R is the new ball lightning radius, and r is the radius of the hole.

4.3 Rendering

In §4.1 and §4.2 the techniques used to animate the motion of a ball lightning were discussed. In this section, the methods used to model a static ball lightning and render a single frame are examined. The rendering procedure is identical for both non-deformable and deformable motion.

Rendering a final ball lightning image is a three step process. First, there are two distinct rendering phases. A different technique is used to render the emissive plasma particles of the ball lightning from that used for the background scene. Both techniques could be merged into one rendering phase, but for this work the ball lightning is rendered separately from the background scene. The third phase is to composite these two resulting images.

In §4.3.1 the basic ball lightning model is discussed. Also in that section, the rendering technique is discussed. In the following section, the methods used to composite the ball lightning image with a raytraced background scene are detailed. The raytracing technique was reviewed in §3.1, so the discussion will not be repeated here.

4.3.1 Basic Ball Lightning

Even though dispute exists (see §2.5), this work assumes that ball lightning has a plasma nature. As described in §2.3, a plasma is a super-heated gas. Thus it can be approximated with a fluid model. Since modelling plasma at the atomic particle level is intractable, the number of particles in the simulation is reduced to a computationally feasible number by letting each particle represent a unit of plasma. Furthermore, recall from §2.3, that particles (or ions) in a plasma have a large electromagnetic volume of influence. That is to say that plasma ions strongly attract and repel each other depending upon their charge. This is different from an inert gas whose molecules only interact if they collide. Unfortunately, including this property in a simulation would be very expensive. In the future when the detailed structure of ball lightning is understood, it may be necessary to perform an accurate plasma simulation in order to obtain more physically accurate results. Until that time, approximations will have to suffice.

For this work, a non-deformable ball lightning is stored as a location, a radius, and a colour. The colour is stored as red, green, blue, and alpha channels (RGBA). It is convenient for this model to let 0 represent perfect transparency and 1 represent perfect opacity. In this way, the total transparency for a pixel is the sum of the alpha values projected onto that pixel. The user can also specify a *glow width* and a *glow colour*. The glow width and colour are used to simulate a *shell* which has sometimes been described in ball lightning sightings.

Associated with the ball lightning is a particle system[104]. Each particle represents a unit of plasma and is assigned a random velocity vector with the a user supplied magnitude. This user supplied magnitude is called the *particle speed*. As mentioned above, the particles do not interact with each other. If a particle is about to move outside the volume of the ball lightning, it is given a new, random, direction. Finally, each particle is initialized with a lifetime. The user supplies an *average lifetime* and a *lifetime delta*. The lifetime distribution for this project is uniform, which

gives the ball lightning a soft looking decay. With each frame, the remaining lifetime of each particle is decreased until it reaches zero. At this point, the particle is no longer considered to be emissive.

Particles are represented as a 3D point. Raytracing individual particles is not appropriate since the probability of a ray-particle intersection is almost zero. Another reason to not raytrace the plasma particle system is that plasma is an emissive light source. It is more realistic to treat each unit of plasma as a light source than as an object with reflective and transmissive properties.

To render a ball lightning, 1000–300000 particles may be used. With the number of required particles it is impossible to treat each as a point light source in a ray tracer. As a consequence, a splatting (or forward mapping) mechanism is used to render the ball lightning. Splatting is discussed in §3.2, but for the sake of clarity, a quick review of the important points is provided here.

The output image buffer (sometimes referred to as a *screen* or a *raster*) is initialized to be perfectly black and transparent. In other words the output buffer is initialized with all zeros. The particle set is traversed. Each particle's position is mapped through a projection transformation. For this project a typical raytracing perspective transformation[113] is used. If the particle intersects a pixel in the output buffer (or in raytracing terms — if the ray from the eye to the particle intersects the screen plane) then it's colour contribution (including alpha channel) is added to the existing buffer value. Every particle is assigned the same colour, unless the user specifies a *glow width* greater than zero. Then the colour of a particle is determined by computing its radial distance from the center of the ball lightning. Note that the red, green, blue, and alpha channels are all capped at a maximum value of 1.0.

This is how the output image is generated for a particle set which represents a ball lightning. The only required information for each particle is the position in world coordinates and the colour (including alpha value). It does not matter whether the particle set represents a spherical ball lightning or one that is deforming through a

hole.

4.3.2 Compositing

Note that in the previous section, the output image only displays the ball lightning. No other scene objects are displayed. These are rendered separately using standard raytracing techniques. Further note that the background scene must only be raytraced once for each view point in an animation. Since a detailed rendering is time consuming to produce, it saves a lot of computing time if the rendering process is split up into two steps.

In order to properly composite a ball lightning image and a raytraced background scene, there is one detail concerning the output of a ball lightning image that must be discussed. When raytracing the background scene, the *z-buffer* algorithm[63] is used for occlusion detection. A z-buffer has the same dimensions as the output image. Typically each z-value is initialized to a really large number that is close to the maximum value that can be represented with the floating point number system of the machine. If an object is struck by a ray, its distance to the eye point is computed and compared with the value stored in the z-buffer. If this computed distance is less than the stored z-value, the shading calculations are performed and the z-buffer value is replaced with the computed distance.

After the background scene is raytraced, the z-buffer is output. This z-buffer is used as input to the ball lightning rendering program. When rendering a particle, the distance between the particle and the eye point is computed. If this distance is greater than that stored in the z-buffer, then the particle is ignored. The z-buffer is not updated when rendering a ball lightning image. Using the z-buffer in this way makes the compositing process simple since occluded ball lightning plasma is not rendered.

Once the background and the ball lightning images are complete, the compositing process is simple. The final image is composited pixel-by-pixel. If C_{bl} is the colour

stored for a pixel in the ball lightning image, and C_s is the colour stored in the corresponding pixel of the background scene, then the red, green, and blue components of the final image pixel, C_f , are computed as

$$C_{f.r} = (C_{bl.\alpha}) C_{bl.r} + (1 - C_{bl.\alpha}) C_{s.r}$$

$$C_{f.g} = (C_{bl.\alpha}) C_{bl.g} + (1 - C_{bl.\alpha}) C_{s.g}$$

$$C_{f.b} = (C_{bl.\alpha}) C_{bl.b} + (1 - C_{bl.\alpha}) C_{s.b}$$

where $C_{bl.\alpha}$ is the alpha component of the ball lightning image pixel.

There is one limitation with this compositing process. A ball lightning cannot pass behind a transparent object in the scene. In order to implement this feature, the above equations would need to include the alpha value for the background scene and z-buffer information for both images.

Chapter 5

Conclusion

This thesis presents the first computer graphics model of ball lightning. The model is based on the underlying physics of ball lightning; but as discussed in Chapter 2, the physical nature of the phenomenon is not well understood. Thus the approach taken has been to use existing computer graphics techniques that are easy to implement (see Chapter 3) in order to approximate deformation of the ball lightning; and to use fluid dynamical results to describe the path taken by the ball lightning when affected by an air current. In this way customizable animations of ball lightning can be created, with a reasonable amount of automation.

This chapter first demonstrates the results of this thesis in §5.1. Then in §5.2, efficiency issues are considered. Future considerations are presented in §5.3, before the concluding remarks are made in §5.4.

5.1 Results

A novel model for simulating the ball lightning phenomenon is presented in this thesis. A combination of common numerical and computer graphics techniques are used to animate the ball lightning. Motion of the ball lightning through the air toward a hole can be easily obtained by numerically solving a set of differential equations,

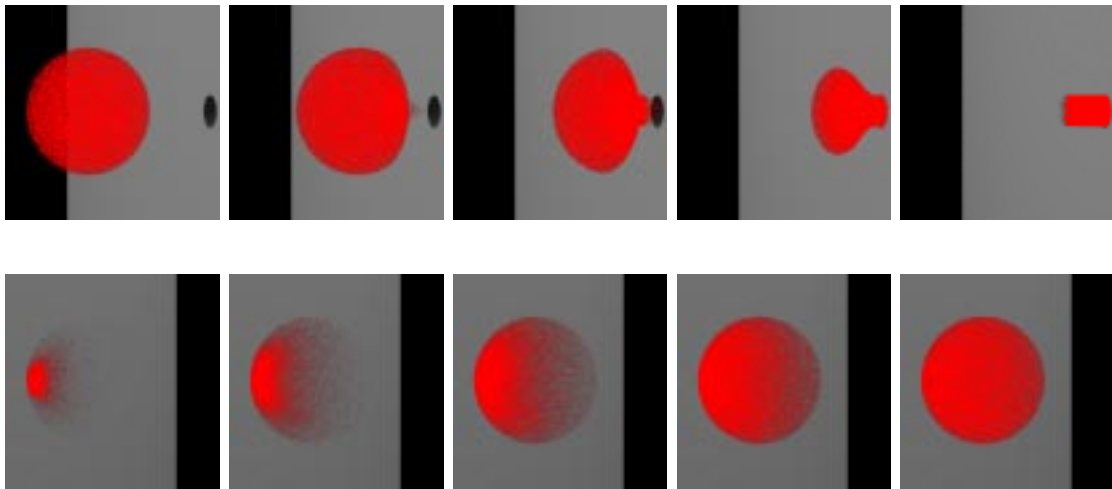


Figure 5.1: Deformation of a ball lightning through a hole in a wall. This sequence of images shows selected frames of an animation of a ball lightning which is passing through a hole in a wall.

using standard techniques. Deformation of a ball lightning through a small opening is simulated by using efficient computer graphics techniques, that are easy to implement.

Figure 5.1 is a sequence of images from an animation of a ball lightning passing through a hole in a wall. Notice the curved shape of the deformation as the ball lightning approaches the wall. The shape is controlled by a *blob* function as discussed in Chapter 4. Concentric blob functions deform the ball lightning until it takes the form of a jet which represents the hole in the wall.

There are many parameters to the ball lightning which can be used to obtain desired visual results. Figure 5.2 is a screen capture of the graphical user interface (GUI) used to test the various parameters. The left hand side of the GUI controls the various model parameters. The right hand side controls the camera angles and video output parameters. The visual parameters are most important to this section and are discussed below. As a technical detail, the GUI was implemented with the QT technology using the concepts provided in Dalheimer's book[34]. The *Create Animation* button invokes the simulation with the parameters specified by the GUI controls. The simulation generates a series of scene description files that describe the

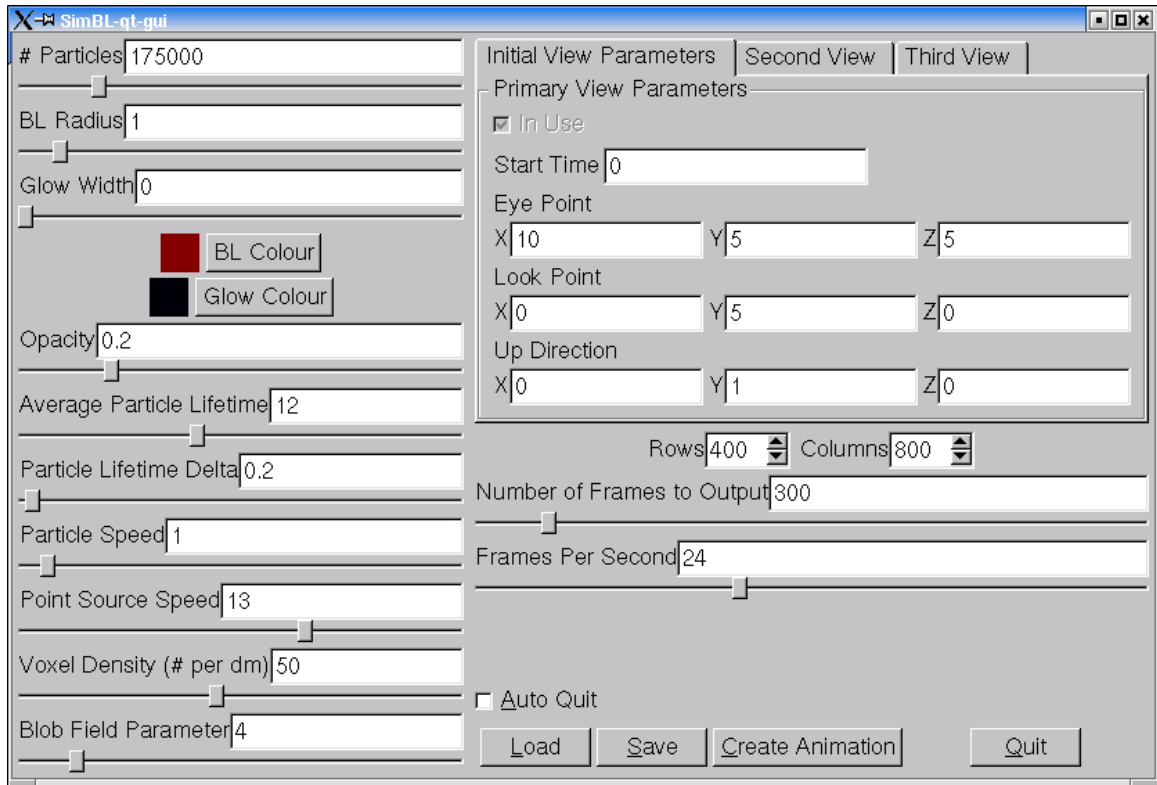


Figure 5.2: GUI used to configure visual ball lightning properties.

motion of the ball lightning particles.

Figure 5.3 demonstrates the effects of varying the number of particles in a ball lightning rendering. In this sequence of images, each particle is opaque. Therefore, each pixel in the output image that is struck by a particle receives no colour contribution from the background scene. Note that each particle is assigned the colour $(0.235, 0, 0)$, which is reasonably dim. In Figure 5.3(b), there are 75000 opaque particles. Notice how some pixels have only been struck by a few particles and as such, the pixel is a very dark red. Other pixels have been struck by many particles and are bright red. Figure 5.3(a) is mostly dark, whereas Figure 5.3(d) is almost completely red.

Figure 5.4 demonstrates the effect of altering the opacity of the particles of a ball lightning. Notice the obvious transparency of the ball lightning in Figures 5.4(a)–

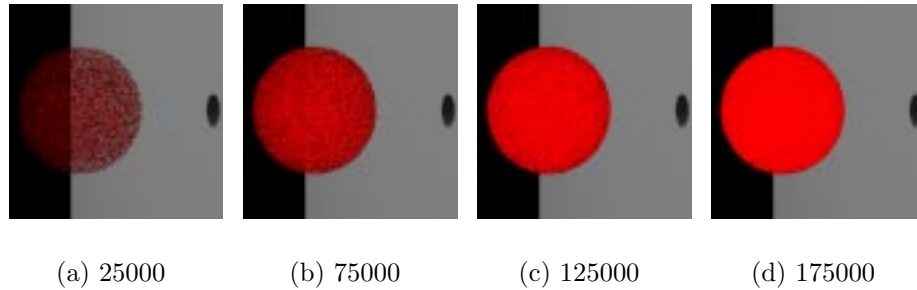


Figure 5.3: Increasing the number of particles of a ball lightning. The particles are rendered with an opacity of 1.0, which makes each pixel that is struck by a particle opaque. The number of particles in each image is shown.

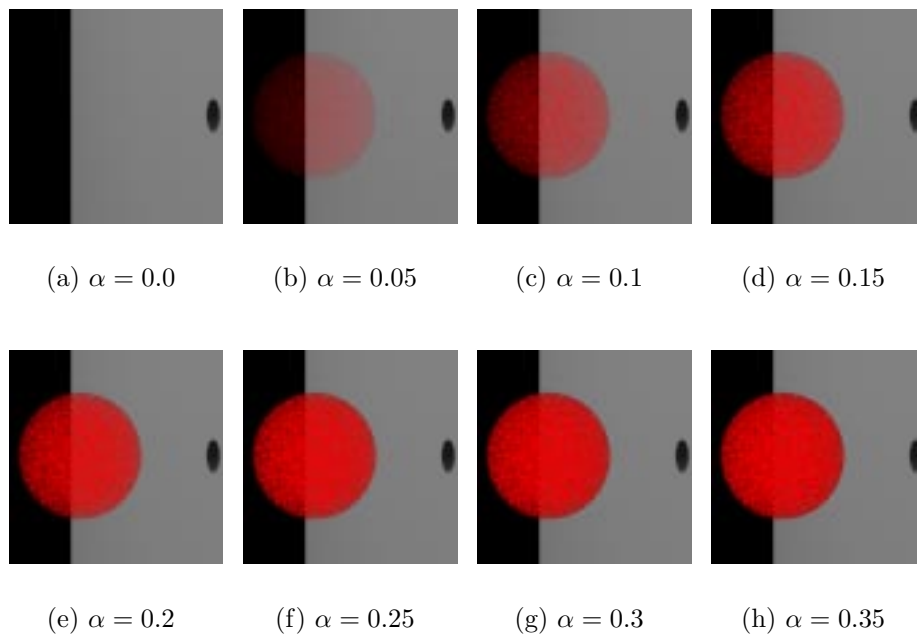


Figure 5.4: Increasing the opacity of the particles of a ball lightning rendered with 70000 particles. Image (a) is rendered with an opacity of 0. Opacity increases with a step size of 0.05 in each image.

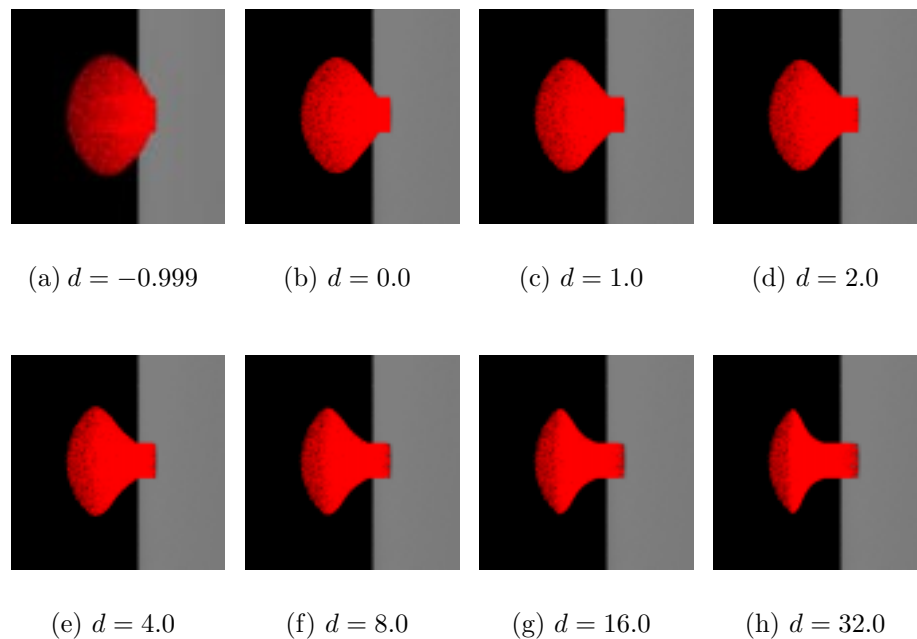


Figure 5.5: Varying the “blob” function field parameter yields drastically different deformations of the ball lightning as it enters the hole in the wall. The field parameter, d , increases non-linearly for images (a)–(h).

5.4(e), and the opacity in Figure 5.4(h). Figures 5.4(f) and 5.4(g) have a slight transparency. The particles in Figure 5.4(a) have a transparency of $\alpha = 0.0$, which makes the ball lightning perfectly transparent. The particles in Figure 5.4(b) have a transparency of 0.05, and are just barely visible. In Figure 5.4(h), the ball lightning has almost no transparency. This is due to the fact that each particle contributes a value of 0.35 for the transparency to the pixel is mapped to; and as such, if three or more particles map to the same pixel, then the transparency component of each pixel will sum to a value greater than 1.0. (Recall that RGB and α values are capped at 1.0, since colour normalization is being used.)

Figure 5.5 demonstrates the results of varying the field parameter, d , of the *blob* function[14]. In Figure 5.5(a), the ball lightning is *ballooning* toward the hole in the wall; whereas in Figure 5.5(h), the ball lightning takes on a mushroom shape. Figure 5.5 clearly demonstrates the utility of using the blob function to deform the ball

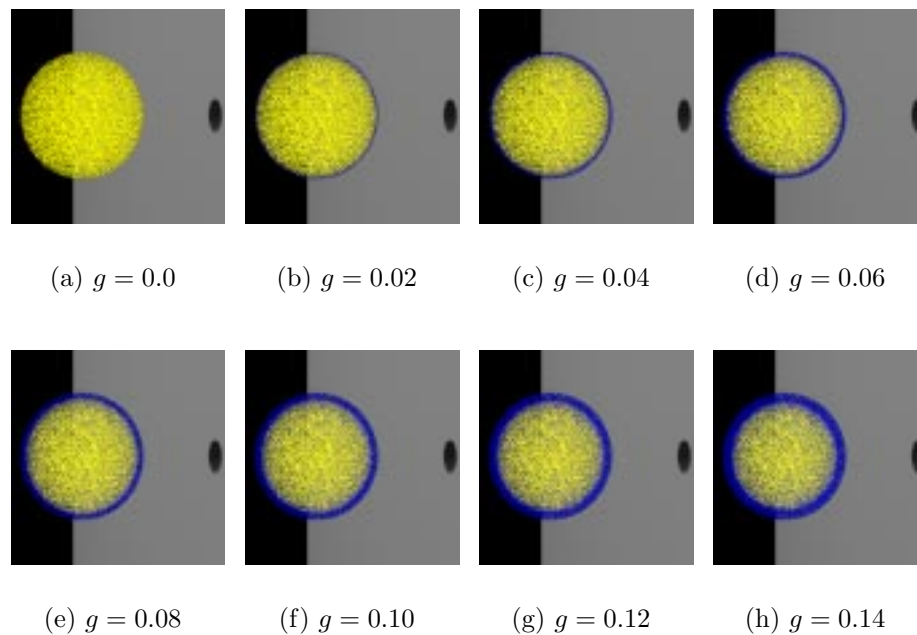


Figure 5.6: Varying the glow width parameter, g , creates different effects for the ball lightning. In image (a) there is no glowing shell. In images (b)–(h) the colour of the glowing shell contributes to the colour of the ball lightning.

lightning. The controllability is very valuable when attempting to mimic eyewitness reports of the phenomenon.

Figure 5.6 demonstrates one of the visual parameters that can be used to effect the look of the ball lightning model — that is the *glow width*, which is denoted g . The glow width parameter is related to three other parameters: *radius*, *colour*, and *glow colour*. As mentioned earlier, the radius of the ball lightning is specified in decimeters. Similarly, the glow width is specified in decimeters, and the value must be less than the radius. The two colours are specified as an RGB triple, whose values are in the range of $[0, 1]$.

When outputting a ball lightning scene file, there is one thing to consider: is the ball lightning being deformed or not? For a non-deformable ball lightning rendering, particles that are a radial distance less than $r - g$ are coloured with the ball lightning colour, where r is the radius. Particles with a radial distance greater than $r - g$ are

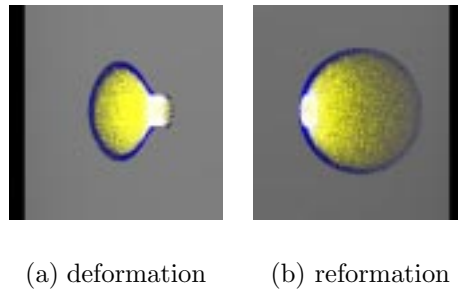


Figure 5.7: This figure illustrates the effects of using a non-zero value for the *glow width* parameter for a deforming ball lightning. Image (a) shows the ball lightning entering a hole in a wall. Image (b) illustrates the reformation of the ball lightning on the other side of the hole.

rendered with the glow colour.

It is less convenient to render a ball lightning that is deforming through a hole in the wall with this two colour system. Before the ball lightning begins to deform, each particle is assigned the appropriate colour based on radial distance. Then the colour associated with each particle is used to render the ball lightning, instead of radial distance. The results of this are shown in Figure 5.7. Good results are obtained for Figure 5.7(a) because concentric blob functions are used and the particles are advected concentrically. When the ball lightning is reforming after passing through the hole, the radius and the glow width are used once again to determine the particles colour, as shown in Figure 5.7(b).

The *average particle lifetime* and *particle lifetime delta* attributes control the lifetime of the ball lightning. The lifetime of each particle is determined randomly from these two parameters. The lifetime is chosen with a uniform distribution in the range $[\mu - \delta, \mu + \delta]$, where μ represents *average particle lifetime*, and δ represents *particle lifetime delta*. Using a large value for the lifetime delta will make the ball lightning fade away more slowly.

The *particle speed* parameter (specified in dm/s) is used to specify the speed that the particles move within a non-deformable ball lightning. Altering this parame-

ter does not greatly affect the animation if there is a sufficient number of particles. Although, if the speed is set to zero then there is no internal motion for the ball lightning, and the animation has an unrealistic, static look. If there are very few particles, then an animation rendered with a slow particle speed will be distinguishable from one rendered with a high particle speed. Unfortunately, it is not easy to demonstrate this with an example in print.

There is one technical detail to worry about with the implementation of the *particle speed* parameter. If the particle speed is an order of magnitude smaller than ball lightning radius, then there is no difficulty; but as the magnitude of the particle speed approaches the linear distance of the ball lightning radius, then a particle may move far outside the ball lightning within the time span of one frame¹. Thus, to advance the animation, each frame must be broken down into smaller time steps.

The *point source speed* parameter is used to specify the magnitude for the vectors in the voxel volume portion of the simulation, which determine how fast the ball lightning proceeds through the hole in the wall. This parameter does not affect the visual quality of the ball lightning animation. It only affects the amount of time necessary for the ball lightning to proceed through the hole in the wall.

The *voxel volume density* is the final parameter to discuss in this section. This parameter is specified in voxels/dm. A larger voxel density will consume more memory resources, but will have the potential to be more accurate. For the animation depicted in Figure 5.1, a ball lightning with a radius of 1 dm was rendered with a density of 50 voxels/dm. The total amount of memory required by the simulation was 278.8 MB. More discussion on efficiency issues are provided in §5.2.

¹The standard duration of a frame is $\frac{1}{24}$ th of a second.

Memory requirements for various voxel densities				
Voxel density (voxels/dm)	25	50	75	100
Maximum Requirement (MB)	8.58	68.66	231.74	549.32
Practical Requirement (MB)	5.95	36.76	122.89	296.00

Table 5.1: Memory requirements for implementing a voxel volume with various voxel densities. The theoretically calculated maximum memory requirement for each density is listed in the second row. The third row displays the actual amount of memory allocated by the simulation. Note that some memory saving enhancements are employed.

5.2 Efficiency Considerations

In this section, efficiency issues are discussed. The model for rendering an animation of a ball lightning discussed in Chapter 4 of this thesis is reasonably efficient. There is, of course, room for improvement. This will be discussed in §5.3.

Simulation

As described in §4.1, a non-deformable ball lightning is represented with a particle system. Particle systems are well understood and are quick and efficient when used for simulation purposes[104]. For a non-deformable ball lightning the particles are constrained with a simple Euclidean distance calculation. The most time consuming aspect of simulating a non-deformable ball lightning is the output of the ball lightning scene description files to disk.

Simulation of a ball lightning deforming through a hole is much more computationally expensive. There are two factors which largely affect the efficiency of this part of the simulation. These are: voxel density, and number of particles. Increasing the voxel density increases the memory requirements cubically. If the voxel volume can be contained in main memory², then it is only the initialization phase that is slowed down. This is due to the fact that the containing voxel for a given particle is

²For this thesis, *main memory* refers to the random access memory (RAM) of the machine. It is defined as the fast storage device that contains the currently executing program and the program data.

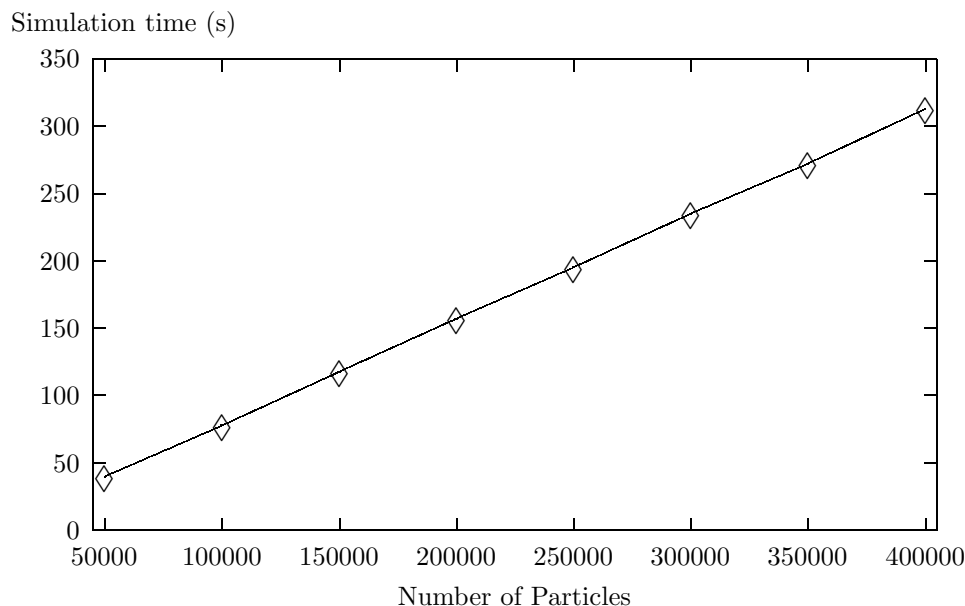


Figure 5.8: This plot shows the relationship between the number of particles and the simulation time. Notice the linearity of the graph.

computed quickly. (See §4.2 for details.) On the other hand, once the voxel volume is too large to be contained in the computer's main memory, then the simulation slows down enormously. This is due to the fact that voxels are accessed randomly, and because main memory must be supplemented by using the computer's disk, or permanent storage device. It is typical for a computer's disk to be an order of magnitude slower than the main memory.

Table 5.1 summarizes the amount of required memory for various voxel volume densities. The first row lists the voxel density. The second row shows a simple calculation of the maximum amount of memory required to initialize every voxel of the respective voxel volumes. Not all voxels need to be initialized — for example, voxels radially distant from the hole in the wall can be ignored. Thus the third row of Table 5.1 displays the total memory usage by the simulation for each density. Notice the dramatic increase in memory usage as density increases. Trials show that a voxel density of 25–50 voxels/dm are sufficient for most simulations.

The second factor which slows down the simulation of a deforming ball lightning

Effect of increasing number of particles on rendering time								
Number of particles ($\times 1000$)	50	100	150	200	250	300	350	400
Rendering time (s)	0.40	0.59	0.77	0.97	1.13	1.46	1.52	1.73

Table 5.2: Increasing the number of particles affects the rendering time .

is the number of particles. Increasing the number of particles increases the running time of the simulation linearly. Each particle accesses a voxel which is stored in a random portion of memory. Thus hardware devices such as memory caches do not improve performance of the system. Figure 5.8 is a plot that demonstrates the linear relationship between number of particles and simulation time.

Note that increasing the number of particles also increases the memory requirements linearly. For all the animations produced in this work, the memory requirements for the voxel volume strongly outweighed the memory requirements of the particle system. To further lower the memory requirements of the particle system, when necessary, each particle was assigned a reference to a colour instead of storing a unique colour for each particle.

Rendering

The *splatting* method (discussed in §3.2) used to render a ball lightning is very efficient. Table 5.2 provides some timings for rendering ball lightning images containing various numbers of particles. Figure 5.9 is a plot of the data in Table 5.2. The relationship between number of particles and rendering time is approximately linear³. Note that the rendering times are all less than two seconds. Thus the splatting technique is very efficient. Consequently, the bottle neck with rendering ball lightning images with this model is the time required to read the input files off of the computer's disk.

As mentioned above, one of the most time consuming aspects of the rendering

³It is difficult to get accurate measurements because the rendering time is so short. Hence the plot in Figure 5.9 is not as smooth as the plot in Figure 5.8.

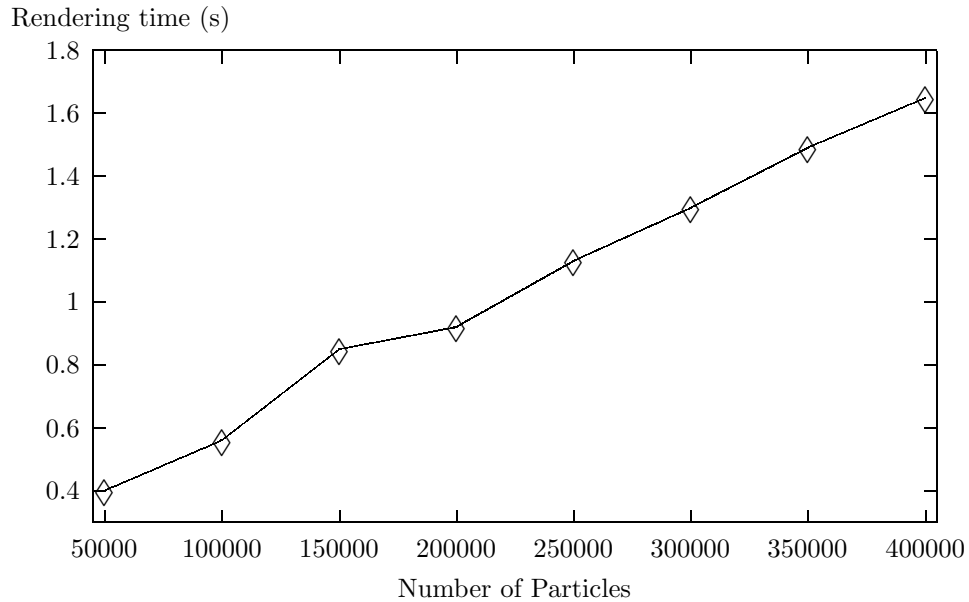


Figure 5.9: This is a plot of the data in Table 5.2. It shows how the rendering time increases linearly with number of particles.

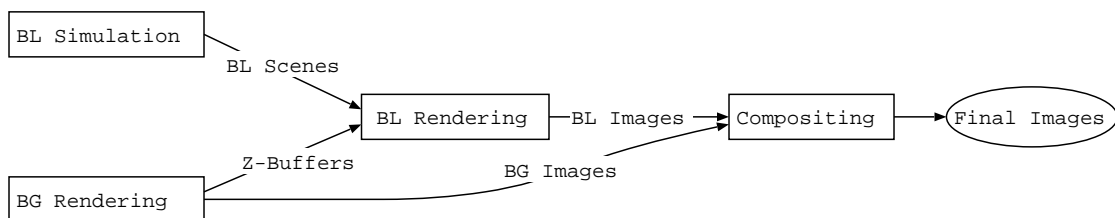


Figure 5.10: This figure describes the simulation rendering pipeline. The ball lightning (BL) simulation generates ball lightning scene description files. Simultaneously, a raytracer generates a set of high detail background images (one per camera position), and the corresponding z-buffer files. The ball lightning rendering phase uses the output ball lightning scene files and the z-buffer files as input, and outputs a set of ball lightning images. Finally, the background (BG) images and the ball lightning images are composited into a final image.

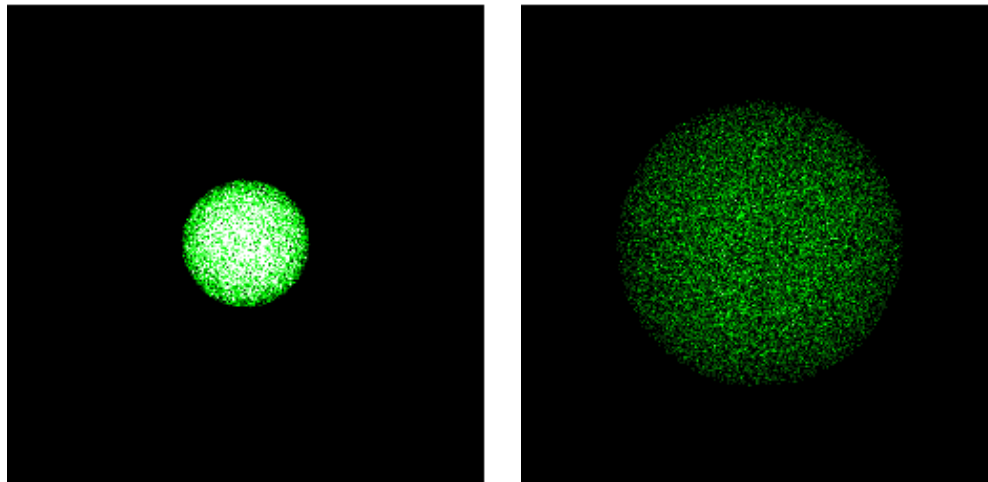
process described in §4.3 is disk I/O. Figure 5.10 summarizes the rendering process. To create an animation of a ball lightning, hundreds of ball lightning scene description files are output by the simulation. For example, a ten second animation requires 240 scene files to be output. For each camera angle in the final animation, one high detail scene (which does not contain the ball lightning) is rendered. When rendering these high detail scenes, the respective z-buffers are output. These z-buffers are used as input to ball lightning rendering phase. Each ball lightning scene file must be read in one at a time, in order to render a ball lightning image. Finally, each ball lightning image file is composited with a background scene file in order to output the final image. There are many inefficiencies introduced due to the superfluous reading from, and writing to, the computer's disk. How to overcome some of these difficulties will be discussed in §5.3.

Ease of Implementation

Ease of implementation is a very important efficiency consideration. The computer graphics techniques utilized in the model and described in Chapter 4 are all straight forward and easy to implement. As such, results can be obtained quickly. Particle systems, splatting, voxel volumes, blob functions, vector arithmetic, and bounding spheres are all used regularly in the discipline of computer graphics. On the other hand, *not all* of these techniques may be used in every specialty. None-the-less, there are numerous texts that describe the necessary implementation details.

The mathematics required to implement a numerical solution to a set of ordinary differential equations can seem oppressive to many software developers. Crenshaw[33] has written a practical text for the mathematically challenged that provides extensive code samples. Furthermore, solving this set of differential equations is not strictly necessary and can be omitted from the model. Using a spline curve to represent the motion of a ball lightning is a possible simplification.

The most challenging aspect to implement for this model is the voxel volume.



(a) Far proximity

(b) Near proximity

Figure 5.11: These two images demonstrate how a lack of adaptation causes artifacts when the proximity of the ball lightning changes sufficiently. Image (a) shows a ball lightning that is far away from the viewer. It has been rendered with 100000 particles. Image (b) is the same ball lightning viewed up close. As the ball lightning approaches the viewer, more particles are required since their colour contributions are splatted on a larger area of the image plane.

Care must be taken any time a continuous space is discretized into voxels. *Off-by-one* errors are easy to introduce, and sometimes small *epsilon* values must be used for comparisons.

5.3 Future Considerations

In this section some future considerations are discussed. The most severe limitation of this project is the lack of adaptation. Figure 5.11 demonstrates this problem. Figure 5.11(a) is a typical ball lightning viewed from a distance. The ball lightning is rendered with 100000 particles. In Figure 5.11(b) the same ball lightning with the same number of particles has approached the viewer. Since the same number of particles are used for the rendering, and since they contribute to a larger area of the view plane, the colour of the ball lightning is strongly dimmed. Adding a feature to

adaptively change the number of particles according to the ball lightning's proximity to the viewer would be necessary to fix this problem.

The model described in this thesis uses a very simple design for animating the internal motion of a ball lightning. Very little is assumed about the internal structure of the ball lightning. This is largely because most ball lightning sightings occur at a distance. Sometimes, close encounters are reported and fine details have been observed[3]. In these reports, ball lightning is often described as having an internal structure that resembles the fluff from a poplar tree or knotted thread. This thesis makes no attempt to simulate such internal structure. In the future, experiments could be performed in order to improve upon this. For example, the "inverse" particle system animation method described by Ebert in chapters six and seven of Ebert et al.[40] could be used to add turbulence that may improve the visual quality of an animation of a close encounter. One report provided in [60] stated that a ball lightning was "composed of a vast number of smaller balls, in fact dots." Therefore, making use of a particle system is a realistic approximation for some events.

For the voxel volume initialization phase of the simulation (described in §4.2.2), one unrealistic simplification was made. The majority of the advection vectors have the same magnitude. This problem is evident in Figure 5.5(h). One can see how condensed the plasma particles have become in comparison to Figure 5.5(a). This issue should be addressed in future versions of the simulation. One possible solution to this problem is to use the gradient of the blob function to appropriately scale the advection vectors in the voxel volume.

As mentioned in §4.2.2, a static radius is used for a ball lightning that is reforming from a hole in a wall. It would be more physically accurate to use a radius that enlarges with time. According to Gaǐdukov[49], a ball lightning will slowly increase in radius as the plasma is ejected from the hole in the wall. In the future it would be good to add such functionality to the simulation to increase the physical reality. Such a feature could be implemented by slowly shifting the center location of the ball

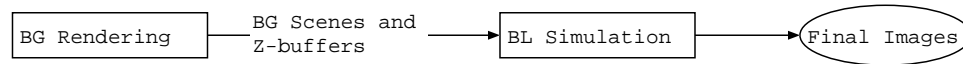


Figure 5.12: This figure represents a proposed rendering pipeline. By putting more functionality into the simulator, fewer temporary files are needed to convert between several small programs. With this pipeline, the background (BG) scenes are first rendered. The outputs are the image files and z-buffers. These are input into the simulation which renders the final images.

lightning as the radius increases with time. Furthermore, volume preservation could be used by counting the number of particles that have passed through the hole in the wall. The number of inflowing particles could be used to increase the radius with a simple formula used to compute the volume of a sphere. Recall that $V = \frac{4}{3}\pi r^3$. Thus as particles flow into the volume, the radius should increase by a factor of the cube root of the volume.

The rendering pipeline is complex and makes use of too many temporary files. Figure 5.12 demonstrates a proposed rendering pipeline, which should sufficiently decrease the computing time necessary to generate an animation of ball lightning. This proposed rendering pipeline implements more of the functionality in the simulation, which reduces the number of temporary files required. This would decrease the total computing time required to render an animation, but not the amount of CPU time.

It should be noted here that ball lightning is emissive — that is to say it is a light source. Ball lightning is not treated as a light source in this work. To implement such a feature is not difficult; one would simply place a coloured light source at the center of the ball lightning. However, this would *greatly increase* the computing time of the simulation since the complex background image would need to be rendered for each frame of the animation as opposed to just once.

The last improvement to be considered here is to use computer graphics hardware to increase performance. Graphics hardware works by projecting primitives onto the view plane. This is very similar to the splatting methods used for the rendering of this model. In fact, graphics hardware implementations usually have support for a point

primitive[143]. The only aspect of this project that would be too slow to perform in real-time is the simulation of the ball lightning as it is advected through the voxel volume. This aspect of the simulation could be precomputed to achieve real-time renderings; or perhaps a simplification could be found so that even the advection is performed in real-time.

5.4 Conclusion

This thesis presents a first attempt at a computer graphics model for simulating ball lightning. The motion of a ball lightning in the force field of a current is computed by numerically solving a set of ordinary differential equations that have been provided in the physics literature. Simple computer graphics techniques are used to approximate the deformation of the ball lightning through a hole in the wall. The shape of the deformation can be controlled by modifying a single parameter, thus providing a mechanism that can be used to match the approximation with observed ball lightning events.

Simulating and rendering of the ball lightning is efficient, robust, and easy to implement. This work presents the first step required in order to produce a convincing animation of ball lightning. Some of the future work that is required is discussed.

This thesis contributes to ball lightning research by attempting to validate a dynamical system of equations provided in the literature. Numerically solving the system yielded a natural-looking, curvilinear path that described the ball lightning motion. However, in the literature it has been noted that ball lightning sometimes follows a path with sharp changes in direction. The dynamical simulation investigated in this work does not seem to be able to reproduce such sharp changes in direction. A more complex system is required to produce such effects.

The model described in this thesis has obvious contributions to the computer graphics industry. An animation of a ball lightning can be used in flight simulators

since ball lightning events have been reported by pilots. Furthermore, a ball lightning could be used to add drama to an animated movie feature. Other applications for this simulation can be found by physicists studying the nature of ball lightning. It would be useful tool to allow eyewitnesses of ball lightning events use the visual parameters described in this thesis to generate a picture of what they saw. Written and verbal accounts from laypeople who have seen the phenomenon would be much more helpful to researchers if a picture could be used to support their story.

Ball lightning is a very elusive phenomenon. The model proposed in this thesis will hopefully help to shed some light on its nature.

Bibliography

- [1] John Abrahamson. Ball lightning from atmospheric discharges via metal nanosphere oxidation: from soils, wood or metals. *Philosophical Transactions — Series A*, 360:61–88, January 2002.
- [2] John Abrahamson. Preface. *Philosophical Transactions — Series A*, 360:3, January 2002.
- [3] John Abrahamson, A. V. Bychkov, and V. L. Bychkov. Recently reported sightings of ball lightning: Observations collected by correspondence and Russian and Ukrainian sightings. *Philosophical Transactions — Series A*, 360:11–35, January 2002.
- [4] John Abrahamson and James Dinniss. Ball lightning caused by oxidation of nanoparticle networks from normal lightning strikes on soil. *Nature*, 403:519–521, February 2000.
- [5] A. M. Adrianov and V. I. Sinitsyn. Erosion-discharge model for ball lightning. *Soviet Physics Technical Physics*, 22(11):1342–1347, November 1977.
- [6] V. Ya. Aleksandrov, E. M. Golubev, and I. V. Podmoshenskii. Aerosol mode of ball lightning. *Soviet Physics Technical Physics*, 27(10):1221–1224, October 1982.
- [7] M. D. Altschuler, L. L. House, and E. Hildner. Is ball lightning a nuclear phenomenon? *Nature*, 228:545–547, November 1970.
- [8] Stephen Andrilli and David Hecker. *Elementary Linear Algebra*. Brooks/Cole Publishing Company, Toronto, Canada, 1998.

- [9] Masaki Aono and Toshiyasu L. Kunii. Botanical tree image generation. *IEEE Computer Graphics & Applications*, 4(5):10–34, May 1984.
- [10] Arthur Appel. Some techniques for shading machine renderings of solids. In *American Federation of Information Processing Societies*, volume 32, pages 37–45, 1968.
- [11] Edward Argyle. Ball lightning as an optical illusion. *Nature*, 230:179–180, March 1971.
- [12] D. E. T. F. Ashby and C. Whitehead. Is ball lightning caused by antimatter meteorites? *Nature*, 230:180–182, March 1971.
- [13] George I. Babat. Electrodeless discharges and some allied problems. *Journal of the Institution of Electrical Engineers*, 94(Part III):27–37, 1947. Reprint Available in [108].
- [14] Gladimir V. G. Baranoski and Jon Rokne. An efficient and controllable blob function. *Journal of Graphics Tools*, 6(4):41–54, 2002.
- [15] Gladimir V. G. Baranoski and Jon G. Rokne. Using a HPC system for the simulation of the trajectories of solar wind particles in the ionosphere. In *High Performance Computing Conference*, pages 14–16, Victoria, B.C., June 2000.
- [16] Gladimir V. G. Baranoski, Jon G. Rokne, Peter Shirley, Trond Trondsen, and Rui Bastos. Simulating the aurora borealis. Technical report, The University of Calgary, 2000.
- [17] James Dale Barry. Ball lightning. *Journal of Atmospheric and Terrestrial Physics*, 29:1095–1101, 1967.
- [18] James Dale Barry. *Ball Lightning and Bead Lightning*. Plenum Press, New York, New York, 1980.
- [19] Jules Bloomenthal. Modelling the mighty maple. In *Proceedings of the 12th Annual Conference on Computer Graphics and Interactive Techniques (SIGGRAPH'85)*, volume 19, pages 305–311, July 1985.

- [20] Jules Bloomenthal, editor. *Introduction to Implicit Surfaces*. Morgan Kaufmann Publishers, Inc., San Francisco, CA, USA, 1997.
- [21] Walther Brand. *Der Kugelblitz*. Verlag von Henri Grand, Hamburg, 1923. English translation available as a NASA technical report[22].
- [22] Walther Brand. Ball lightning. Technical Report NASA TT F-13,228, National Aeronautics and Space Administration, Washington D.C., 20546, February 1971.
- [23] K. A. Bromley. Ball lightning. *Nature*, 226:252, April 1970.
- [24] G. H. Brown. Ball lightning. *The Meteorological Magazine*, 86:375, 1957.
- [25] C. E. R. Bruce. Ball lightning. *Nature*, 202(4936):996–997, June 1964.
- [26] A. V. Bychkov, V. L. Bychkov, and John Abrahamson. On the energy characteristics of ball lightning. *Philosophical Transactions — Series A*, 360:97–106, January 2002.
- [27] V. L. Bychkov. Polymer-composite ball lightning. *Philosophical Transactions — Series A*, 360:37–60, January 2002.
- [28] C. Maxwell Cade and Delphine Davis. *The Taming of Thunderbolts*. Abelard-Schuman, New York, 1969.
- [29] Steuart Campbell. Ball lightning through the window glass? *Journal of Meteorology*, 22:216–218, 1997.
- [30] Steuart Campbell. Ball lightning and window panes. *Journal of Meteorology*, 23:235–236, 1998.
- [31] Robert L. Cook. Shade trees. *Computer Graphics*, 18(3):223–231, July 1984.
- [32] Arthur E. Covington. Ball lightning. *Nature*, 226:252–253, April 1970.
- [33] Jack W. Crenshaw. *Math Toolkit for Real-Time Programming*. CMP Books, Lawrence, Kansas, USA, 2000.
- [34] Matthias Kalle Dalheimer. *Programming with QT*. O’Reilly, second edition, January 2002.

- [35] Alexandre Dauvillier. Foudre globulaire et réactions thermonucléaires. *Comptes Rendus de l'Académie des Sciences*, 245:2155–2156, December 1957.
- [36] B. V. Davidov. Radkaia fotografia sharovi molnii. *Priroda*, 47(1):96, 1958.
- [37] René Descartes. *Discourse on Method, Optics, Geometry, and Meteorology*. Hackett Publishing Company, Inc., Indianapolis, IN, USA, revised edition, 2001. Translated, with Introduction, by Paul J. Olscamp.
- [38] Yoshinori Dobashi, Tsuyoshi Yamamoto, and Tomoyuki Nishita. Efficient rendering of lightning taking into account scattering effects due to clouds and atmospheric particles. In *Ninth Pacific Conference on Computer Graphics and Applications*, pages 390–397, October 2001.
- [39] Robert A. Drebin, Loren Carpenter, and Pat Hanrahan. Volume rendering. *Computer Graphics*, 22(4):65–74, 1988.
- [40] David S. Ebert, F. Kenton Musgrave, Darwyn Peachey, Ken Perlin, and Steven Worley. *Texturing & Modeling: A Procedural Approach*. AP Professional — An Imprint of Academic Press, San Diego, California, USA, 1998.
- [41] S. Eliezer and Y. Eliezer. *The Fourth State of Matter: An Introduction to Plasma Science*. Institute of Physics Publishing, Philadelphia, Pennsylvania, second edition, 2001.
- [42] V. G. Endeian. Ball lightning as electromagnetic energy. *Nature*, 263:753–755, October 1976.
- [43] Gerald Farin. *Curves and Surfaces for CAGD*. Morgan Kaufmann, San Francisco, California, fifth edition, 2002.
- [44] Pavol Federl and Przemyslaw Prusinkiewicz. Modelling fracture formation in bilayered materials, with applications to tree bark and drying mud. In *Western Computer Graphics Symposium Proceedings 2002*, pages 29–35, 2002.
- [45] Murray Felsher. Ball lightning. *Nature*, 227:982, August 1970.

- [46] H. T. Flint. On the problem of ball lightning. *Quarterly Journal of the Royal Meteorological Society*, 65:532–535, October 1939.
- [47] Gideon Frieder, Dan Gordon, and R. Anthony Raynolds. Back-to-front display of voxel-based objects. *IEEE Computer Graphics & Applications*, 5(1):52–60, January 1985.
- [48] N. I. Gaídukov. Equations of motion of ball lightning in the field of a point source. *Soviet Physics Doklady*, 33(8):571–573, August 1988.
- [49] N. I. Gaídukov. Motion of ball lightning in an airflow through a wide circular opening in a flat screen. *Soviet Physics Technical Physics*, 34(2):181–184, February 1989.
- [50] N. I. Gaídukov. Hydrodynamic model of the passage of ball lightning through a narrow slot in a flat screen. *Soviet Physics Technical Physics*, 36(11):1223–1227, November 1991.
- [51] J. J. Gilman. Cohesion in ball lightning. *Applied Physics Letters*, 83(11):2283–2284, September 2003.
- [52] Andrew Glassner. The digital ceraunoscope: Synthetic thunder and lightning. Technical report, Microsoft Corporation, 1999.
- [53] Andrew Glassner. Andrew Glassner’s notebook: The digital ceraunoscope: Synthetic thunder and lightning, part 1. *IEEE Computer Graphics & Applications*, 20(2):89–93, March/April 2000.
- [54] Andrew Glassner. Andrew Glassner’s notebook: The digital ceraunoscope: Synthetic thunder and lightning, part 2. *IEEE Computer Graphics & Applications*, 20(3):92–96, May/June 2000.
- [55] E Gold. Thunderbolts: The electrical phenomena of thunderstorms. *Nature*, 169(4301):561–563, April 1952.
- [56] Robert A. Goldstein and Roger Nagel. 3-D visual simulation. *Simulation*, 16(1):25–31, January 1971.

- [57] Robert K. Golka. Laboratory-produced ball lightning. *Journal of Geophysical Research*, 99(D5):10679–10681, May 1994.
- [58] B. L. Goodlet. Lightning. *The Journal of the Institution of Electrical Engineers*, 81:1–56, 1937.
- [59] Robert Greenler. *Rainbows, Halos, and Glories*. Cambridge University Press, New York, 1980.
- [60] A. I. Grigor'ev, I. D. Grigor'eva, and S. O. Shiryaeava. Ball lightning penetration into closed rooms: 43 eyewitness accounts. *Journal of Scientific Exploration*, 6(3):261–279, 1992.
- [61] Charles W. Hamilton. Sustained, localized, pulsed-microwave discharge in air. *Nature*, 188(4756):1098–1099, December 1960.
- [62] Peter H. Handel and Jean François Leitner. Development of the maser-caviton ball lightning theory. *Journal of Geophysical Research*, 99(D5):10689–10691, May 1994.
- [63] Donald Hearn and M. Pauline Baker. *Computer Graphics: C Version*. Prentice Hall, Upper Saddle River, New Jersey, 1997.
- [64] E. L. Hill. Ball lightning as a physical phenomenon. *Journal of Geophysical Research*, 65(7):1947–1952, July 1960.
- [65] E. L. Hill. Ball lightning. *American Scientist*, 58:479, 1970.
- [66] Graham K. Hubler. Fluff balls of fire. *Nature*, 403:487–488, February 2000.
- [67] William F. Hughes and John A. Brighton. *Schaum's Outlines: Fluid Dynamics*. McGraw-Hill, Toronto, Canada, third edition, 1999.
- [68] W. J. Humphreys. Ball lightning. *Proceedings fo the American Philosophical Society*, 76:613–626, 1936.
- [69] R. C. Jennison. Ball lightning. *Nature*, 224:895, November 1969.

- [70] John Clark Johnson. *Physical Meteorology*. The Technology Press of MIT and John Wiley and Sons, Inc., New York, 1954. pp. 315–316.
- [71] Peter L. Kapitsa. O prirode sharovoi milnii (the nature of ball lightning). *Doklady Akademii Nauk SSSR*, 101(2):245–248, 1955. Reprint Available in [108].
- [72] William J. Kaufmann. *Universe*. W. H. Freeman and Company, fourth edition, 1994.
- [73] Douglas Scott Kay and Donald Greenberg. Transparency for computer synthesized images. In *6th Annual Conference on Computer Graphics and Interactive Techniques (SIGGRAPH'79)*, pages 158–164, Chicago, Illinois, USA, 1979.
- [74] A. G. Keul. Possible ball lightning colour photograph from sankt gallenkirch, vorarlberg, austria. *Journal of Meteorology*, 17(167):73–82, March 1992.
- [75] A. G. Keul. Ball lightning photographs — testing the limits. *Journal of Meteorology*, 21(207):82–88, 1996.
- [76] G. I. Kogan-Beletskii. The nature of ball lightning. *Priroda*, 6:71–73, 1957. Translation Available in [108].
- [77] Paul Kruszewski. A probabilistic technique for the synthetic imagery of lightning. *Computers & Graphics*, 23(2):287–293, April 1999.
- [78] Hendrik Kück, Christian Vogelgsang, and Günther Greiner. Simulation and rendering of liquid foams. In *Graphics Interface 2002*, pages 81–88, 2002.
- [79] Yu. P. Ladikov. Magneto-vortex rings. In Donald J. Ritchie, editor, *Ball Lightning: A Collection of Soviet Research in English Translation*, pages 51–60. Consultants Bureau Enterprises, Inc., New York, 1961.
- [80] Brendan Lane and Przemyslaw Prusinkiewicz. Generating spatial distributions for multilevel models of plant communities. In *Graphics Interface 2002*, pages 69–87, 2002.
- [81] David Laur and Pat Hanrahan. Hierarchical splatting: A progressive refinement algorithm for volume rendering. *Computer Graphics*, 25(4):285–288, 1991.

- [82] Reiner Lenz, Bjorn Gudmundsson, and Per E. Danielsson. Display of density volumes. *IEEE Computer Graphics & Applications*, 6(7):20–29, July 1986.
- [83] Steven J. Leon. *Linear Algebra With Applications*. Prentice-Hall, Inc., New Jersey, USA, fourth edition, 1994.
- [84] Pedro Lilienfeld. Ball lightning. *Nature*, 226:252, April 1970.
- [85] J. J. Lowke. A theory of ball lightning as an electric discharge. *Journal of Physics D: Applied Physics*, 29:1237–1244, 1996.
- [86] J. J. Lowke, M. A. Uman, and R. W. Liebermann. Toward a theory of ball lightning. *Journal of Geophysical Research*, 74(28):6887–6898, December 1969.
- [87] David K. Lynch and William Livingston. *Colour and Light in Nature*. Cambridge University Press, second edition, 2001.
- [88] Tomas Möller and Ben Trumbore. Fast, minimum storage ray-triangle intersection. *Journal of Graphics Tools*, 2(1):21–28, 1997.
- [89] F. Kenton Musgrave. Prisms and rainbows: A dispersion model for computer graphics. In *Graphics Interface 1989*, pages 227–234, 1989.
- [90] Von Th. Neugebauer. Zu dem problem des Kugelblitzes. *Zeitschrift für Physik*, 106:474–484, 1937. English translation available from the Met Office⁴.
- [91] Karl Nickel. A model for ball lightning and bead lightning. Technical report, Australian National University, March 1986.
- [92] Y. H. Ohtsuki and H. Ofuruton. Plasma fireballs formed by microwave interference in air. *Nature*, 350:139–141, March 1991.
- [93] Yoshi-Hiko Ohtsuki, Masashi Kamogawa, and Hideho Ofuruton. Co-seismic ball lightning of 1995 Hanshin-Awaji earthquake in Japan and 1999 Chi-Chi earthquake in

⁴<http://www.metoffice.co.uk/>

- Taiwan. In *7th international symposium on ball lightning (ISBL'01)*, St. Louis, Missouri, USA, July 2001. Abstract available online at <http://home.planet.nl/icblsec/> at time of writing.
- [94] Marcel Ouellet. Earthquake lights and seismicity. *Nature*, 348:492, December 1990.
- [95] Eric Paquette, Pierre Poulin, and George Drettakis. The simulation of paint cracking and peeling. In *Graphics Interface 2002*, pages 59–68, 2002.
- [96] Bui Tuong Phong. Illumination for computer generated pictures. *Communications of the ACM*, 18(6), June 1975.
- [97] Brian Pippard. Ball of fire? *Nature*, 298:702, August 1982.
- [98] James R. Powell and David Finkelstein. Ball lightning. *American Scientist*, 58:262–280, 1970.
- [99] A. J. Preetham, Peter Shirley, and Brian Smits. A practical analytic model for daylight. In *Proceedings of the 26th Annual Conference on Computer Graphics and Interactive Techniques (SIGGRAPH'99)*, pages 91–100, 1999.
- [100] Przemyslaw Prusinkiewicz. *The Algorithmic Beauty of Plants (The Virtual Laboratory)*. Springer Verlag, 1990.
- [101] Antonio F. Rañada and José L. Trueba. Ball lightning an electromagnetic knot? *Nature*, 383:32, September 1996.
- [102] Warren D. Rayle. Ball lightning characteristics. Technical Report TN-D-3188, National Aeronautics and Space Administration: Lewis Research Center, Cleveland, Ohio, January 1966.
- [103] K. Todd Reed and Brian Wyvill. Visual simulation of lightning. In *Proceedings of the 21st Annual Conference on Computer Graphics and Interactive Techniques (SIGGRAPH'94)*, volume 28, pages 359–364, July 1994.
- [104] William T. Reeves. Particle systems — a technique for modeling a class of fuzzy objects. *ACM Transactions on Graphics*, 2(2):91–108, April 1983.

- [105] R. Reiter. *Phenomena in Atmospheric and Environmental Electricity*. Elsevier, New York, 1992.
- [106] Herbert S. Ribner and Dipankar Roy. Acoustics of thunder: A quasilinear model for tortuous lightning. *The Journal of the Acoustical Society of America*, 72(6):1911–1925, December 1982.
- [107] Donald J. Ritchie. Reds may use lightning as weapon. *Missiles and Rockets*, August 1959.
- [108] Donald J. Ritchie, editor. *Ball Lightning: A Collection of Soviet Research in English Translation*. Consultants Bureau Enterprises, Inc., New York, 1961.
- [109] Dipankar Roy. A Monte Carlo model of tortuous lightning and the generation of thunder. Technical Report 243, The University of Toronto Institute for Aerospace Studies, Toronto, Canada, February 1981.
- [110] Sir Basil Schonland. *The Flight of Thunderbolts*. Oxford University Press, Oxford, second edition, 1964.
- [111] V. D. Shafranov. On equilibrium magnetohydrodynamic configurations. In *International Conference on Ionization Phenomena in Gases*, pages 990–997, Venice, Italy, June 1957.
- [112] V. D. Shafranov. On magnetohydrodynamical equilibrium configurations. *Soviet Physics JETP*, 6(9):545–554, 1957. Reprint Available in [108].
- [113] Peter Shirley. *Realistic Ray Tracing*. A. K. Peters Ltd., 2000.
- [114] Paul A. Silberg. On the question of ball lightning. *Journal of Applied Physics*, 32(1):30–35, January 1961.
- [115] Stanley Singer. The unsolved problem of ball lightning. *Nature*, 198(4882):745–747, May 1963.
- [116] Stanley Singer. *The Nature of Ball Lightning*. Plenum Press, New York, New York, 1971.

- [117] Stanley Singer. Great balls of fire. *Nature*, 350:108—109, March 1991.
- [118] Stanley Singer. Ball lightning—the scientific effort. *Philosophical Transactions — Series A*, 360:3, January 2002.
- [119] B. M. Smirnov. The properties and the nature of ball lightning. *Physics Reports*, 152(4):177–226, August 1987.
- [120] B. M. Smirnov. Physics of ball lightning. *Physics Reports*, 224(4):151–236, March 1993.
- [121] B. M. Smirnov. Radiation of some fractal structures. *International Journal of Theoretical Physics*, 32(8):1453–1464, 1993.
- [122] Alvy Ray Smith. Plants, fractals, and formal languages. In *Proceedings of the 11th Annual Conference on Computer Graphics and Interactive Techniques (SIGGRAPH'84)*, volume 18, pages 1–10, July 1984.
- [123] Brian Smits. Efficiency issues for ray tracing. *Journal of Graphics Tools*, 3(2):1–14, 1998.
- [124] B. Sosorbaram, T. Fujimoto, K. Muraoka, and N. Chiba. Visual simulation of lightning taking into account cloud growth. In *Computer Graphics International 2001 Proceedings*, pages 89–95, July 2001.
- [125] Mark Stenhoff. *Ball Lightning: An Unsolved Problem in Atmospheric Physics*. Kluwer Academic / Plenum Publishers, New York, New York, 2000.
- [126] C. F. Talman. A case of ball lightning. *Bulletin of the American Meteorological Society*, 11:110–111, May 1930.
- [127] Spencer W. Thomas. Dispersive refraction in ray tracing. *Visual Computer*, 2(1):3–8, January 1986.
- [128] W. M. Thornton. On thunderbolts. *Philosophical Magazine and Journal of Science*, 21(125):630–634, May 1911.

- [129] Lewi Tonks. Electromagnetic standing waves and ball lightning. *Nature*, 187(4742):1013–1014, September 1960.
- [130] Chi Fu (Mark) Tse. Personal communication, January 2002.
- [131] D. J. Turner. Ball lightning through the window glass? a reply. *Journal of Meteorology*, 22:219–221, 1997.
- [132] D. J. Turner. The interaction of ball lightning with glass window panes. *Journal of Meteorology*, 22:52–64, 1997.
- [133] D. J. Turner. Ball lightning and window panes. a reply. *Journal of Meteorology*, 23:236–238, 1998.
- [134] D. J. Turner. The fragmented science of ball lightning (with comment). *Philosophical Transactions — Series A*, 360:107–152, January 2002.
- [135] M. A. Uman. Some comments on ball lightning. *Journal of Atmospheric and Terrestrial Physics*, 30:1245–1246, 1968.
- [136] Martin A. Uman. *The Lightning Discharge*. Academic Press, Orlando, Florida, 1987.
- [137] W. K. R. Watson. A theory of ball lightning formation. *Nature*, 185(4711):449–450, February 1960.
- [138] Alan Watt and Mark Watt. *Advanced Animation and Rendering Techniques: Theory and Practise*. Addison-Wesley, Don Mills, Ontario, 1992.
- [139] Lee Westover. Interactive volume visualization. In *1989 Chapel Hill Workshop on Volume Visualization*, pages 9–16, Chapel Hill, North Carolina, USA, 1989.
- [140] Lee Westover. Footprint evaluation for volume rendering. *Computer Graphics*, 24(4):367–376, 1990.
- [141] Turner Whitted. An improved illumination model for shaded display. *Communications of the ACM*, 23(6), June 1980.

- [142] A. Wittmann. In support of a physical explanation of ball lightning. *Nature*, 232:625, August 1971.
- [143] Mason Woo, Jackie Neider, Tom Davis, and Dave Shreiner. *OpenGL[®] Programming Guide*. Addison Wesley, Don Mills, Ontario, 1999.
- [144] E. R. Wooding. Ball lightning. *Nature*, 199(4890):272–273, July 1963.
- [145] V. V. Yankov. Behavior of a conducting gaseous sphere in a quasi-stationary electromagnetic field. *Soviet Physics JETP*, 9(2):388–391, 1959. Reprint Available in [108].
- [146] V. V. Yankov. Dynamics of a conducting gaseous sphere in a quasi-stationary electromagnetic field. *Soviet Physics JETP*, 10:158–160, 1959. Reprint Available in [108].
- [147] P. D. Zimmerman. Energy content of Covington’s lightning ball. *Nature*, 228:853, November 1970.